

6.4.2 Structural Analysis

The DHLW WP must be shown to comply with all regulations and requirements that govern the containment of radionuclides. The regulations that the design must meet include 10 CFR 20, 10 CFR 60, and 40 CFR 191. These requirements state that the WP must remain intact as a unit for containing waste and provide for the safe handling of the waste, at least until the end of the period of retrievability. Therefore, the repository and the WPs must be designed to preserve the option of waste retrieval throughout this period. The WP must also be capable of sustaining normal handling, packaging, and operational loads without loss of containment. Furthermore, it must be shown that the WP can survive design-basis accidents either without loss of containment or with a limited release of radionuclides.

The most damaging loads the DHLW WP must be able to endure are the accident loads. The accident scenarios analyzed for the WPs are a WP 2-m drop, a WP slap down, and a starter tunnel rock fall onto the WP. To be conservative, the acceptance criteria will be to show that there is no breaching of the pour canisters or the inner or outer barriers, excluding the outer barrier skirt (the extensions of the outer barrier cylinder used for handling purposes). Material failure in the outer barrier skirts is acceptable because the skirts are not part of the containment barrier. Plastic deformation of the barriers is also acceptable during these accidents provided that there is no breaching of the material. The material properties used in the calculations are given in Table 6.4-4. For these analyses, the inner and outer barrier are assumed to be at 60°C and the pour canisters and glassified waste are assumed to be at 250°C. These temperatures are only estimates made for selecting temperature-dependent material properties for use in the analyses to improve the accuracy of the solution over using room temperature properties. The density inputs for the model were calculated to match the mass of each component with its mass given in Table 6.1-4, so density is not included in the material properties table. Material behavior is approximated in the model with elastic/plastic bilinear stress-strain curves for the materials.

6.4.2.1 Waste Package 2-m Drop Accident Analysis

Prior to licensing, the WP must be shown to be capable of surviving certain accident conditions without resulting in a breach of radionuclide containment. One possibly damaging accident is to drop the WP. The maximum height to which the WP is assumed to be lifted during transportation is 2 m (CRWMS M&O 1995n). Therefore, this height is selected for the WP drop analysis.

A rock fall could potentially occur in the starter tunnel or main drift while the WP is in transit, or in the emplacement drift after the WP has been emplaced. The main difference between these cases is the height from which the rock falls. The starter tunnel height is greater than either the main drift or emplacement drift height, so the starter tunnel rock fall is considered to be limiting.

Table 6.4-4. Material Properties Table for Defense High-Level Waste Waste Package Models

| Material | Temp. | Yield Strength S_y | Ultimate Tensile Strength S_u | Elastic Modulus E | Poisson's Ratio ν | Percent Elongation |
|----------------------|-------|-------------------------|------------------------------------|-----------------------|--------------------------|--------------------|
| C71500 | 60°C | 153 MPa ^a | 358 MPa ^a | 143 GPa ^b | 0.28 ^c | 46 ^b |
| Alloy 825 | 60°C | 304 MPa ^d | 642 MPa ^d | 203 GPa ^d | 0.42 ^d | 45 ^d |
| 304L Stainless Steel | 250°C | 113 MPa ^e | 399 MPa ^e | 179 GPa ^e | 0.30 ^e | 40 ^b |
| Glassified Waste* | 250°C | - | - | 62.7 GPa ^f | 0.20 ^f | - |
| Rock* | - | - | - | 32.7 GPa ^g | 0.22 ^g | - |

Table Notes:

* The stresses in the glass and rock are not of concern because the waste form is not part of the containment or internal structure, and the rock is conservatively assumed not to fail; therefore, the allowables for the glassified waste and the rock are not important, and because the glassified waste and the rock are not evaluated plastically, the percent elongation is not required.

a. Cohen, A. and W.S. Lyman 1986. (Values are found by linear interpolation of the presented data.)

b. *Metals Handbook Ninth Edition, Volume 3, Properties and Selection: Stainless Steels, Tool Materials and Special-Purpose Metals, American Society for Metals, 1980. p. 747* (Values found by linear extrapolation of data.)

c. *Metals Handbook Tenth Edition, Volume 2, Properties and Selection: Nonferrous Alloys and Special-Purpose Materials, 1990.*

This reference provides the shear modulus for C71500 @ 20°C: $G = 57 \text{ GPa}$.

The elastic modulus of C71500 @ 20°C: $E = 146 \text{ GPa}$ (*Metals Handbook Ninth Edition, Volume 3, Properties and Selection: Stainless Steels, Tool Materials and Special-Purpose Metals, American Society for Metals, Metals Park, Ohio 1980*)

$$\nu = -1 + E/2G = 0.28$$

d. INCO Alloys International 1992. (pp. 2-3)

e. ASME 1992. (Section II, Part D, Subpart 2, Table TM-1)

f. MEMS 1990. (Properties of General Borosilicate Glass at room temperature are assumed to be representative for these analyses and are used only to provide stiffness for the glass.)

g. YMP 1994a

This hypothetical accident condition is a free drop of the WP from a height of 2 m onto a flat, essentially unyielding horizontal surface. The horizontal surface cannot be perfectly unyielding because that would require a surface with infinite stiffness. Because such a surface cannot be modeled, these analyses use the next best option; an essentially unyielding surface which has a very high stiffness. The case analyzed is one in which the WP strikes the ground at an angle that puts the center of mass directly above the point of impact. These conditions cause the highest loads on the WP outer barrier and therefore are expected to cause the most damage. The model described and the analysis results given in this section are taken from the *Finite-Element Analysis of Rock Fall onto Defense High-Level Waste Package* (CRWMS M&O 1996a).

6.4.2.1.1 Description of Finite-Element Model for 2-m Drop

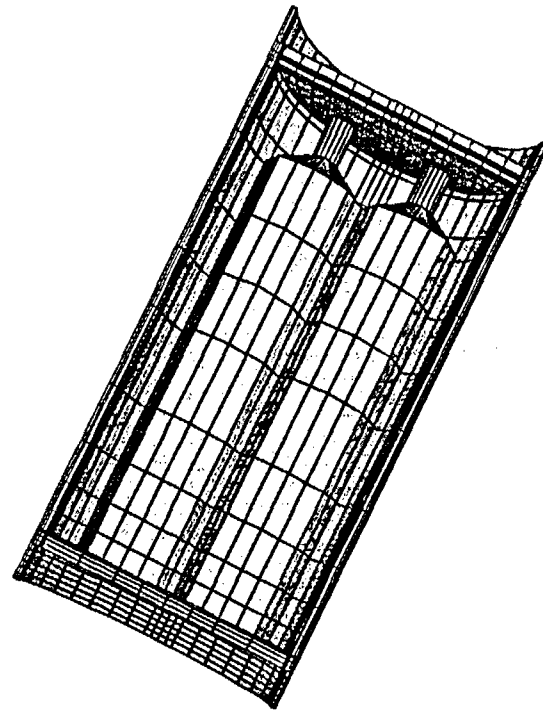
The ANSYS 5.0A finite-element analysis code is used for the structural analysis of the WP 2-m drop accident scenario. Three-dimensional brick elements are used in modeling all parts of the WP. Some capabilities of the element used to perform this nonlinear transient dynamic analysis are plasticity, large deflection, and large strain.

The model developed for the 2-m drop analysis of the DHLW WP is a one-half symmetry, three-dimensional finite-element model, shown in Figure 6.4-17. The analysis incorporates the outer barrier and lids, inner barrier and lids, and the Savannah Pour Canister with glassified waste. The mass of the canister guide is included in the mass of the inner barrier, but the structure itself is not included because it is not a critical structural member of the WP. Material specifications of the outer barrier, inner barrier, pour canisters, and glass are defined by their individual property tables. The outer barrier is given the properties of C71500, the inner barrier is given the properties of Alloy 825, the pour canister is given the properties of 304L stainless steel, and the glass is given the properties of general borosilicate glass.

The WP is symmetric about a plane that runs along the longitudinal axis, so only half of the WP is modeled, and symmetry boundary constraints are placed on the symmetry plane. This approach has been verified on a simple model, which shows that stress distribution results obtained for both half and full models are identical in terms of normal and shear stress components. Stress plots have been given in Figures 6.5-52 and 6.5-53. Taking advantage of the symmetry reduces the model size, allowing more detail in the half that is modeled. However, even with the half model, the element mesh must remain somewhat coarse to keep run times down and maintain manageability of the output files.

Therefore, some other simplifications have been made to the model:

- The model is constructed as if the inner and outer barriers are fabricated as one piece. It is not yet known if the WP will be fabricated in this manner, but using this assumption prevents the need for contact elements between the inner and outer barriers. It is best to avoid the use of contact elements wherever possible to prevent convergence problems and to reduce the model size and run times. While the inner and outer barriers are treated as contiguous, there is an element border between the inner and outer barrier and the appropriate material properties are used for each barrier.



ANSYS 5.0 A
JAN 30 1996 .

ELEMENTS

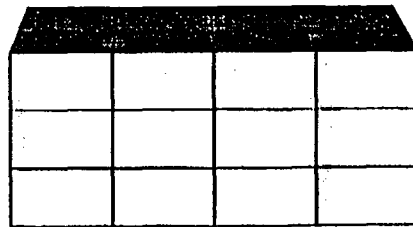


Figure 6.4-17. Defense High-Level Waste Waste Package 2-m Drop Model

- The gaps between the pour canisters and the inner barrier side walls and the gaps between pour canisters are closed by increasing the outer diameter of the pour canisters. The inner diameter is also increased to keep the moment of inertia constant. By keeping the modulus of elasticity, moment of inertia, and length of the glass pour canister the same, the stiffness remains the same. The pour canister is also modeled as being fixed to the bottom lid of the inner barrier. These modifications are made to prevent the need for contact elements inside the WP model. Another modification is that the pour canisters are modeled as octagonal cylinders rather than circular cylinders because ANSYS meshing operations will not permit meshing of the volume between tangent circular cylinders, a condition that occurs without this modification. The pour canisters are further simplified in geometry at the ends to ease model creation. The flange on the bottom of the pour canister is simplified to a flat plate having the nominal flange thickness and an angle of 90° to the canister wall. The top flange was simplified to a ramped reduction in diameter with a smaller solid cylinder on top. These simplifications are likely to increase the stress output in the regions of the pour canisters and are considered conservative.
- The density of each material has been slightly modified so that the mass of each component of the model will match that calculated in Table 6.1-4. This is necessary because the polygonal approximation of round members changes the volume slightly. Also, the density of the inner barrier is adjusted to include the mass of the canister guide.

The simplifications are deemed reasonable because, for conceptual design, overall system response is more important than the discrete calculation of stresses in the various radii and corners that a finer mesh allows. These discrete calculations will be performed at a later design stage.

The only force acting on the WP is its own mass times gravity. Maximum linear momentum transfer of the WP will occur along a vertical plane passing through its center of gravity, so the WP has been rotated 26.66° with respect to the vertical plane. This rotation puts the center of mass directly above the contact point with the ground, causing the WP to be in an orientation that will result in maximum plastic deformation on the outer barrier skirt. The distance from the flat surface to the WP bottom edge is 2 m.

6.4.2.1.2 Barrier Response to 2-m Drop

As is described in the previous section, the drop considered is a corner drop with the WP rotated 26.66° from vertical. A corner drop can be separated into two individual drop events: initial impact and slap down. For WP impact angles near vertical, the initial impact dominates and the WP response resembles the condition of an end drop. For impact angles near horizontal, the slap down phase dominates and the assembly response resembles the condition of a side drop (SNL 1992a, pp. 53-64). A corner drop of 26.66° with respect to the vertical axis resembles the condition of an end drop and results in the largest deformation pattern on the barrier. Thus, the effect of second impact on the opposite end of the WP will not be critical when compared to the first impact. The slap down case is analyzed separately and the results are given in Section 6.4.2.2.

The skirt on the outer barrier behaves as an impact limiter during the WP 2-m corner-drop accident scenario. The linear momentum of the WP in the vertical direction results in maximum damage on

the skirt in terms of elastic and plastic deformations. Figure 6.4-18 shows the principal stress distribution (S_1) on the WP and on the locally deformed region in the vicinity of the contact area with the flat surface.

An outer barrier breach can occur by ductile tearing as a result of excessive stress or strain. Sharp curvature bending of the impacted WP corner is the reason for very high stress magnitudes, which may result in ductile rupture. Since the skirt functions as an impact limiter in this accident condition, failure is expected at this location of the DHLW disposal container. Failure is acceptable in the skirt because a failure in this region will not cause loss of radionuclide containment. As can be observed in Figure 6.4-19, the effect of impact is not critical in any regions of the outer barrier other than the skirt.

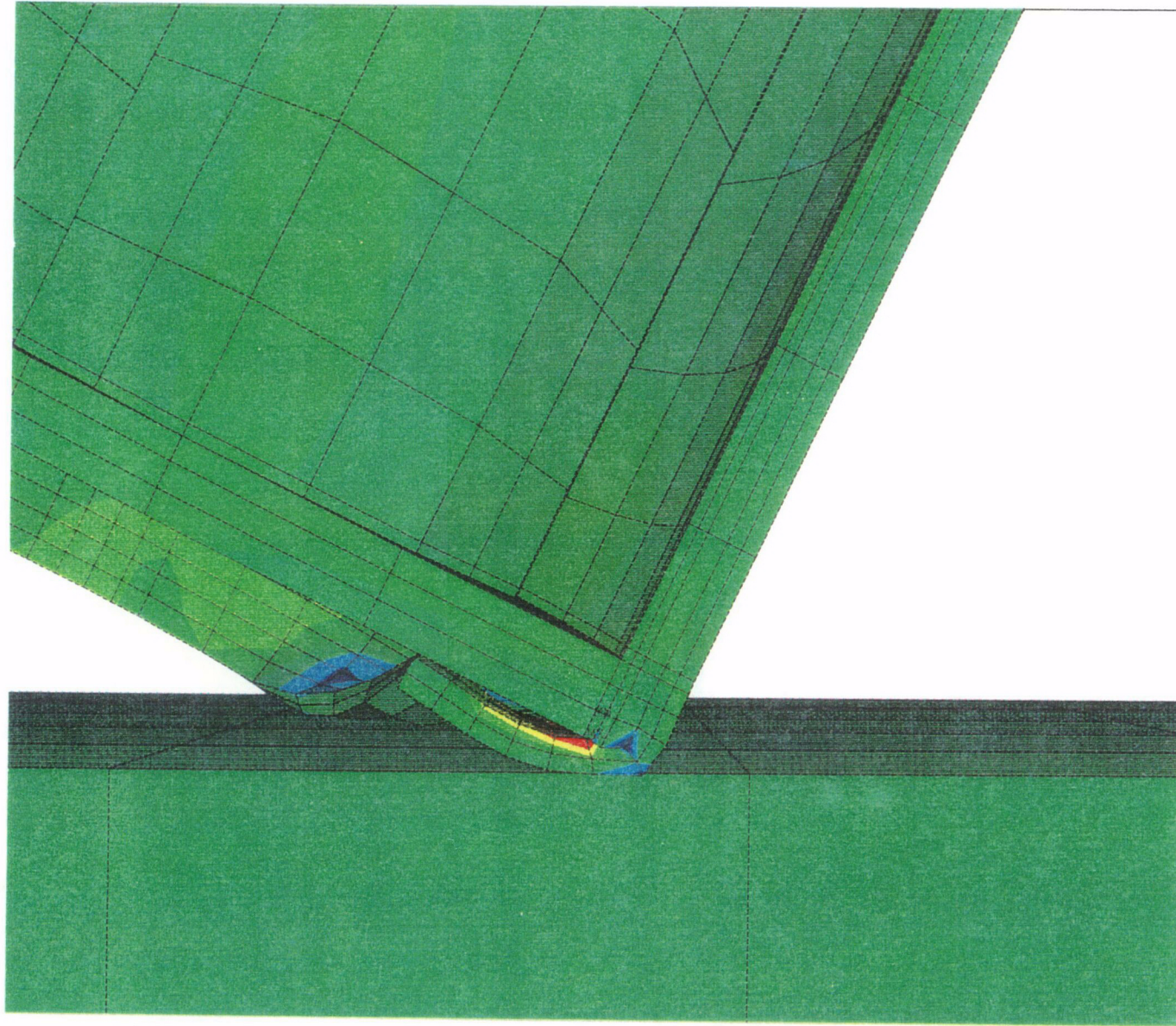
The inner surface of the skirt makes a 90° angle with the WP outer lid at the location where the skirt is extended from the container. This sharp corner could be eliminated by introducing a corner radius during the manufacturing process. This might slightly reduce the excessive deformation of the skirt by decreasing the stress concentration factor at the corner. However, the effect of a corner radius would still not be able to prevent the skirt from deforming plastically because the dynamic loading on the skirt is very high.

The maximum stress and strain magnitudes were obtained in the vicinity of the outer barrier skirt where it is flattened due to the impact. The maximum principal stress magnitude on the WP is 504 MPa (see Figure 6.4-18). This is above the ultimate tensile strength of the outer barrier material (358 MPa). Therefore, some localized material failure may occur in the region of impact of the skirt. However, the maximum principal stress magnitude in the model, excluding the skirt, is 323 MPa (see Figure 6.4-19). This indicates that the peak stress in the outer barrier, excluding the skirt, is below the ultimate tensile strength of the material (358 MPa). Therefore, it can be concluded that there is no material failure in the outer barrier other than in the skirt.

The results of this analysis indicate that the WP will retain its structural integrity during a 2-m drop accident since the stress magnitudes are below the ultimate tensile strength in the inner and outer barriers, excluding the skirt. There will be gross plastic deformation of the skirt, as well as some minor plastic deformation of the outer barrier.

6.4.2.1.3 Pour Canister Response to 2-m Drop

In the DHLW WP, the pour canister is the innermost barrier of the multibarrier design (though it is not credited for waste isolation analysis) and part of the internal structure. Therefore, it must provide separation and mechanical stability of the waste forms (YMP 1994b). To ensure that the pour canister is meeting these requirements, it must be verified that no material failure occurs in the pour canister during the WP 2-m drop accident. The pour canister used in this analysis is the Savannah Pour Canister. Because of the size of the model, the modeling of the pour canister has been simplified, so the stresses obtained from the model for the pour canister must be taken as approximate. They should be a good indication of the order of magnitude of the stresses in the pour canister and may indicate whether more detailed analyses are required and whether potential problems exist.



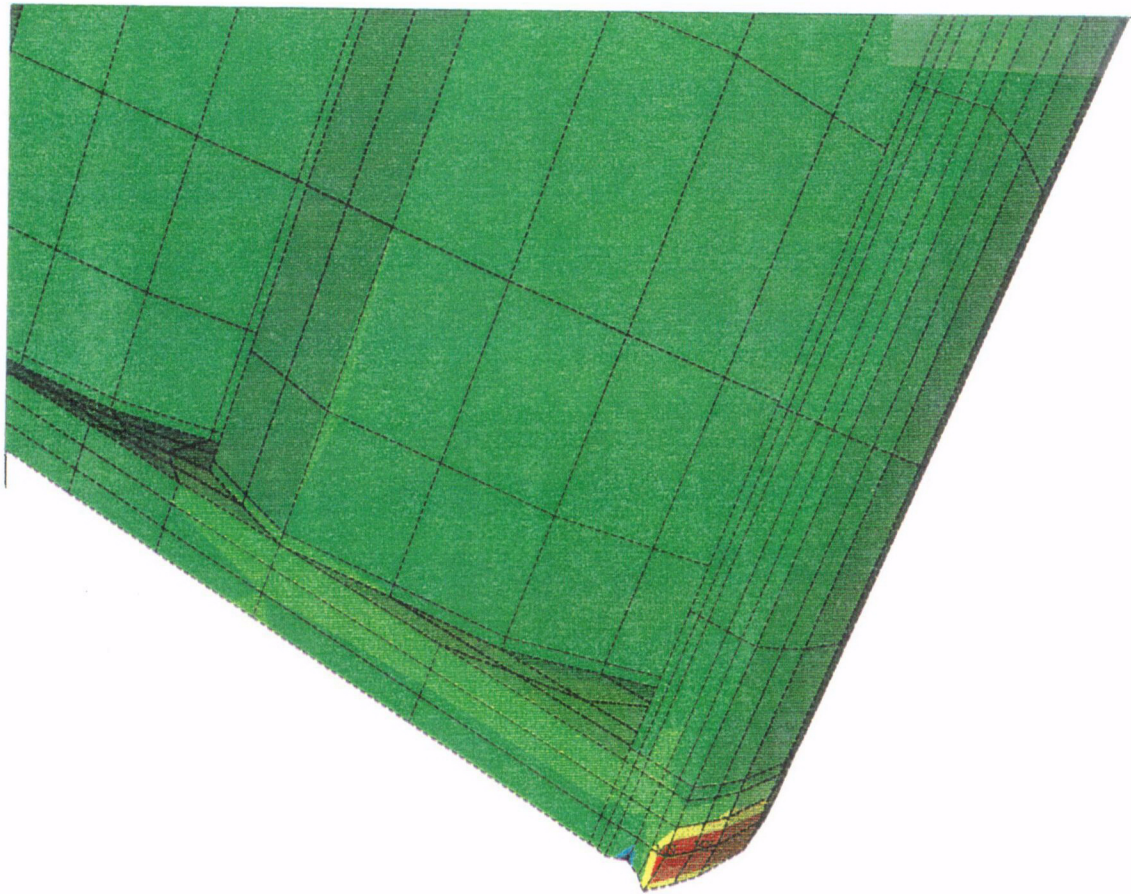
ANSYS 5.0 A
JAN 30 1996

NODAL SOLUTION
STEP=3
SUB =74
TIME=.683134
STRESS (Pa)
S1 (AVG)
MIN =-.387E+09
MAX =.504E+09

| | |
|--------------|-----------|
| Dark Blue | -.387E+09 |
| Blue | -.288E+09 |
| Light Blue | -.189E+09 |
| Green | -.899E+08 |
| Light Green | .911E+07 |
| Yellow-Green | .108E+09 |
| Yellow | .207E+09 |
| Orange | .306E+09 |
| Red | .405E+09 |
| Dark Red | .504E+09 |

Figure 6.4-18. Defense High-Level Waste Waste Package 2-m Drop Stress Contour

C 21



ANSYS 5.0 A
JAN 30 1996

NODAL SOLUTION
STEP=3
SUB =69
TIME=.679384
STRESS (Pa)
S1 (AVG)
MIN =-.376E+09
MAX =.323E+09

| | |
|--------------|-----------|
| Dark Blue | -.376E+09 |
| Blue | -.299E+09 |
| Light Blue | -.221E+09 |
| Green | -.143E+09 |
| Light Green | -.654E+08 |
| Yellow-Green | .123E+08 |
| Yellow | .901E+08 |
| Orange | .168E+09 |
| Red-Orange | .246E+09 |
| Red | .323E+09 |

Figure 6.4-19. Defense High-Level Waste Waste Package 2-m Drop Stress Contour (Without Skirt)

C 22

The maximum stresses in the pour canister were located on the bottom surface. The maximum principal stress magnitude on the pour canister is 32.0 MPa (see Figure 6.4-20). When the ultimate tensile strength of the pour canister (399 MPa) is compared to the first principal stress value (32.0 MPa), it can be concluded that no localized material failure occurs in the pour canister. The stresses in the pour canisters are extremely low and should be of little concern.

6.4.2.2 Waste Package Slap Down Accident Analysis

A corner drop can be separated into two individual drop events: initial impact and slap down. For impact angles near horizontal, the slap down phase dominates and the assembly response resembles the condition of a side drop (SNL 1992a). Initial impact is analyzed in Section 6.4.2.1. The hypothetical slap down accident condition analyzed here is that of a WP striking a flat, essentially unyielding horizontal surface. The model described and the analysis results given in this section are taken from the *Finite-Element Analysis of Slap Down of Defense High-Level Waste Package* (CRWMS M&O 1995j).

6.4.2.2.1 Description of Finite-Element Model for Slap Down

The ANSYS 5.0A finite-element analysis code is used for the structural analysis of the WP slap down accident scenario. The model used is a modification of the model used in the WP 2-m drop analysis. The initial orientation of the WP for the slap down model is shown in Figure 6.4-21. The modifications to the WP 2-m drop model are as follows:

- The unyielding surface has been raised so that it is in contact with the bottom edge of the WP.
- The initial angle of rotation of the WP has been increased from 26.66° from vertical to 35° from vertical. This moves the center of mass of the canister outside the initial contact footprint, ensuring that the WP will fall on its side rather than upright itself. Ideally, a value just above 26.66° should be used, but to get ANSYS to begin the solution, the moment created between the pivot and center of mass had to be large enough to initiate rotation. Angles less than 35° were tried, but they would not initiate rotation. Potential energy calculations indicate that the energy lost due to the use of 35° instead of 26.66° is less than 2 percent, leading to a difference in the stresses of less than 1 percent. Because this is likely to be smaller than the accuracy of the solution, this difference is neglected.
- The contact element area has been expanded to include a larger portion of the unyielding surface along nearly its entire length and the side of the outer barrier on which the WP will fall.
- The contact point between the WP and the unyielding surface is constrained from horizontal motion to create a pivot point about which the WP will rotate.

6.4.2.2.2 Barrier Response to Slap Down

A fixed axis rotation of the WP is followed by an impact on the flat surface. Since the WP is initially at rest, having an angle of 35° with respect to vertical, the potential energy is converted into kinetic energy before the impact. The kinetic energy is transformed into strain energy by elastic and plastic deformations on the WP after the impact. Deformation on the flat surface is negligible when compared to the WP response at the impact region because the stiffness value assigned to the flat surface is much larger than the WP stiffness.

A linearly varying deceleration distribution between the pivot and the opposite end of the WP leads to a loading distribution of similar characteristics. Thus, dynamic load, deformation, and stress magnitudes on the WP vary from one end to the other.

Figure 6.4-22 illustrates the first principal stress distribution on the WP. As can be seen in the figure, the maximum principal stress magnitude is 496 MPa and is located on the inner surface of the inner barrier near the attachment of the upper lid. The maximum tensile stress is less than the ultimate tensile strength of the inner barrier material (642 MPa), so it can be concluded that the slap down accident will not result in a breach of the inner barrier. The first principal stress distribution in the outer barrier is shown in Figure 6.4-23. As can be seen in the figure, the maximum tensile stress in the outer barrier is 270 MPa and it occurs in the lid. The maximum tensile stress is less than the ultimate tensile strength of the outer barrier material (358 MPa), so it can be concluded that the outer barrier will not fail.

The results of this analysis indicate that the WP will retain its structural integrity during a slap down accident since the stress magnitudes are below the ultimate tensile strength in the inner and outer barriers.

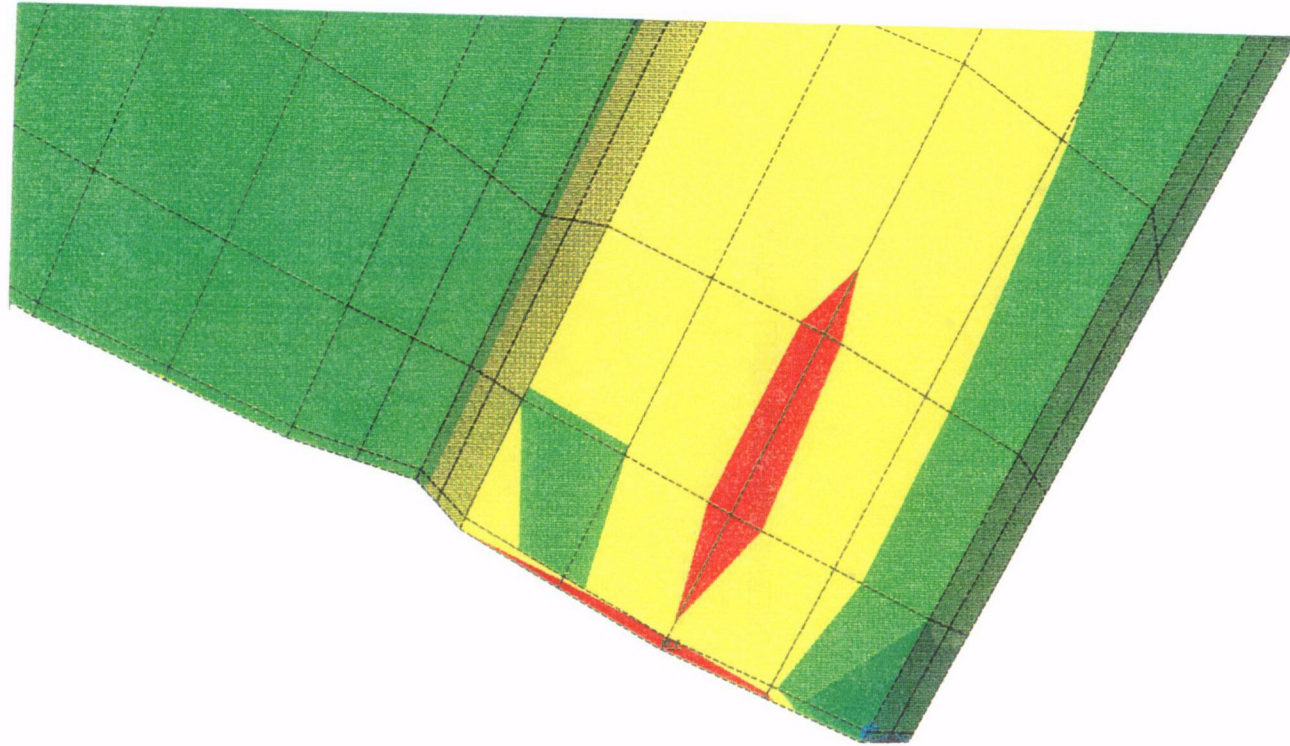
6.4.2.2.3 Pour Canister Response to Slap Down

As stated in Section 6.4.2.1.3, it must be verified that no material failure occurs in the pour canister. Stress results in the pour canisters from this analysis must be taken as approximate due to simplifications made during modeling.

The maximum principal stresses in the pour canisters are about 186 MPa and are located at the bottom edge of the canisters. The stresses in this region are artificially increased by the simplifications made to the model for the slap down accident, but they are still well below the ultimate tensile strength of the pour canister material (399 MPa). Therefore, the best estimate indicates that the pour canisters will not fail.

6.4.2.3 Analysis of Rock Fall onto Waste Package

The DHLW WP is designed to be drift emplaced, so it may be subjected to a tunnel collapse or an individual rock fall. The rock load could be the result of rock expansion and rock fall or by rock instability caused by a phase transformation in the rock. Because of the possibility for this accident, the WP is designed with a robust outer barrier.

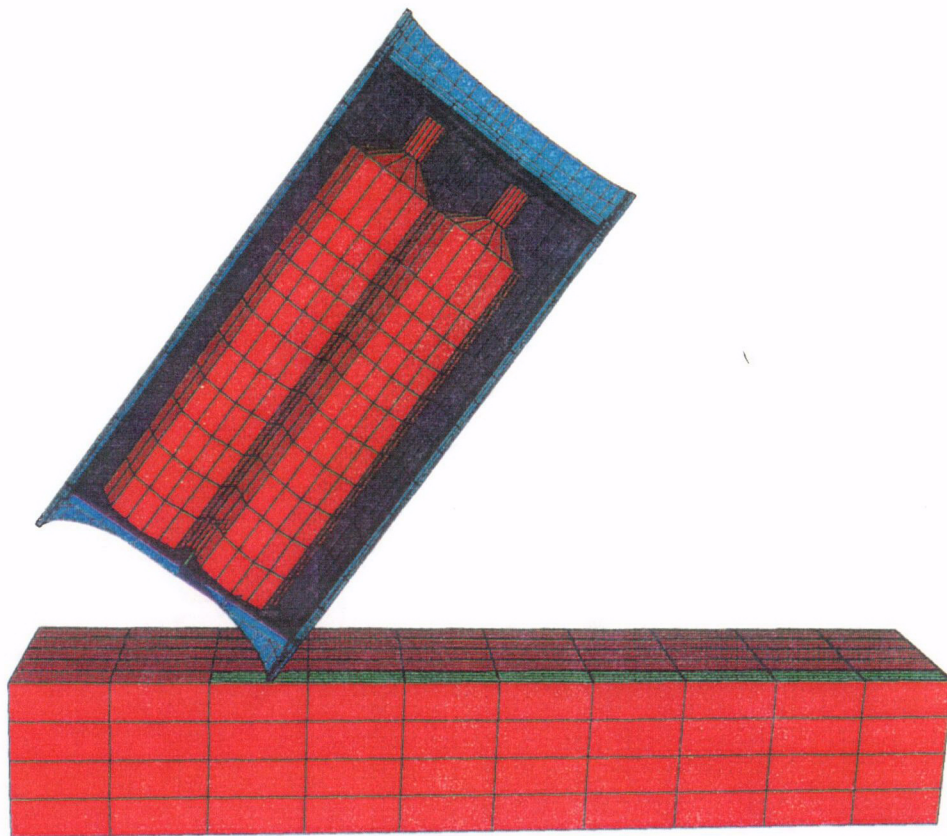


ANSYS 5.0 A
JAN 30 1996

NODAL SOLUTION
STEP=3
SUB =73
TIME=.682384
STRESS (Pa)
SI (AVG)
MIN =-.495E+08
MAX =.320E+08

| | |
|--------------|-----------|
| Dark Blue | -.495E+08 |
| Blue | -.404E+08 |
| Light Blue | -.314E+08 |
| Green | -.223E+08 |
| Light Green | -.133E+08 |
| Yellow-Green | -.420E+07 |
| Yellow | .486E+07 |
| Orange | .139E+08 |
| Red | .230E+08 |
| Dark Red | .320E+08 |

Figure 6.4-20. Defense High-Level Waste Waste Package 2-m Drop Stress Contour of Pour Canisters



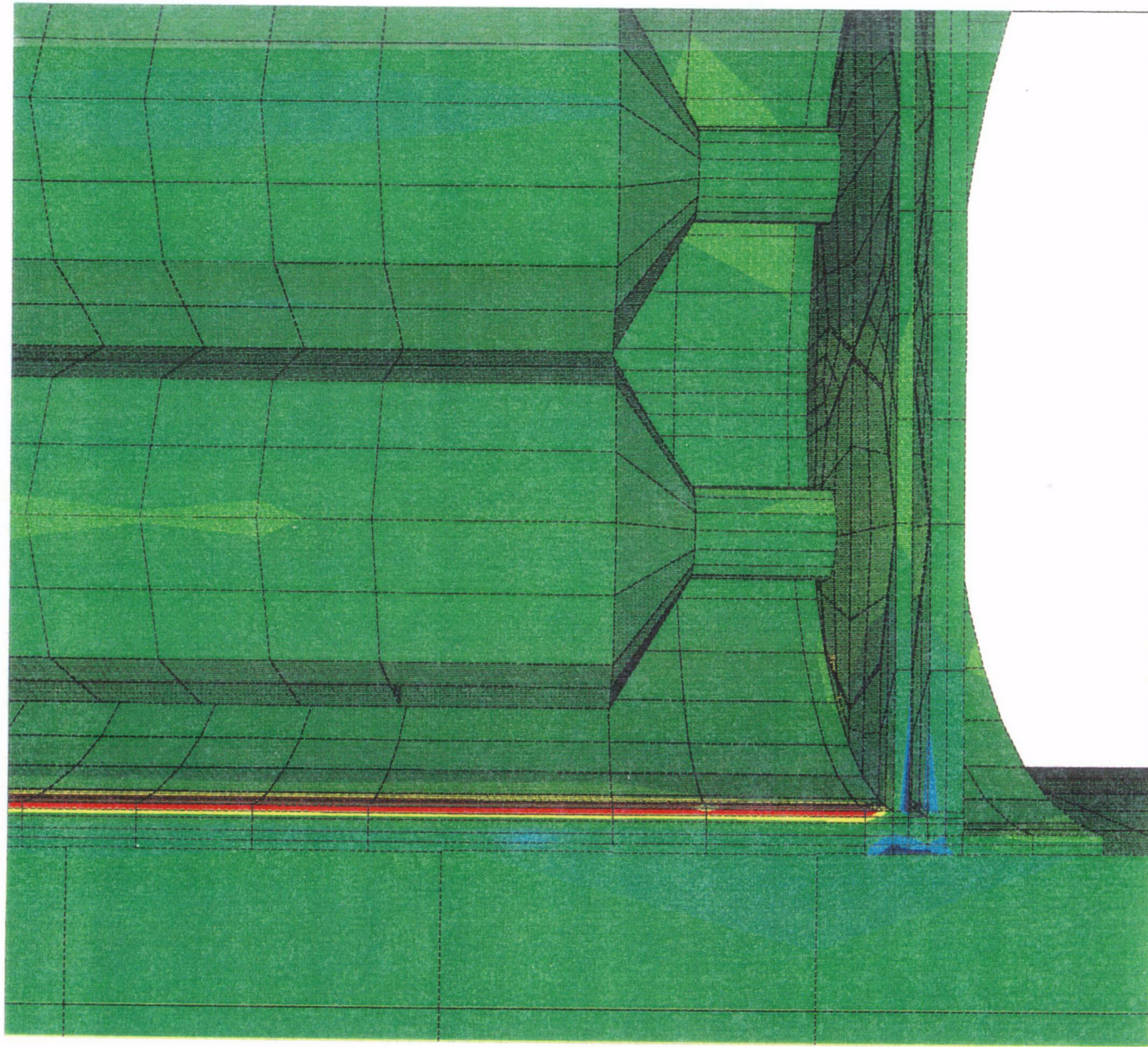
ANSYS 5.0 A
MAY 6 1995

ELEMENTS
TYPE NUM

XV = -.97203
YV = .197251
ZV = -.127477
*DIST=9.607
XF = .662475
YF = .823258
ZF = 2
A-ZS=-2.058
CONE=25
FACE HIDDEN

Figure 6.4-21. Defense High-Level Waste Waste Package Slap Down Model

C24



ANSYS 5.0 A
DEC 7 1995

NODAL SOLUTION
STEP=3
SUB =5
TIME=1.407
STRESS (Pa)
S1 (AVG)
MIN = -.407E+09
MAX = .496E+09

| | |
|--------------|-----------|
| Dark Blue | -.407E+09 |
| Blue | -.307E+09 |
| Light Blue | -.206E+09 |
| Green | -.106E+09 |
| Light Green | -.569E+07 |
| Yellow-Green | .947E+08 |
| Yellow | .195E+09 |
| Orange | .296E+09 |
| Red | .396E+09 |
| Dark Red | .496E+09 |

Figure 6.4-22. Defense High-Level Waste Waste Package Slap Down Stress Contour

C 25

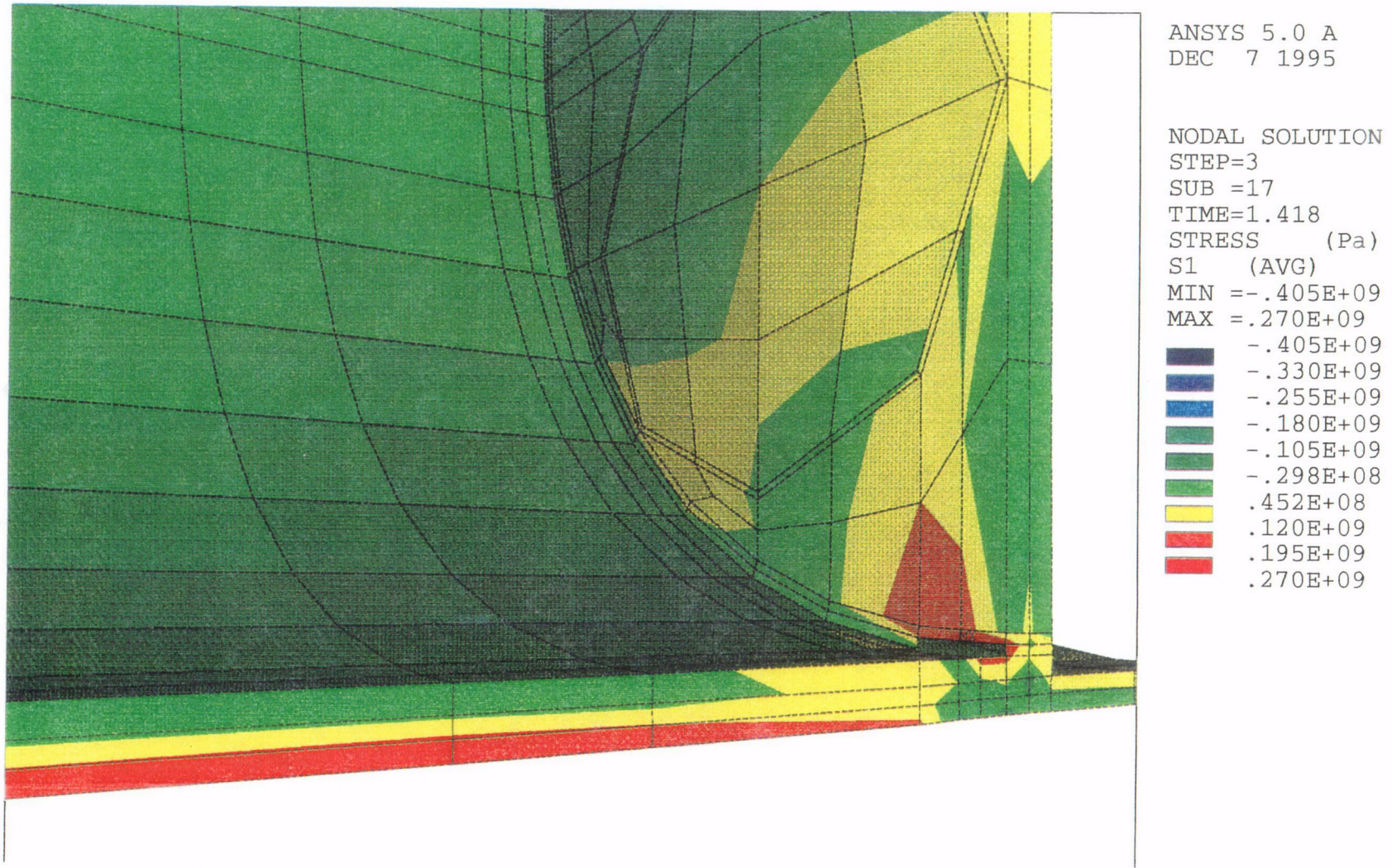


Figure 6.4-23. Defense High-Level Waste Waste Package Slap Down Stress Contour (Outer Barrier Only)

C 26

A rock fall could potentially occur in the starter tunnel or main drift while the WP is in transit, or in the emplacement drift after the WP has been emplaced. The main difference between these cases is the height from which the rock falls. The starter tunnel height is greater than either the main drift or emplacement drift height, so the starter tunnel rock fall is considered to be limiting.

The following conservative assumptions are made for the rock fall analysis in the starter tunnel:

- The WP is assumed to be sitting on the invert of the starter tunnel. It will actually be on a transporter, raising it some distance above the invert, thus reducing the fall height.
- The WP is assumed to be completely unprotected. It will actually be inside a shielded transporter, which may be expected to provide some impact protection.

The probability of a rock fall onto the WP in the starter tunnel is low due to the following reasons:

- The WP is not stored in the starter tunnel, but rather just passes through. Therefore, the WP spends very little time there, reducing the probability of an accident.
- Rock bolts and shotcrete are used to support the roof of the starter tunnel, decreasing the probability of a rock fall.

The model described and the analysis results given are taken from the *Finite-Element Analysis of Rock Fall onto Defense High-Level Waste Package* (CRWMS M&O 1995k).

6.4.2.3.1 Description of Finite-Element Model for Rock Fall Accident

The ANSYS 5.0A finite-element analysis code is used for the structural analysis of the rock fall accident scenarios. The model for this analysis is a modification of the model used in the WP 2-m drop analysis (see Figure 6.4-24). The modifications to the model are as follows:

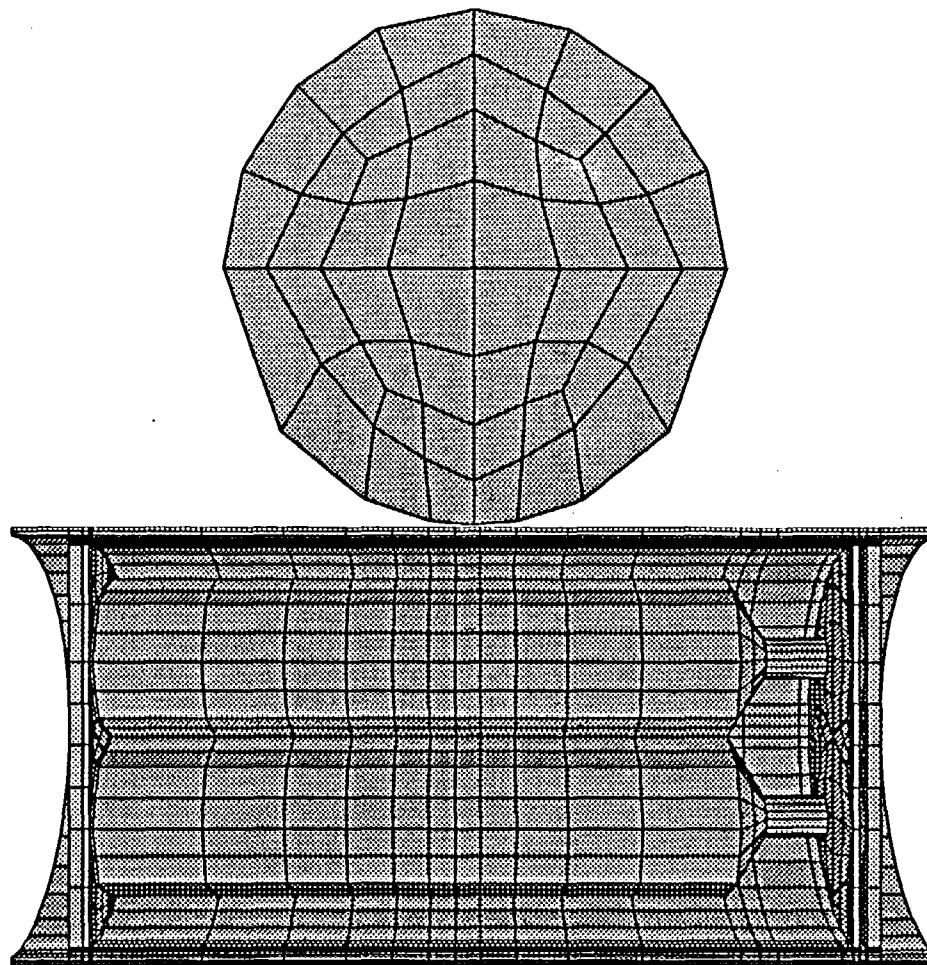
- The unyielding surface is removed. It is replaced by a half-symmetry model of a spherical rock located midway along the WP at a prescribed distance from the bottom of the WP and having the same plane of symmetry and symmetry constraints.
- The axis of the WP is perpendicular to the direction of gravity and radial constraints are placed at the ends of the WP outer barrier to simulate the emplacement supports. A longitudinal constraint is also placed on one node at one of the supports to add stability to the model since the friction between the supports and the WP is not present in the model to prevent rigid body motion.
- The contact element area has been changed to include the section midway along the top of the outer barrier and the bottom of the rock.

The geometry of the WP remains identical to the WP 2-m drop model except that element sizes have been adjusted so that there is a higher concentration of elements in areas of high stress, and a lower concentration of elements in areas of low stress. The only force acting on the rock is its own mass times gravity. Reaction forces exist in the WP at the support locations due to the mass of the WP and gravity.

ANSYS 5.0 A
AUG 7 1995

DISPLACEMENT
STEP=3
SUB =1
TIME=1.276
RSYS=0
DMX =7.984

*DSCA=1
XV =-1
YV =-.328E-11
ZV =.111E-15
*DIST=7.787
*XF =1.941
*YF =1.615
*ZF =-.642009
A-ZS=-90
CONE=25
FACE HIDDEN



ROCK FALL ONTO DHLW WP

Figure 6.4-24. Defense High-Level Waste Waste Package Rock Fall Model (Shown Just Prior to Impact)

6.4.2.3.2 Barrier Response to Rock Fall Accident

The WP barrier experiences localized plastic deformation in the area of impact of the rock. The maximum tensile stresses are seen on the inner surface of the inner barrier. The tensile stresses in the outer barrier are also high, but have been found to be lower than in the inner barrier. The stresses in the inner and outer barriers away from the area of rock impact have been found to be relatively low, so they are not studied in depth.

An initial rock fall scenario was run with the rock falling from the starter tunnel height onto the WP resting unprotected on the invert, the fall height being 7.996 m. The mass of the rock was assumed to be 6000 kg. This rock size proved to be more than can be taken by this WP because of its relatively thin outer barrier wall; the outer barrier wall of the DHLW WP is one half the thickness of the Multi-Purpose Canister WP outer barrier wall. The maximum principal stress output from the transient dynamic analysis is 641 MPa and is in the inner barrier (see Figure 6.4-25). This principal stress is nearly equal to the ultimate tensile strength of the inner barrier material (642 MPa). However, the maximum principal stress in the outer barrier is 436 MPa (see Figure 6.4-26), which is greater than the ultimate tensile strength of the outer barrier material (358 MPa). Using a correlation between kinetic energy and strain energy given in Section 6.5.2.3.1 (Equation 6.5-2), the rock size that will cause the maximum principal stress in the outer barrier to be equal to the ultimate tensile strength of the outer barrier material is determined to be about 4040 kg. With a rock density of 2297 kg/m³ (YMP 1994a), this corresponds to a rock with a diameter of approximately 1.49 m.

6.4.2.3.3 Pour Canister Response to Rock Fall Accident

As in the previous two accident scenarios, the requirement is that no material failure occurs in the pour canisters.

The pour containers do not experience any significant load for the configuration analyzed in the rock fall accident. It is possible that the WP will be rotated 45°, giving a potentially more critical orientation for the pour canisters. However, the current design does not provide for a means to hold the pour canisters in place inside the WP other than the canister guide at one end. Therefore, assuming that filler material is not used, the pour canisters will settle to the bottom of the WP away from the point of rock impact, leaving a large gap between the pour canister and the inner barrier. This gap is approximately 0.18 m. If it is assumed that the canister guide holds one end in place, the gap at mid span will be about half of this value, around 0.09 m. The maximum deflection for the fall of a 4040 kg rock is found by extrapolating from the available data. Analyses indicate that the maximum deflection for a 10,000 kg rock fall is 0.147 m, and the maximum deflection for a 6000 kg rock fall is 0.098 m. Extrapolating for a 4040 kg rock fall indicates that the maximum deflection in the WP barriers is 0.074 m. The approximated displacement value is less than the gap, 0.09 m, so the loads imparted onto the pour canisters under these conditions, if any, would be very small.

6.4.2.4 Conclusions Drawn from Structural Evaluation

The WP 2-m drop accident scenario results in a localized material failure around the region of impact in the outer barrier skirt. However, there is no material failure in any region of the inner or outer barrier other than in the outer barrier skirt. It is also concluded that the maximum principal stress in the pour canisters is below the material yield strength. Therefore, the overall WP response reveals that there will be no loss of radionuclide containment due to a WP drop from a height of 2 m.

The slap down accident scenario does not result in a breach in any part of the inner or outer barriers. The maximum principal stress in the pour canister is also below the ultimate tensile strength of the pour canister material. Therefore, the WP will not fail during a slap down accident.

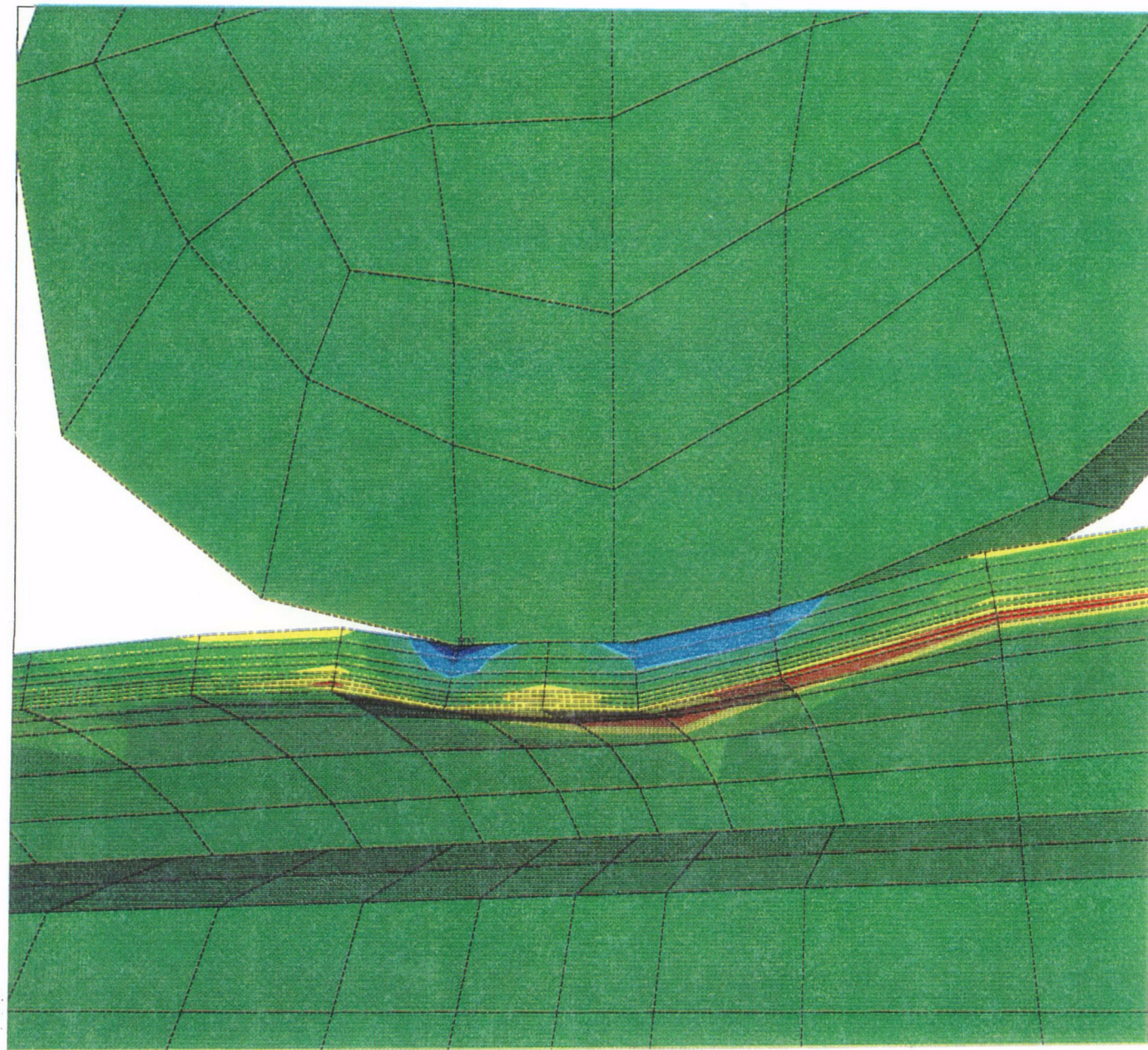
The rock fall accident analysis indicates that the maximum rock size that may fall onto the WP in the starter tunnel without breaching either the inner or outer barrier is 4040 kg, corresponding to a rock with a diameter of 1.49 m. This value could be increased, if it is found to be necessary, by increasing the thickness of one or both of the barriers. The maximum rock size which can fall onto the WP is still being determined. Based on preliminary data and analysis of likely rock falls, the pour canisters should not see any significant loads due to rock fall accidents and should be in no danger of breaching.

6.4.3 Criticality Analysis

The DHLW canister design analyzed is taken from the *Characteristics of Potential Repository Wastes* report (DOE 1992b). The Savannah River Site HLW glass and pour canister characteristics are assumed representative for that from all Department of Energy sites. The Savannah River Site glass composition is taken from the Characteristics Database (ORNL 1993b).

The DHLW form consists of four glass-filled pour canisters situated in a two-barrier disposal package. No internal basket structure for holding the pour canisters in place has been designed.

Pu-239 is the predominant long-lived fissile isotope in DHLW glass. U-235 is present only at natural levels (0.7 percent) in the uranium included in the glass makeup. Based on optimum moderation and reflection, the minimum critical concentration of Pu-239 in an aqueous solution is 7 gm/liter according to the *Nuclear Safety Guide*, (NRC 1978). The concentration of Pu-239 in the DHLW glass is nominally 0.35 g/liter and is not under optimum conditions. Calculations are provided below to demonstrate the degree of subcriticality of the DHLW glass disposal container.



ANSYS 5.0 A
AUG 7 1995

NODAL SOLUTION
STEP=3
SUB =9
TIME=1.283

S1 (Pa)
DMX =8.063
SMN =-.654E+09
SMX =.641E+09

| | |
|--------------|-----------|
| Dark Blue | -.654E+09 |
| Blue | -.510E+09 |
| Light Blue | -.366E+09 |
| Green | -.222E+09 |
| Light Green | -.783E+08 |
| Yellow-Green | .655E+08 |
| Yellow | .209E+09 |
| Orange | .353E+09 |
| Red-Orange | .497E+09 |
| Red | .641E+09 |

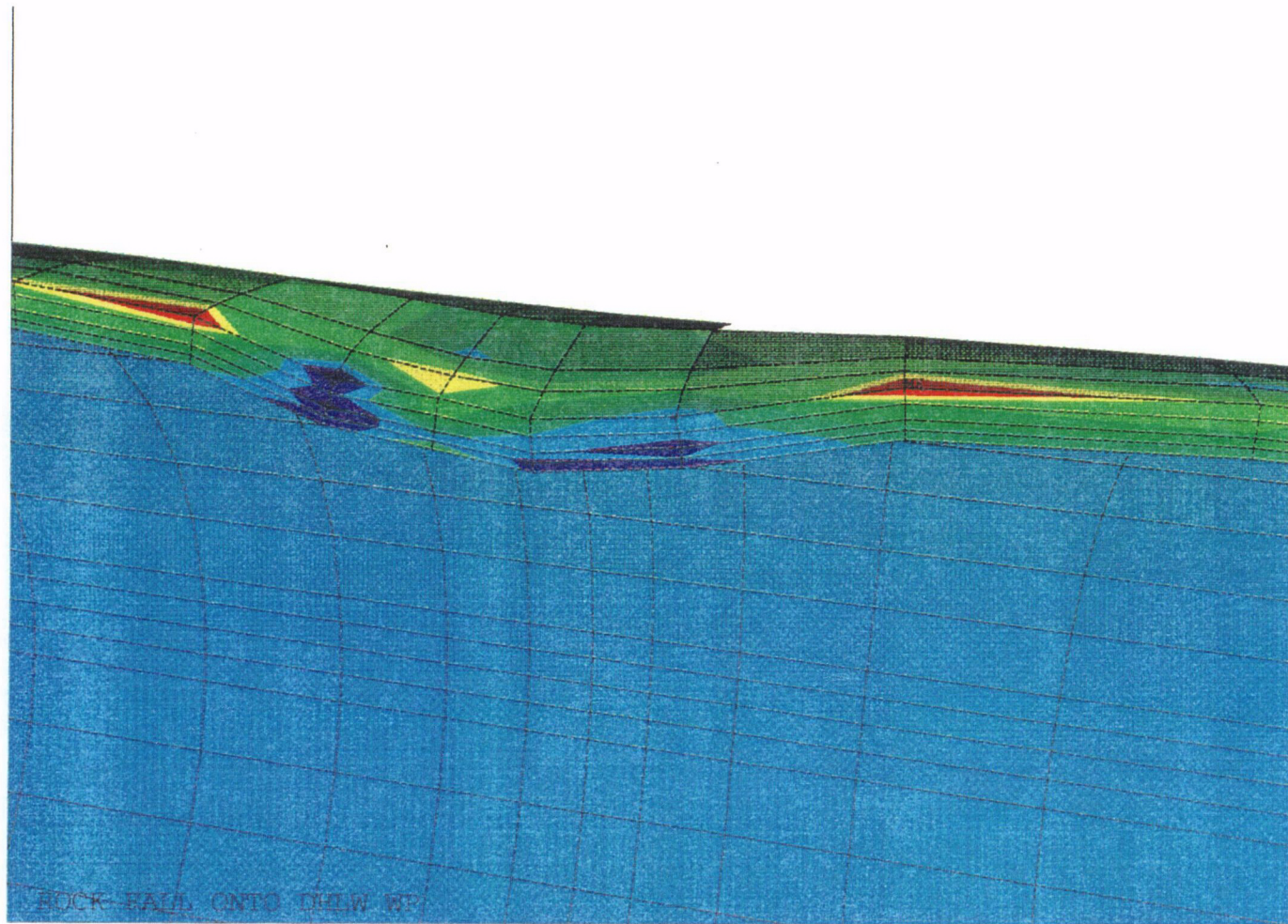
C27

Figure 6.4-25. Defense High-Level Waste Waste Package Stress Contour for Fall of 6000 kg Rock

B000000000-01717-5705-00027 REV 00

6.4-51

March 1996



ANSYS 5.0 A
AUG 7 1995

NODAL SOLUTION
STEP=3
SUB =27
TIME=1.295
S1 (Pa)
DMX =.091268
SMN =-.152E+09
SMX =.436E+09
-.152E+09
-.865E+08
-.212E+08
.441E+08
.109E+09
.175E+09
.240E+09
.305E+09
.371E+09
.436E+09

C28

Figure 6.4-26. Defense High-Level Waste Waste Package Stress Contour of Outer Barrier for Fall of 6000 kg Rock

6.4.3.1 Codes, Biases, and Isotopic Inventory Generation

The analysis method employed to ensure criticality control for disposal in the MGDS uses the MCNP computer program, Version 4.2, developed by Los Alamos National Laboratory (ORNL 1992). MCNP (Monte Carlo Neutron and Photon Transport) is a three-dimensional Monte Carlo particle transport program with a generalized geometry capability that allows the development of detailed, accurate models of the systems of interest. MCNP is used to calculate the effective multiplication factors (k_{eff}) for the various designs and configuration of interest. MCNP has been thoroughly benchmarked against criticality experiments and other criticality computer programs. MCNP Version 4.2, has been approved (verified and validated) for quality assurance criticality work according to the Civilian Radioactive Waste Management System Management and Operating Contractor Quality Administrative Procedures.

An associated continuous energy cross-section set based on the Evaluated Nuclear Database Files, ENDF/B-V, is used by MCNP. This library provides much more detail than multi-group, cross-section sets. The continuous energy cross-section library is not spectrum weighted (biased) and, therefore, is not limited in its applicability.

There are biases and uncertainties associated with a criticality calculation. How these biases and uncertainties are treated in criticality calculations is covered in the American National Standard on *Criticality Safety Criteria for the Handling, Storage, and Transportation of Light Water Reactor (LWR) Fuel Outside Reactors* (ANSI/ANS-8.17). The fresh fuel bias and uncertainty for MCNP is approximately 0.015 (CRWMS M&O 1994i). The preliminary SNF bias and uncertainty is approximately 0.06 (CRWMS M&O 1994i). The SNF bias and uncertainty is higher because of additional factors such as isotopics and axial effects. The SNF bias and uncertainty is applied to the DHLW glass for this conceptual work. The Characteristics Database (ORNL 1993b) was used to provide physical and isotopic composition information (high-level waste database) for the DHLW glass. The Characteristics Database has been qualified for quality assurance work under the Management and Operating Contractor program.

6.4.3.2 Defense High-Level Waste Modeling Assumptions

The canister was modeled as essentially filled up to the neck with a height of 2,742.6 mm. This translates into approximately 22 percent more material in the canisters than indicated in the reference (ORNL 1993b), since the canister is actually only filled 80 percent by volume when cooled. A 2x2 array at a center-to-center spacing of 640 mm (30.4 mm edge-to-edge) of these canisters is then reflected on the X and Y surfaces, creating an infinite array in two dimensions. The spacing of the canisters represents a reasonable representation of that in a WP. The array is modeled from the centerline up (reflected on the centerline) axially. A water reflector (air for "normal" case) 150 mm thick was placed above the canisters.

For SNF, the isotopes were reviewed and the isotope importance was determined by generating macroscopic neutron absorption cross-sections in both the thermal and fast/resonance ranges for each of the isotopes being examined. Based on the results of the long-term isotope importance evaluations, a preliminary list of "Principal Isotopes" for long-term criticality control was determined (CRWMS M&O 1994i). The preliminary 31 principal isotopes are shown in Table 6.4-5.

Table 6.4-5. Preliminary List of Principal Long-Term Burnup Credit Isotopes

| | | | | |
|--------|--------|--------|---------|--------|
| O-16 | Mo-95 | Tc-99 | Ru-101 | Rh-103 |
| Ag-109 | Nd-143 | Nd-145 | Sm-147 | Sm-149 |
| Sm-150 | Sm-151 | Sm-152 | Eu-151 | Eu-153 |
| Gd-155 | U-233 | U-234 | U-235 | U-236 |
| U-238 | Np-237 | Pu-238 | Pu-239 | Pu-240 |
| Pu-241 | Pu-242 | Am-241 | Am-242m | Am-243 |
| Cm-245 | - | - | - | - |

Pu-239 is the predominant long-lived fissile isotope in DHLW glass. U-235 is present only at natural levels (0.7 percent) in uranium included in the glass makeup. An additional limit on the number of isotopes in the model was their availability in the MCNP cross-section libraries. Nine of the identified principal isotopes are not available in the standard MCNP cross-section sets. The unavailable isotopes are Mo-95, Tc-99, Ru-101, Nd-143, Nd-145, Sm-147, Sm-150, Sm-151, and Sm-152. The 22 available isotopes are used in the MCNP models. The nine unavailable isotopes are absorbers, and, therefore, not accounting for them is conservative.

The "normal" condition in the repository, both within and surrounding the WP, is a dry environment. The "accident" condition considers the repository and WP as being flooded with water.

6.4.3.3 Standard Evaluation

Five infinite array cases have been run for DHLW glass. The k_{eff} ($\pm 2\sigma$ where σ is the relative error) values calculated are as follow (CRWMS M&O 1996g).

| | |
|---|---------------------|
| DHLW glass, infinite array, Flooded | 0.0073 \pm 0.0003 |
| DHLW glass, infinite array, Dry | 0.0090 \pm 0.0004 |
| DHLW glass, infinite array, Dry, fissile x 100 | 0.2208 \pm 0.0023 |
| DHLW glass, infinite array, Flooded, no absorbers | 0.0742 \pm 0.0020 |
| DHLW glass, infinite array, Dry, no absorbers | 0.1169 \pm 0.0038 |

The k_{eff} results reported are the simple combined average of the track length, absorption, and collision estimates as listed in the last generation print of the MCNP output. The first two cases have the explicit glass description provided in the Characteristics Database. The third case has the concentrations of the fissile isotopes U-235 and Pu-239 multiplied by 100 to demonstrate that even extreme variation of the composition will not be a criticality concern. The fourth and fifth cases are composed of the actinides in silicon dioxide alone, to demonstrate the effect of eliminating absorbers, and, effectively, increase moderation.

The DHLW glass is not of criticality concern in the intact form. No supplemental absorbers are required for the WP. No significant change in reactivity will occur with time.

The WP does contain multiple critical masses of Pu-239 (optimum conditions) if it could be separated and concentrated. A probabilistic analysis is required to determine the credibility of separation/concentration scenarios. A deterministic criticality analysis could then be performed on credible geometries and concentrations.

6.4.4 Shielding Analysis

For the MGDS, the DHLW disposal container, described in Section 6.4, provides some direct shielding function. The disposal containers are designed primarily for containment with materials that also provide shielding. No materials whose only purpose is shielding are located in the WP disposal containers.

A basic property of the WP to be disposed of in the MGDS is high radioactivity. Because limiting the dose to workers is a major radiation protection goal (as low as reasonably achievable), methods for limiting the dose rate to workers have been devised. The two methods are shielding and remote handling. An emplacement transport shield is used for shielding purposes.

The emplacement transport shield strategy uses the incidental shielding of the WP and a shield carried on the WP emplacement transporter to reduce the dose rate. The transport shield can have optimized shield materials, which are not allowed around, or in, the emplaced WP. This strategy relies on remote handling operations.

The target dose rate for the transport shield concept has been set to 10 mrem/hr at 2 m. This dose rate is the same as that specified by the transportation regulation from 10 CFR 71.

6.4.4.1 Codes, Isotopic Inventory, and Source Terms

Shielding analysis has been performed using the ANISNBW computer program Version 4.5HP on Hewlett Packard 9000 730/735 workstations. ANISNBW is a B&W Nuclear Technologies version of the one-dimensional discrete ordinates transport code ANISN-W program developed at Oak Ridge National Laboratory (BWNT 1993a).

Multi-group neutron and photon cross-section data was provided by the BUGLE-80 (ORNL 1980) library.

The Characteristics Database (High-Level Waste Database) was used to provide physical and isotopic composition information for the DHLW glass. The Characteristics Database has been qualified for quality assurance work under the Management and Operating Contractor program. Radionuclide inventories and multiple energy group photon and neutron source terms have been calculated with ORIGEN2 (BWNT 1991) using the material isotopic compositions from Characteristics Database.

6.4.4.2 Defense High-Level Waste Modeling Assumptions

The DHLW WP consists of four glass-filled pour canisters situated in a two-barrier disposal package. The inner barrier is 2 cm (0.79 in.) thick and is composed of 825 Alloy. The outer barrier is 5 cm (1.97 in.) thick and is composed of C71500 Alloy.

The DHLW canister design analyzed is taken from the *Characteristics of Potential Repository Wastes* report (DOE 1992b). The Savannah River Site HLW glass and pour canister characteristics are assumed representative for that from all Department of Energy sites. The Savannah River Site glass composition is taken from the Characteristics Database (ORNL 1993b) and are representative for the time of production. Previous analyses have been performed for compositions representative for 20 years of decay time because it was thought that the glass would not be shipped to the repository for at least that time. Since this is not a documented requirement, the current analysis was performed for glass with no decay, thus providing a bounding analysis.

The waste canisters and internal area of the WP are homogenized in the shielding model. Since the calculations are one-dimensional, the WPs are modeled as infinitely long and doses are conservatively overestimated. No credit was taken for the individual canister wall material.

6.4.4.3 Disposal Container Outer Barrier

The dose rate at 2 m for DHLW WPs with a 5 cm (1.97 in.) outer barrier thickness is 17.2 rem/hr (BWNT 1995a). This is approximately a factor of 5 higher than the dose rate from the 125 ton Multi-Purpose Canister waste package, which is about the same outside diameter. Figure 6.4-27 illustrates the curve for total dose rates at various distances from the outer barrier. The total dose rate is due primarily to gamma radiation with only 0.0024 percent being contributed from neutrons.

Previously, calculations were performed for an earlier WP design with a 0.95 cm (0.37 in.) thick inner barrier and a 10 cm (3.94 in.) thick outer barrier (CRWMS M&O 1994n). These calculations were based on a 20-year decayed glass composition and had a dose rate of 0.13 rem/hr at 2 m from the WP surface. Cobalt-60, with a half-life of 5.27 years, and cesium-137, with a half-life of 30.2 years, are major contributors to the dose outside the package. These isotopes have a significant reduction in activity over the 20-year decay period. This decay, along with nearly 4 cm of additional barrier material, are the major causes of the great difference in dose rates between the two calculations described here. Because of the sensitivity to decay time, calculations will be performed in the future to demonstrate the dose rate as a function of time.

6.4.4.4 Emplacement Transport Shield

The emplacement transport shield strategy places the necessary shielding on the emplacement transporter. This transporter would have sufficient shielding around it to limit the dose rate to an individual to the target levels. Once emplaced underground, the WP would not have sufficient intrinsic shielding to allow unprotected human access to the emplacement drifts.

The conceptual design of the WP emplacement transport shield is as follows: a two-layer approach to shielding was used, with a layer of gamma shielding material followed by a minimal layer of

neutron shielding material. The gamma shield, consisting of a dense material, should be close to the package to reduce the shield weight. The relative contribution of neutrons to the dose rate from the DHLW glass is low and the contribution from secondary gammas in the neutron shield are even less significant. Because of the low contribution of the secondary gammas, a secondary gamma shield as used for SNF waste forms is not required. These shield material layers can be arranged in various configurations (e.g., cylinder, rectangle, and half-cylinder).

The materials analyzed for the transport shield model were 5 percent boron-polyethylene for the neutron shield and lead for the gamma shield. These materials were chosen because they are commonly used in the nuclear industry and their use is well proven as shielding materials. The shielding layers are encased in a thin (0.5 cm) outer layer of stainless steel 316L to provide minimal structural support for the shields and containment for the lead. A 30 cm air gap between the WP and the transport shield for handling equipment and additional structural support was also included.

Calculations were performed with the boron-polyethylene thickness fixed at 0.5 cm and the lead thickness was varied to achieve the target dose rate. The lead transport shield thickness required to meet the target dose rate of 10 mrem/hr at 2 m from the shield surface is 9 cm (3.54 in.) (BWNT 1995b). The transport shield weight is approximately 60 tonnes (66 tons).

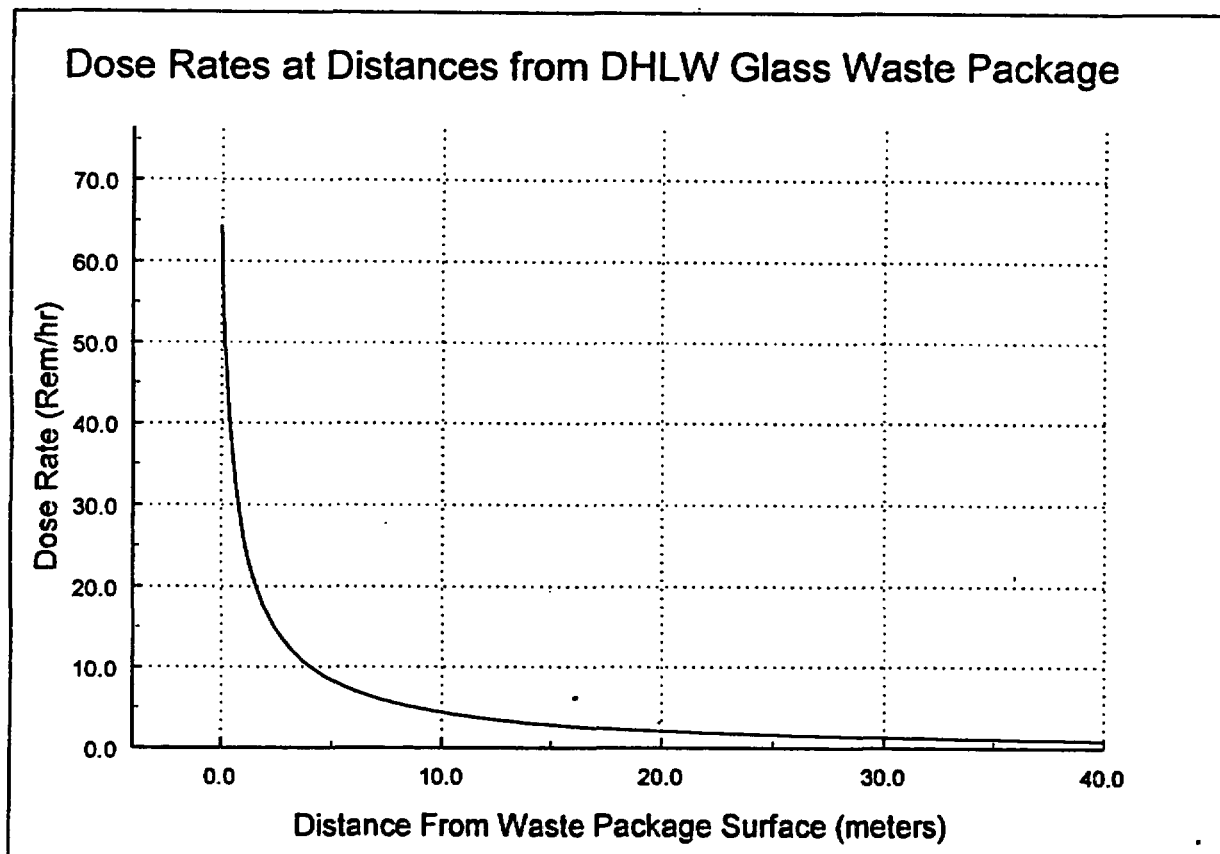


Figure 6.4-27. Dose Rates Away from 5 cm Outer Barrier, Defense High-Level Waste Glass

INTENTIONALLY LEFT BLANK

6.5 CANISTERED FUEL DISPOSAL CONTAINER CONCEPT

The current repository system is based upon the implementation of a CF container as the prime SNF waste handling concept throughout the waste management system as presented in Volume I of the MGDS ACD report. The CF container is a concept which includes dual-purpose or multi-purpose types of containers. To assess the performance of the CF container in a repository environment, the Multi-Purpose Canister (MPC) conceptual design (CRWMS M&O 1994k) was selected to be the basis for evaluation of the CF container concepts. Thus, the use of the term MPC and CF for the purpose of this section are interchangeable. The results presented in this section are specific to the MPC conceptual design and will be different if an alternate MPC design or CF design, such as a dual-purpose container, is selected for use in the MGDS. The analysis presented in this section is representative of the design and operational considerations that the MGDS must examine for any type of CF container that may be selected.

A CF container such as the conceptual MPC (CRWMS M&O 1994k) could be designed to transport SNF from individual nuclear reactor sites to the repository. The conceptual MPC is intended to handle intact SNF from both PWR and BWR reactor types. Thus, with the operational concept presented in Volume I of this report, the majority of the HLW to be emplaced in the repository will be handled with an MPC type of disposal container. The MPC (or any other CF container) may be loaded and sealed at the reactor site and then placed inside a transportation cask for shipment to the repository. The transportation cask, which provides shielding and containment, meets the NRC transportation requirements and can be reused many times.

Upon arrival at the repository, the MPC will be removed from the transportation cask and placed within the multibarrier disposal container. The MPC (or any other type of CF container) will remain sealed unless it is necessary to add filler material, in which case the MPC would be cut open, filler added, and then resealed (note that use of filler material is a design option, and is not included in the nominal design). The MPC conceptual design lifting feature consists of six threaded blind holes in the outer lid; this feature is adequate to lift the complete MPC (including filler material). This same feature would be used to lift the MPC top should the top be cut off for addition of filler material.

The conceptual MPC designs are sized to contain the largest possible number of SNF assemblies, subject to several constraints. Significant constraints include reactor facility crane capacity, repository thermal loading design, SNF cladding temperature limitations for emplacement in the repository, and criticality concerns including burnup credit. The preliminary designs have resulted in small and large MPC design configurations, corresponding primarily to reactor facility crane limitations. Existing crane limitations are nominally 75 ton and 125 ton; the crane hook weight includes the loaded and flooded MPC, transportation cask weight less impact limiters, and lifting yoke. The small MPC design can accommodate 12 PWR SNF assemblies or 24 BWR SNF assemblies. The large MPC design can accommodate 21 PWR SNF assemblies or 40 BWR SNF assemblies.

Design of the MGDS disposal container for a CF container concept is based on the current MPC conceptual design (CRWMS M&O 1994k). Each MPC disposal container design must be specifically tailored to accommodate the various MPCs or other types of CF containers which the industry may produce. The MGDS CF Disposal Container concept is shown on Figure 6.1-1. The

12 PWR/24 BWR MPC disposal container differs only in size from the 21 PWR/40 BWR MPC disposal container.

6.5.1 Thermal Analysis

To capture a majority of the SNF, the WP must be designed and evaluated to accommodate the bounding or limiting case of fresh SNF, which has a thermal output much higher than average. Thus, a design basis SNF can be determined that can be considered the hottest SNF that could be loaded and emplaced in that WP. The detailed Engineered Barrier System/WP evaluation would then represent the hottest WP in the repository at a given thermal loading with average SNF. While all of the WPs (hot and cold) will collectively influence repository temperatures (average SNF characteristics), every WP must meet thermal goals (design basis SNF characteristics). The methodology and selection of design basis SNF for WP design is covered in Section 5.

Given that higher capacity WPs are more likely to exceed thermal goals than smaller ones in the same repository thermal environment, the choice of a design basis SNF is important because it could limit the number of assemblies that can be loaded without exceeding thermal goals for disposal. The limiting thermal goal for large WPs, such as the 21 PWR MPC, is a temperature of no more than 350°C at the SNF cladding. Design bases have been established for WP design (based on the total potential repository inventory) and for MPC procurement (CRWMS M&O 1994j). There are also obsolete design bases that may be used for historical comparisons. Several different design basis SNF types have been used in the following thermal analyses to demonstrate compliance with requirements and to allow comparison with previous evaluations. Table 6.5-1 summarizes the SNF types used. Figure 6.2-4 compared the time-dependent heat decay for each of the SNF types in Table 6.5-1.

Table 6.5-1. Multi-Purpose Canister Thermal Analysis Design Basis

| Organization | SNF Type | SNF Age | SNF Burnup | Initial Heat |
|--------------|----------|----------|------------|--------------|
| MGDS | PWR | 10 years | 48 GWd/MTU | 850 watts |
| MGDS | BWR | 10 years | 49 GWd/MTU | 409 watts |
| MPC | PWR | 20 years | 40 GWd/MTU | 547 watts |
| MPC | BWR | 20 years | 40 GWd/MTU | 265 watts |
| MPC Historic | PWR | 10 years | 40 GWd/MTU | 718 watts |

Design basis SNF will impact the timing of peak temperatures, as well as the magnitude of the peak. The repository host rock temperatures will peak between 10 to 500 years, depending on the thermal loading but will be largely independent of the individual WP design. The WP itself will experience its peak temperature before the rock temperature peaks. The WP peak temperature and its timing will depend on the design basis SNF and the basket/container design. In previous analyses of the large WP (CRWMS M&O 1994i), higher-conductivity SNF baskets were seen to lower and delay the peak temperatures experienced. The choice of the design basis SNF is of key importance. Younger SNF types produce high peak temperatures within the first year, then drop off quickly.

Older SNF (at the same initial areal power density, but not areal mass loading) produces lower and later peaks with more stable and higher long-term temperatures. In the following evaluations, more than one design basis SNF type has been used to illustrate the impacts of the SNF types.

A second key factor in evaluating internal WP temperatures is the determination of peak cladding temperatures. Three methods are available to estimate cladding temperatures inside a storage, transportation, or disposal container. The first and most involved method is to explicitly model the canister and every fuel rod in every assembly within it. This model would directly consider the internal fill gas convection and conduction and a matrix of radiation view factors among the rods. The second method employs the Wooton-Epstein correlation (Wooton-Epstein 1963) to estimate the peak cladding temperature based on the highest steady state temperature in the SNF basket structure. The Wooton-Epstein correlation has historically been the primary tool of transportation/storage cask vendors, as it simplifies the analysis and has been previously accepted by the NRC. The third method of estimating peak cladding temperatures is to prepare a finite-element or finite-difference model of the SNF assembly volume as a smeared solid with internal volumetric heat generation as part of the entire disposal container model. An effective conductivity for the assembly volume can be defined that will approximate the temperature drop across a PWR assembly.

The key to accurate SNF cladding temperature predictions using the effective conductivity method lies in determining the proper conductivity to assume in the assembly volume. Section 6.2.1.2 describes the development of an ANSYS SNF assembly model for the determination of effective conductivities. The temperature-dependent conductivities reported in that section were applied to the homogeneous assembly volumes in the following MPC thermal evaluations. The peak assembly temperatures using the effective conductivity provide a "best-estimate" for peak clad temperatures, which is compared for each case to "conservative" estimations of cladding temperatures using the Wooton-Epstein correlation.

The use of filler material could also affect the determination of WP internal temperatures. The thermal effects of adding filler material to the WP have previously been investigated (CRWMS M&O 1994i). While the addition of material to fill the void space within the WP may be beneficial to criticality control and containment (by inhibiting corrosion and radionuclide release), the thermal effects depend entirely on the type and conductivity of the material used. Iron shot was found not to have a significant effect on peak temperatures; however, other less conductive materials could seriously affect large MPCs where internal temperatures can approach maximum thermal goals.

6.5.1.1 21 PWR Multi-Purpose Canister

A two-dimensional finite-element thermal model of the large 21 PWR burnup credit MPC conceptual design was developed from design drawings supplied in the *MPC Conceptual Design Report* (CRWMS M&O 1994k). Model detail included the separate layers of the basket tube design. Intimate contact was assumed between the layers of stainless steel and aluminum, and also between the tube guides and inner shell. The MPC fill gas was assumed to be helium. The multibarrier disposal container for the 21 PWR MPC, detailed in Appendix B, was also modeled. The analysis is detailed in a supporting design analysis (CRWMS M&O 1995e).

The finite-element code ANSYS was used to model the two-dimensional cross-section of the MPC/WP. Time and position-dependent temperatures for the WP surface were exported from the emplacement model, described in Section 6.2.1.1.1, and applied as time-varying boundary conditions. The other time-varying conditions used in the model were the design basis SNF decay heat outputs applied as volumetric heat generations to the assembly areas of the model and use smeared material properties. The effective conductivity for the assembly area was developed as described in Section 6.2.1.2 and it represents the resistance due to heat transfer in a 15x15 PWR assembly. The heat loads for the assembly areas were interpolated from the Oak Ridge National Laboratory database of SNF characteristics for each of the assumed design basis SNF types. The heat load will decrease logarithmically with time as the fission products decay. The heat loads were applied volumetrically and were multiplied by an axial heat peaking factor to approximate the axial center of the WP with a two-dimensional model. An SNF assembly is much hotter at the mid-length than at the ends, and it is conservative to assume the two-dimensional WP model represents the hottest cross-section of the MPC/WP.

The boundary conditions and heat loads were applied and solved out to 1,000 years for each of the five thermal loading scenarios described in Section 6.2.1.1.1 and for each of the PWR design basis SNF types described in Table 6.5-1. Table 6.5-2 summarizes the peak temperatures and the time of occurrence for each of the cases analyzed. The thermal loading scenarios indicated in Table 6.5-2 are defined in Table 6.2-1, and the design basis SNF descriptions are provided in Table 6.5-1. Both "conservative" estimates of peak cladding temperatures using the Wooton-Epstein correlation and "best estimate" predictions using the effective conductivity method are presented in the table. Peak cladding temperatures using effective conductivity are calculated directly in the ANSYS program. Wooton-Epstein calculations for each time step in the ANSYS analysis were also performed for comparison.

The historic MPC PWR design basis of 10-years-old, 40 GWd/MTU was evaluated so that the current solution results can be compared to the MPC with disposal container analysis reported in the *Initial Summary Report for Repository/Waste Package Advanced Conceptual Design* (CRWMS M&O 1994i) and the *MPC Conceptual Design Report* (CRWMS M&O 1994k). The thermal history for this SNF type at 83 MTU/acre is presented in Figure 6.5-1. Figure 6.5-2 displays the temperature profile across the MPC basket and disposal container for the time of peak internal temperatures (one year). The peak conservative estimate for SNF cladding temperature was 310°C, which can be compared to the previously reported estimate of 337°C (CRWMS M&O 1994i). Both were calculated with the Wooton-Epstein correlation. In that previous analysis, the WP surface temperature was predicted to be 205°C, which resulted in higher cladding predictions for that analysis. There are two reasons for environment temperatures lower than 205°C in the current evaluation. First, and primarily, the WP spacing has been increased from 16 m to 19.5 m to accommodate a 22.5-m drift spacing. A greater WP spacing results in lower near-field temperatures, as described in Section 6.2.1.1.4. Second, the previous analysis used a two-dimensional repository emplacement thermal model, which, compared to a three-dimensional model, conservatively over-predicted near-field temperatures. In general, as more information becomes available and modeling techniques are improved, conservatism will be replaced with greater accuracy in these evaluations.

Table 6.5-2. 21 PWR Multi-Purpose Canister Thermal Analysis Results

| Thermal Load | Design Basis SNF | Peak Cladding | | | | Peak Basket | | MPC shell | | WP Surface | |
|--------------|------------------|-----------------------|-----|---------------|-----|-------------|-----|-----------|-----|------------|-----|
| | | Conservative Estimate | | Best Estimate | | °C | yrs | °C | yrs | °C | yrs |
| | | °C | yrs | °C | yrs | | | | | | |
| High #1 | MGDS | 338 | 0.9 | 318 | 1 | 301 | 2 | 214 | 30 | 188 | 50 |
| | MPC | 287 | 7 | 273 | 8 | 261 | 8 | 207 | 30 | 188 | 50 |
| High #2 | MGDS | 336 | 0.6 | 316 | 0.7 | 298 | 0.9 | 200 | 10 | 165 | 40 |
| | MPC | 281 | 5 | 265 | 6 | 253 | 7 | 189 | 20 | 165 | 40 |
| | Historic | 310 | 0.9 | 291 | 1 | 276 | 2 | 194 | 10 | 165 | 40 |
| Low #1 | MGDS | 333 | 0.3 | 313 | 0.4 | 294 | 0.4 | 181 | 2 | 117 | 8 |
| | MPC | 271 | 1 | 254 | 1 | 240 | 2 | 162 | 4 | 117 | 8 |
| Low #2 | MGDS | 334 | 0.5 | 314 | 0.6 | 296 | 0.7 | 187 | 3 | 131 | 8 |
| | MPC | 276 | 2 | 259 | 2 | 246 | 2 | 171 | 6 | 131 | 8 |
| Low #3 | MGDS | 337 | 0.8 | 318 | 0.9 | 300 | 1 | 197 | 5 | 146 | 10 |
| | MPC | 282 | 3 | 266 | 3 | 253 | 4 | 183 | 8 | 146 | 10 |

Figures 6.5-3 and 6.5-4 display the thermal history of the 21 PWR MPC with disposal container at 83 MTU/acre (20.5 kgU/m²) for the MGDS design basis SNF and the MPC design basis SNF, respectively. The highest temperatures occur for the MGDS design basis SNF owing to its relatively young age of 10 years. The conservative estimate of peak cladding temperature for this case was 336°C, which is less than the thermal design goal (limit) of 350°C. Peak temperatures for the MPC design basis SNF were 55°C less than that for the MGDS design basis.

Peak temperatures inside the WP occur between the time of emplacement and the time of peak drift wall temperatures. At emplacement, the SNF heat load is at its highest but the drift is still cool; by the time of peak drift temperatures, the heat load has decayed so that internal temperature drops are lower. As indicated in Table 6.5-2, the time of peak temperatures varies depending on thermal loading, WP spacing, and the time-dependent WP decay heat (SNF type). For most design basis SNF types, peak WP internal temperatures will occur in less than five years after emplacement even though WP surface temperatures do not peak for 40 years or more.

Figure 6.5-5 displays the temperature contours in the 21 PWR MPC with disposal container at the time of peak temperatures, 0.7 years. The thermal loading for this case was 83 MTU/acre (20.5 kgU/m²) and the MGDS design basis SNF was assumed. Figures 6.5-6, 6.5-7, and 6.5-8 display the temperature contours for the same case at 10, 50, and 100 years, respectively. By 100 years, the temperature drop across the WP (from center to edge) has dropped to less than 50°C.

While 83 MTU/acre is considered a more likely scenario for a high thermal loading, a higher thermal loading of 100 MTU/acre was also evaluated to bound the WP internal temperatures for the full range of possible thermal loadings. Figures 6.5-9 and 6.5-10 display the thermal history of the

21 PWR MPC with disposal container at 100 MTU/acre (24.7 kgU/m²) for the MGDS and MPC SNF design bases, respectively. The combination of short WP spacing and high thermal loading resulted in the highest temperature of all the cases. SNF cladding temperatures peaked at 338°C and average repository horizon temperatures remained above 150°C past 1,000 years. Calculations at Lawrence Livermore National Laboratory (LLNL 1994b) have shown that above boiling conditions will persist for thousands of years at areal mass loadings in this range; however, some temperatures are close to limiting thermal goals.

Figures 6.5-11 and 6.5-12 display the thermal history of the 21 PWR MPC with disposal container at 25 MTU/acre (6.2 kgU/m²) with the long WP spacing (low thermal loading #1) for the MGDS design basis SNF and the MPC design basis SNF, respectively. Peak internal temperatures are similar to those for the high thermal loading because the peaks occur in the first few years before any effects of thermal loading have been realized. Figures 6.5-13 and 6.5-14 display the thermal history of the 21 PWR MPC with disposal container for low thermal loading #2 and for the MGDS design basis SNF and the MPC design basis SNF, respectively. Because the WP spacing is similar to that for high thermal loading #2, similar temperatures are predicted for the first few years of emplacement. However, as thermal loading effects emerge, all of the low thermal loading results converge, as described in Section 6.2.1.1.1. Figures 6.5-15 and 6.5-16 display the thermal history of the 21 PWR MPC with disposal container for low thermal loading #3 and for the MGDS design basis SNF and the MPC design basis SNF respectively. The highest internal temperature for all cases occurred where the MGDS design basis SNF is used and the shortest WP spacing (16.2 m) defines the thermal loading. The peak temperatures occur before drift-to-drift effects emerge such that WP spacing drives the peak near-field temperatures and high thermal loading #1 and low thermal loading #3 have nearly the same peak cladding temperature.

The thermal evaluation of the 21 PWR MPC conceptual design with respect to the repository has considered a number of thermal loading scenarios and design basis SNF types. The repository thermal loading has not been specified and will not be finalized for years. Therefore, the WP thermal behavior has been analyzed for a range of thermal loadings. For each repository thermal loading scenario, a three-dimensional repository emplacement and two-dimensional WP evaluation were performed. The results of the thermal evaluations indicate that the 21 PWR MPC with disposal container design satisfies the thermal limitations for disposal in the MGDS.

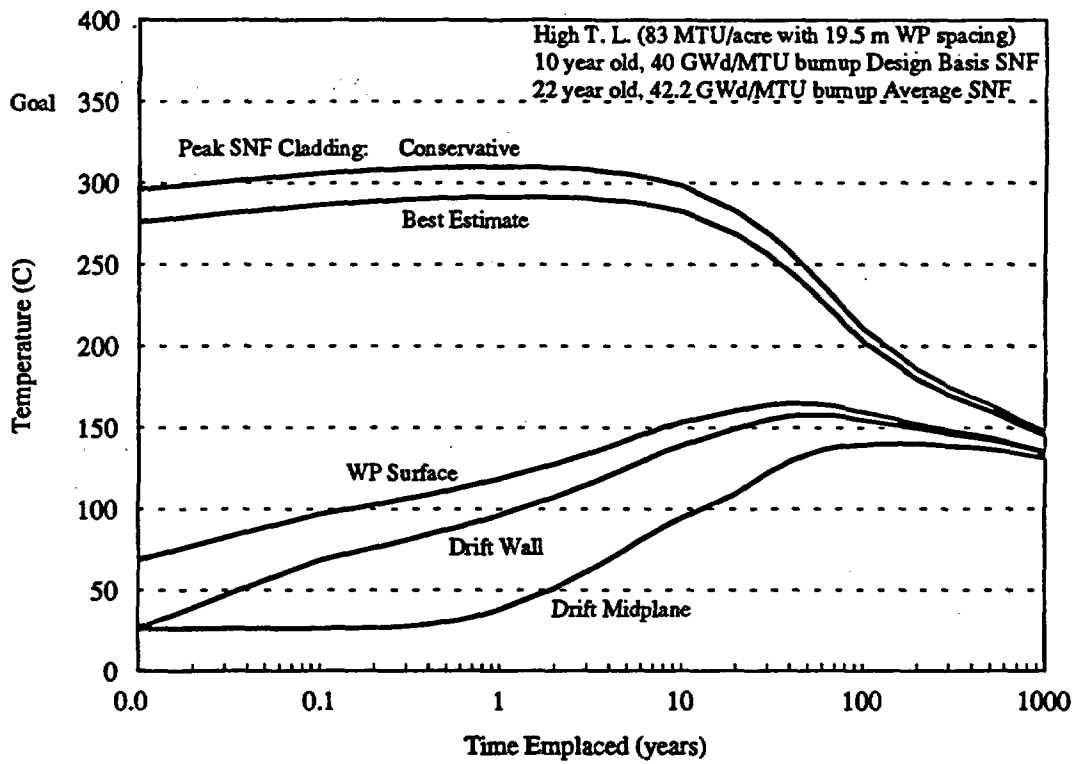


Figure 6.5-1. 21 PWR Multi-Purpose Canister, High Thermal Loading (#2), Historic Design Basis Fuel

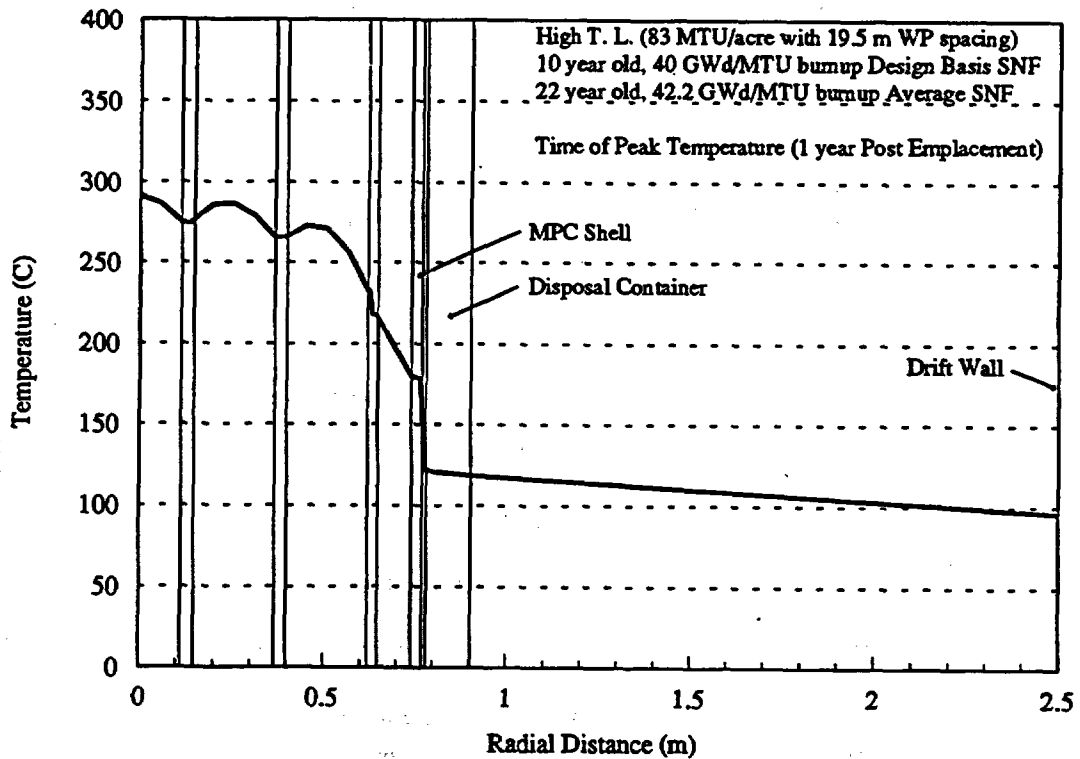


Figure 6.5-2. Temperature Profile in 21 PWR Multi-Purpose Canister

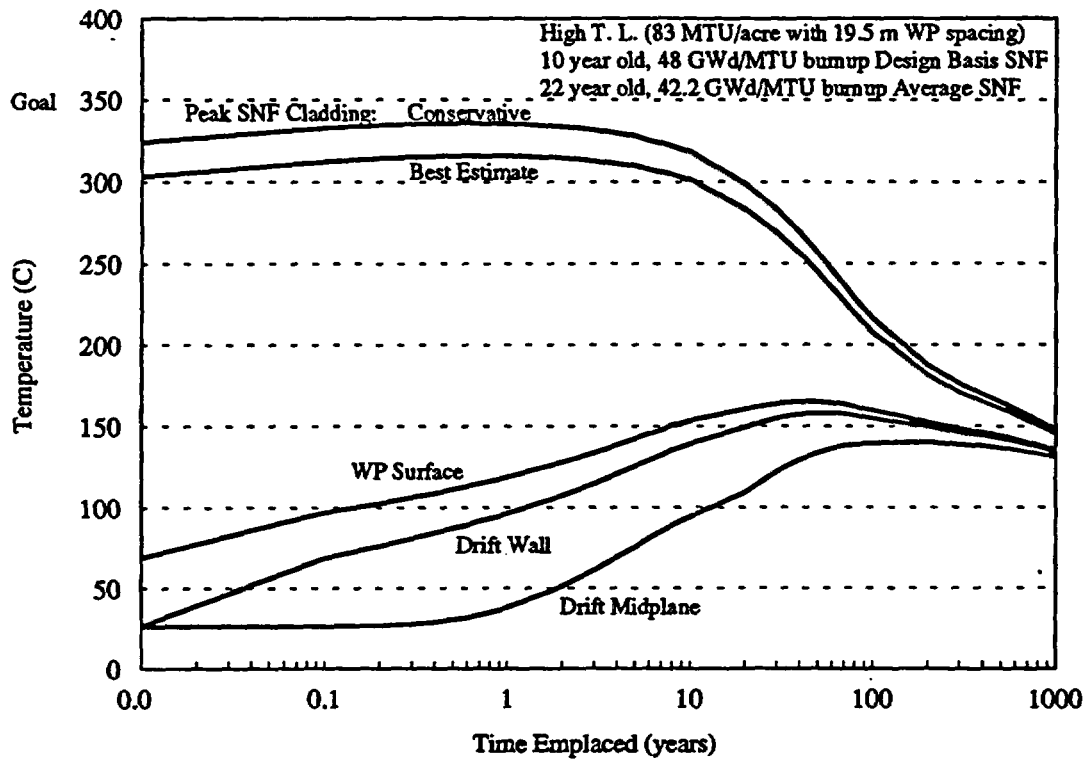


Figure 6.5-3. 21 PWR Multi-Purpose Canister, High Thermal Loading (#2), MGDS Design Basis Fuel

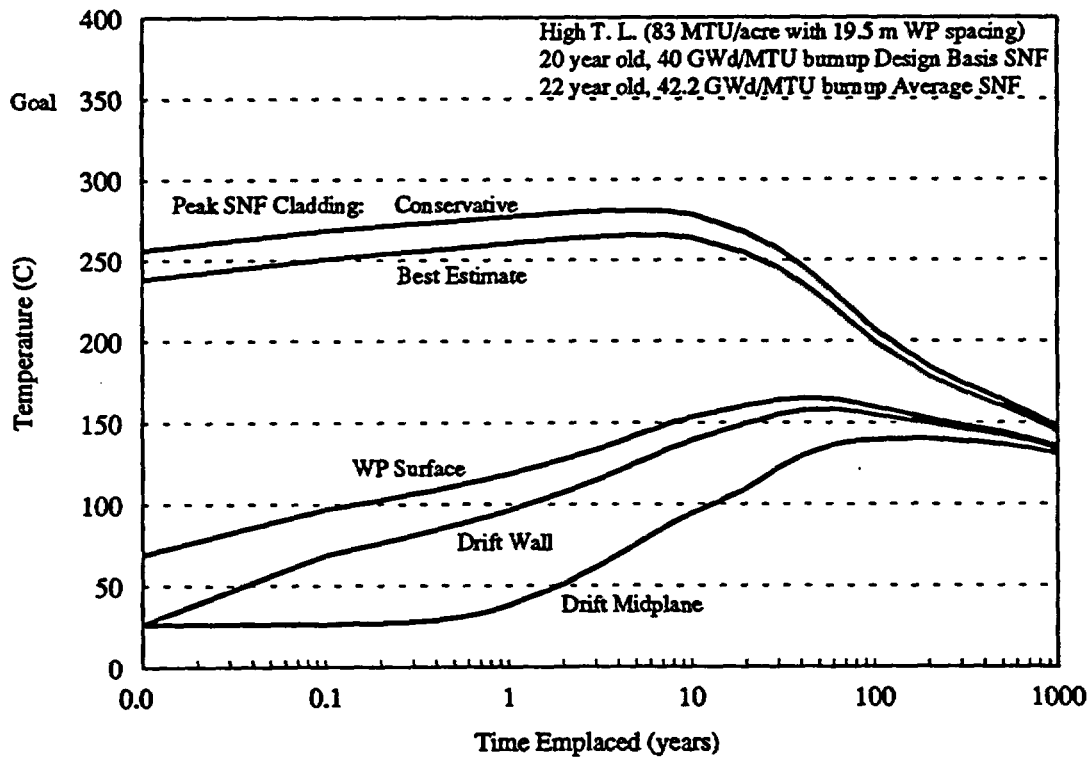
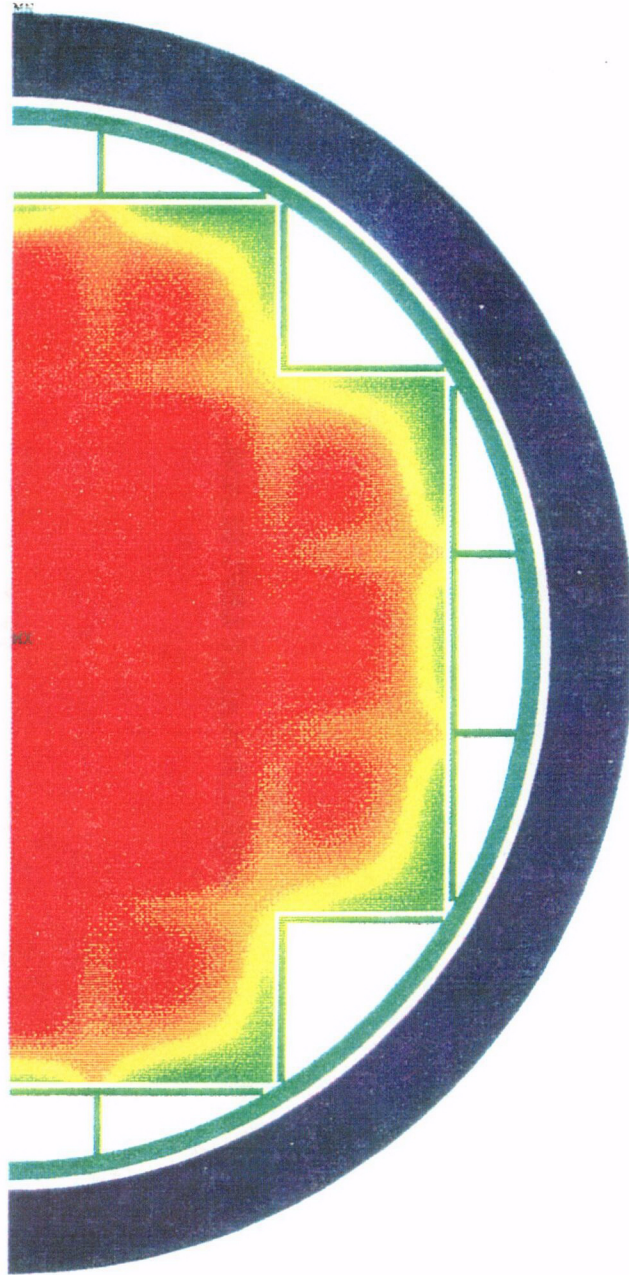


Figure 6.5-4. 21 PWR Multi-Purpose Canister, High Thermal Loading (#2), Multi-Purpose Canister Design Basis Fuel

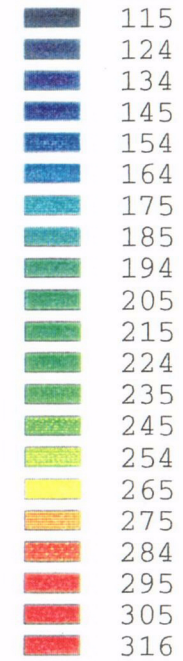


ANSYS 5.0 A
MAR 5 1995

Temperature

Min =113

Max =316



Degrees C

83 MTU/acre

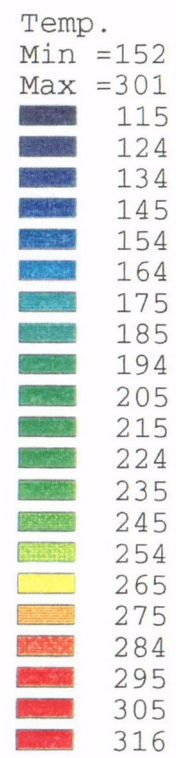
10 year old SNF

48 GWd/MTU

COI

Figure 6.5-5. 21 PWR Multi-Purpose Canister Peak Temperatures at 0.7 Years

ANSYS 5.0 A
MAR 5 1995



Degrees C

83 MTU/acre

10 year old SNF
48 GWd/MTU

CO2

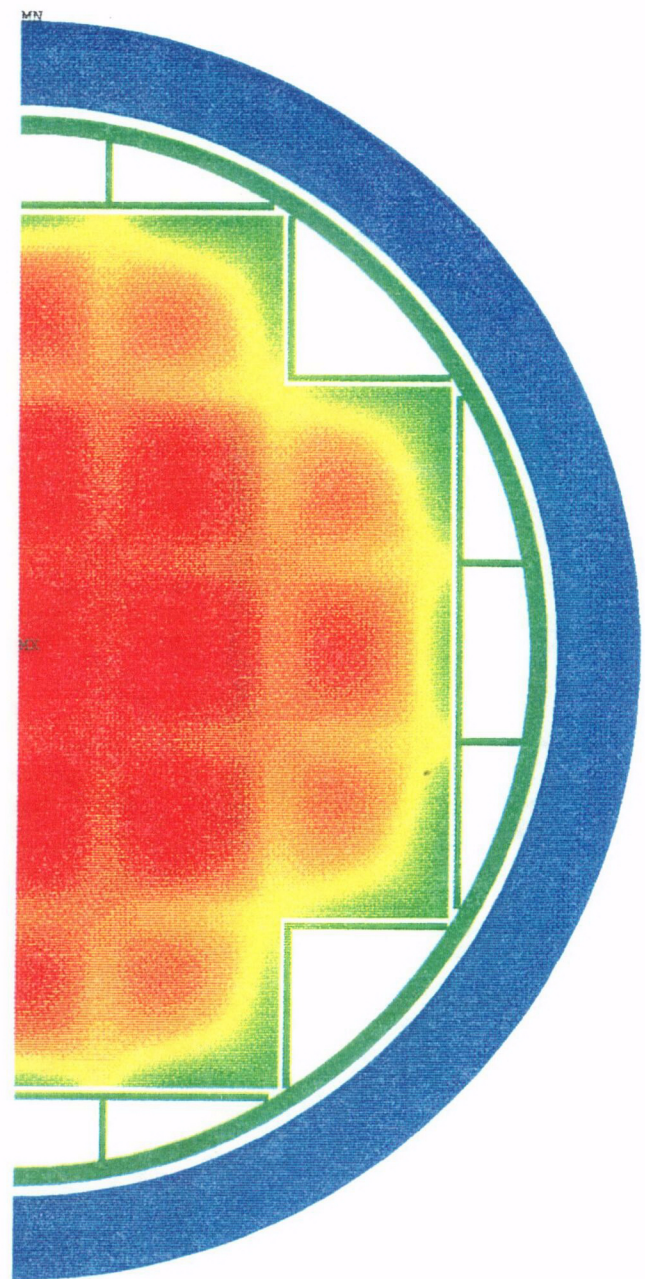
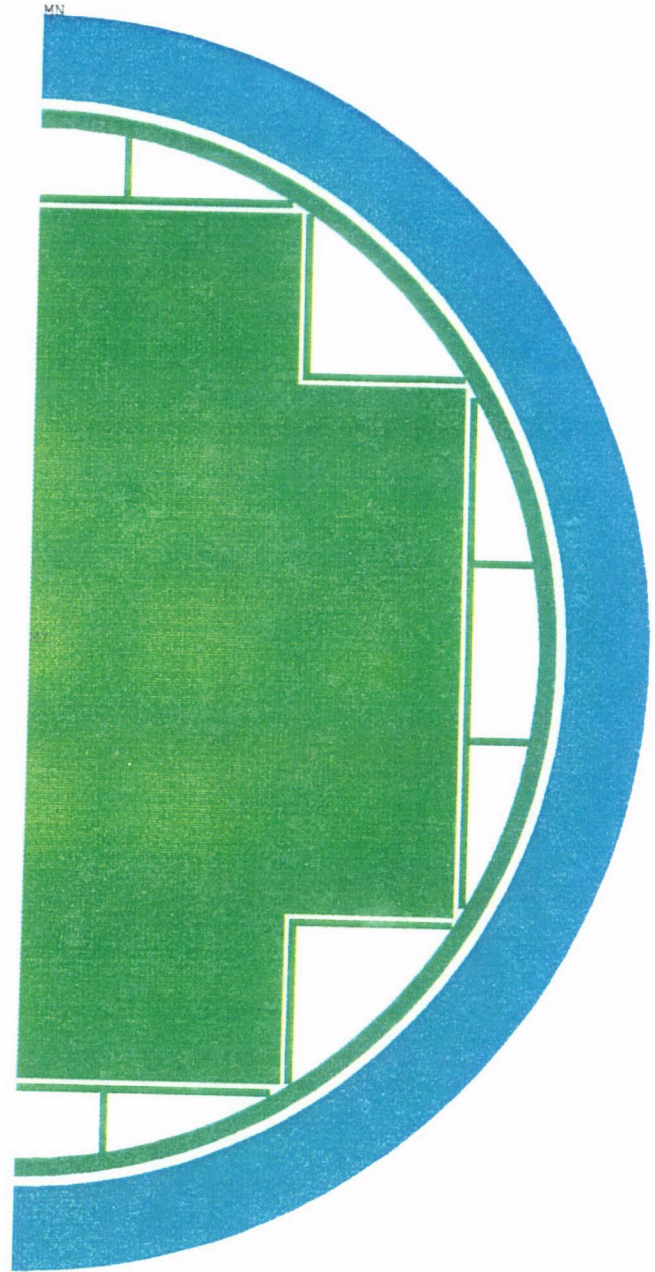


Figure 6.5.6. 21 DWP Multi Purpose Canister Temperatures at 10 Years



ANSYS 5.0 A
MAR 5 1995

Temperature

Min = 164
Max = 245

| |
|-----|
| 115 |
| 124 |
| 134 |
| 145 |
| 154 |
| 164 |
| 175 |
| 185 |
| 194 |
| 205 |
| 215 |
| 224 |
| 235 |
| 245 |
| 254 |
| 265 |
| 275 |
| 284 |
| 295 |
| 305 |
| 316 |

Degrees C

83 MTU/acre

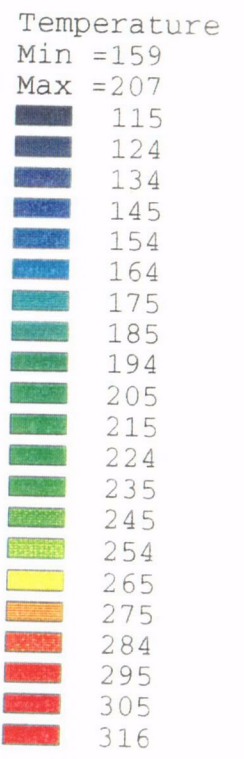
10 year old SNF
48 GWd/MTU

C03

Figure 6.5-7. 21 PWR Multi-Purpose Canister Temperatures at 50 Years



ANSYS 5.0 A
MAR 5 1995



Degrees C

83 MTU/acre

10 year old SNF
48 GWd/MTU

C04

Figure 6.5-8. 21 PWR Multi-Purpose Canister Temperatures at 100 Years

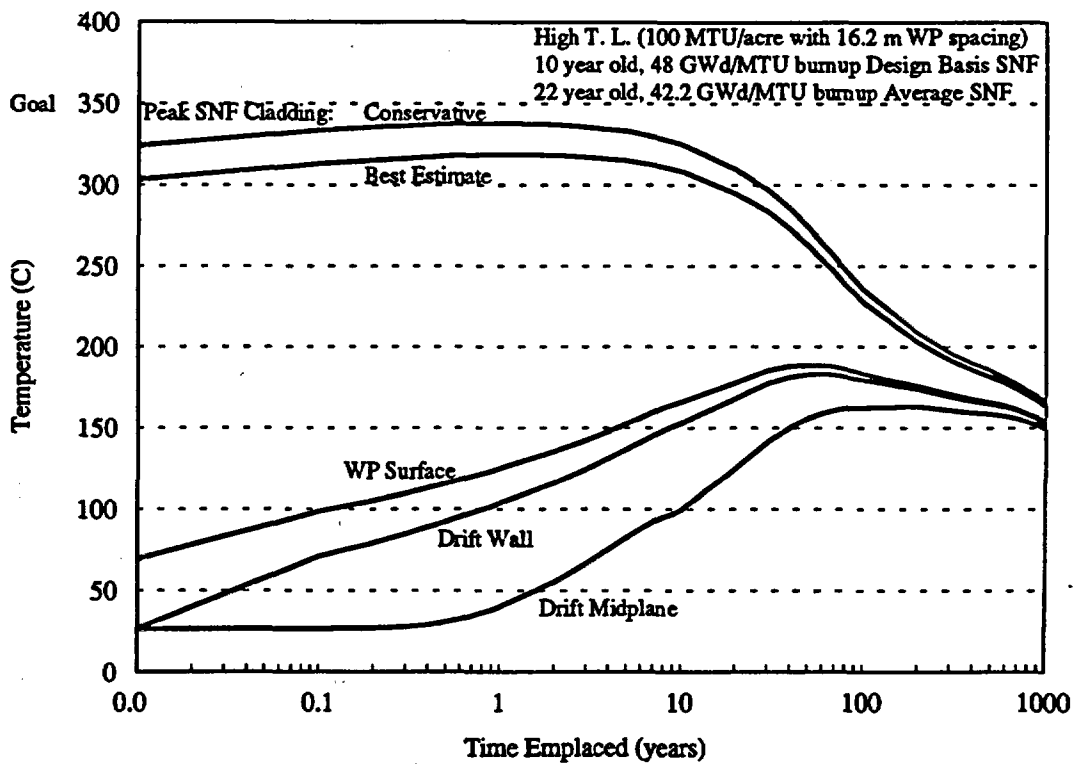


Figure 6.5-9. 21 PWR Multi-Purpose Canister, High Thermal Load (#1), MGDS Design Basis Fuel

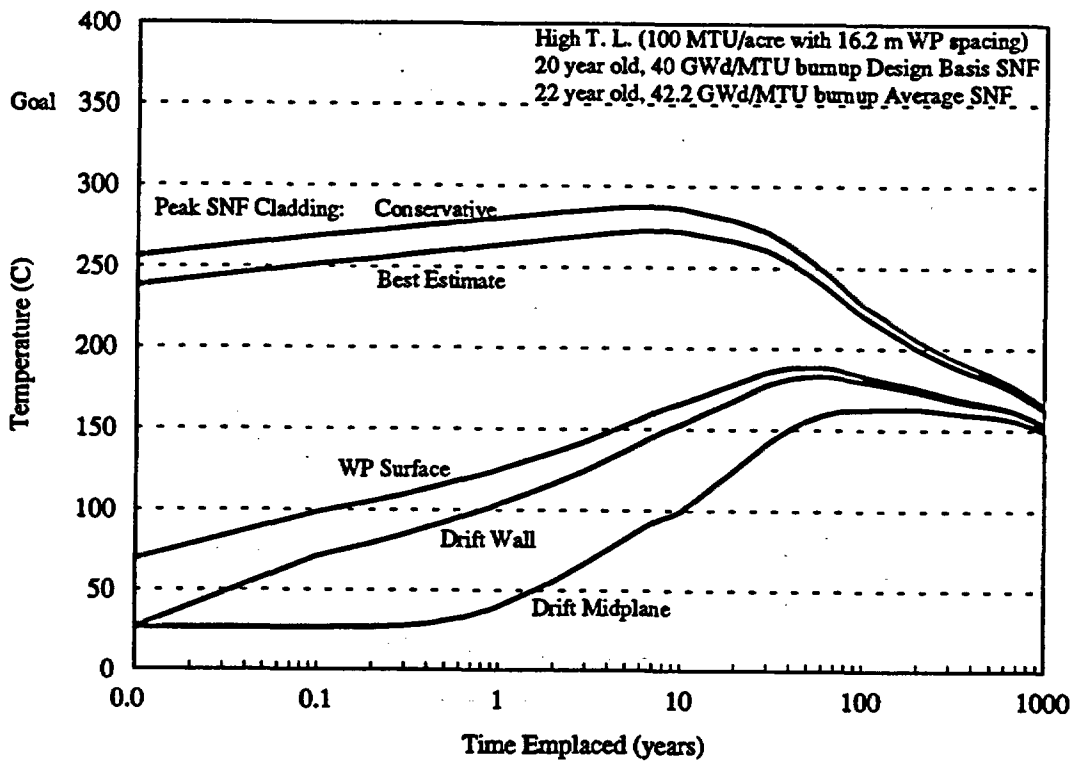


Figure 6.5-10. 21 PWR Multi-Purpose Canister, High Thermal Load (#1), Multi-Purpose Canister Design Basis Fuel

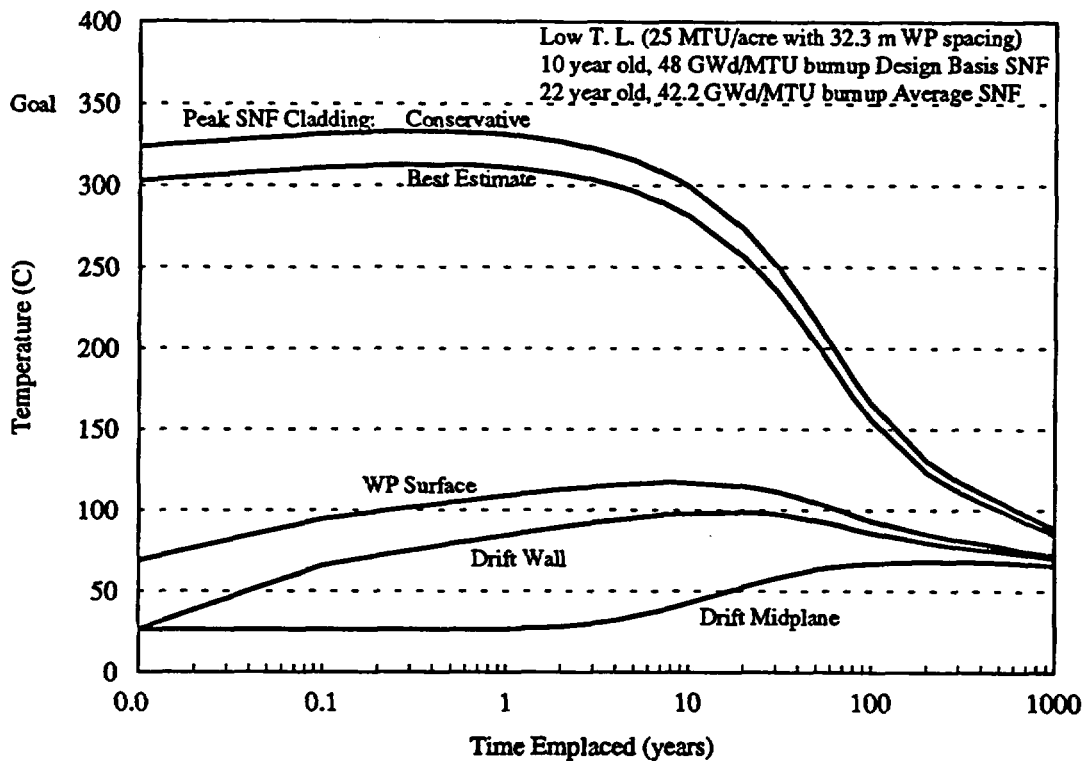


Figure 6.5-11. 21 PWR Multi-Purpose Canister, Low Thermal Load (#1), MGDS Design Basis Fuel

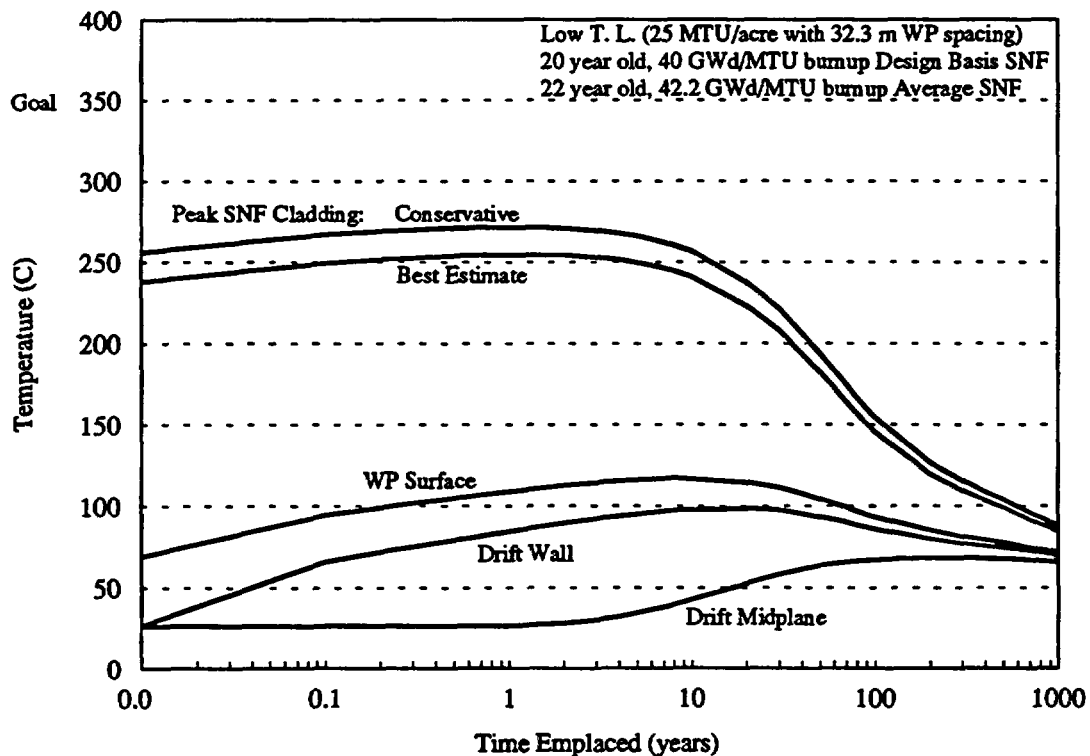


Figure 6.5-12. 21 PWR Multi-Purpose Canister, Low Thermal Load (#1), Multi-Purpose Canister Design Basis Fuel

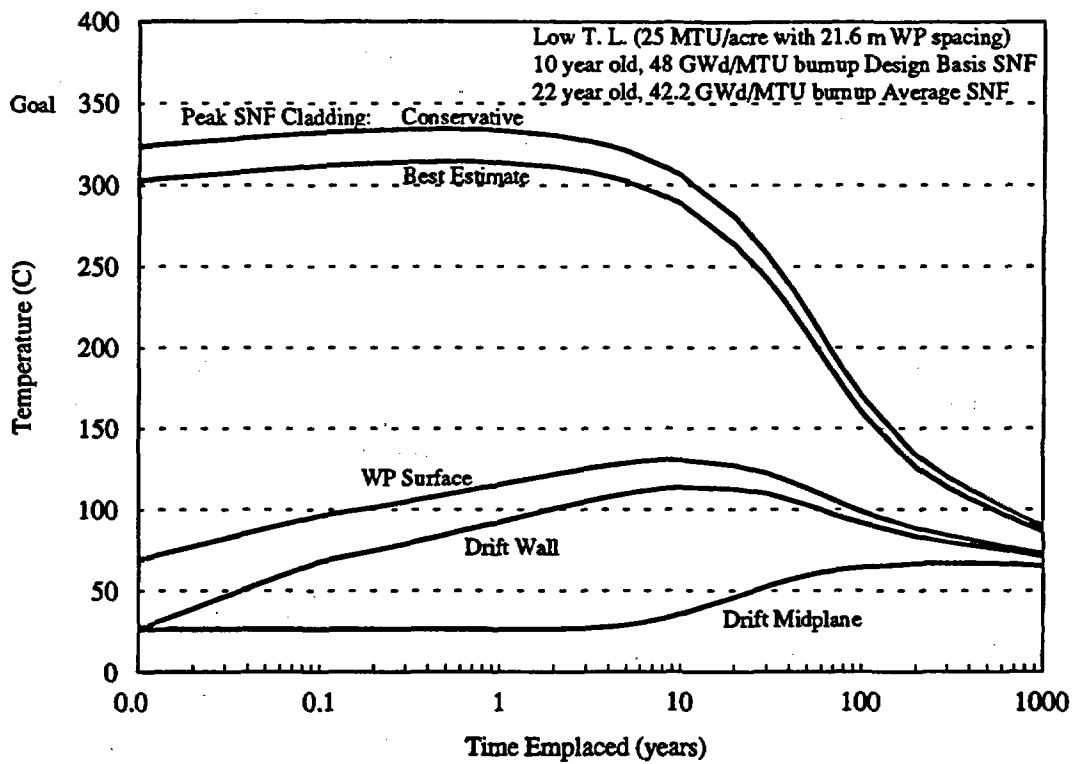


Figure 6.5-13. 21 PWR Multi-Purpose Canister, Low Thermal Load (#2), MGDS Design Basis Fuel

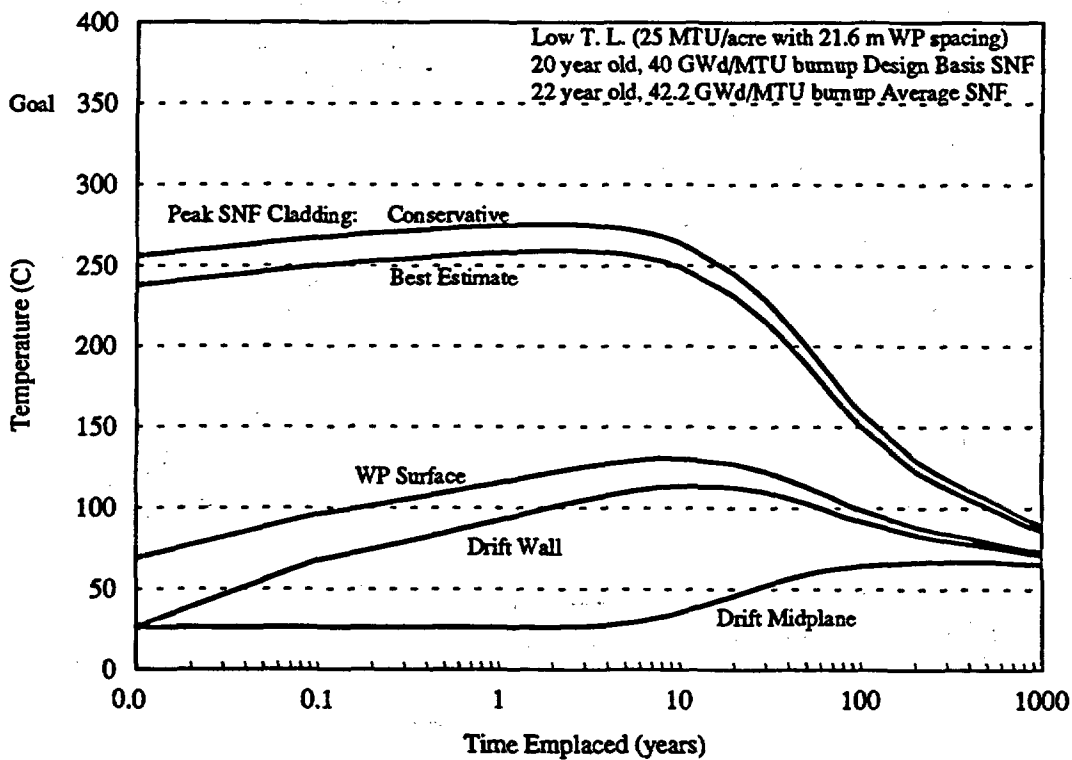


Figure 6.5-14. 21 PWR Multi-Purpose Canister, Low Thermal Load (#2), Multi-Purpose Canister Design Basis Fuel

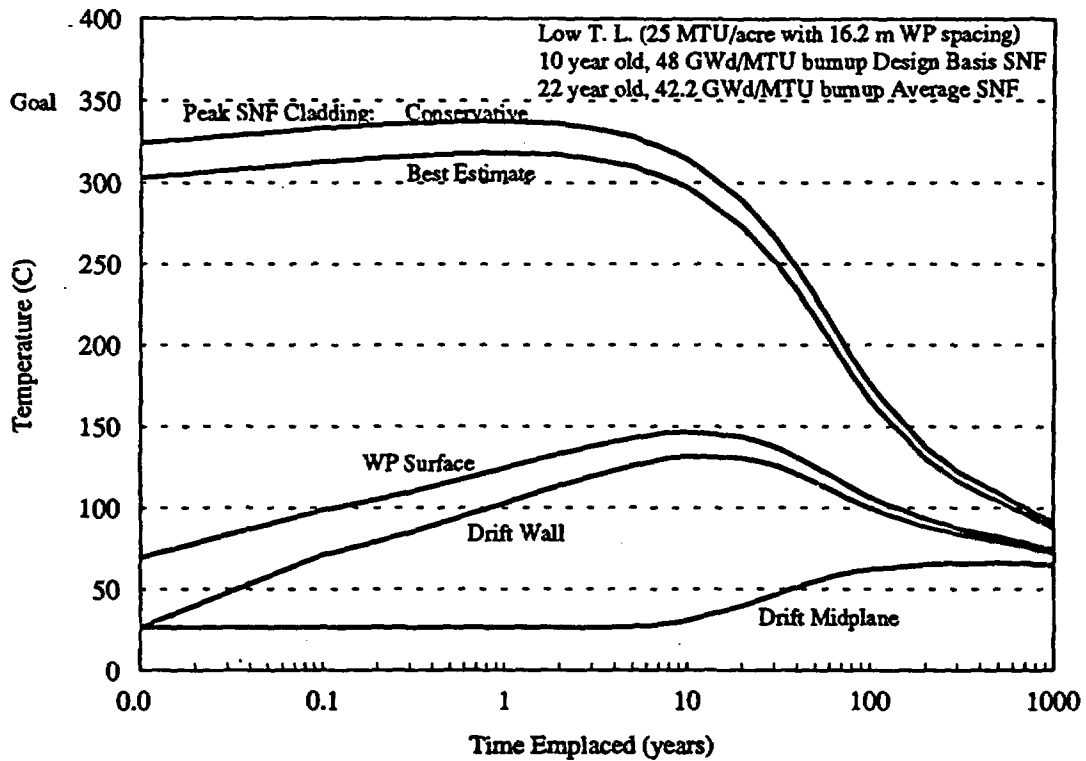


Figure 6.5-15. 21 PWR Multi-Purpose Canister, Low Thermal Load (#3), MGDS Design Basis Fuel

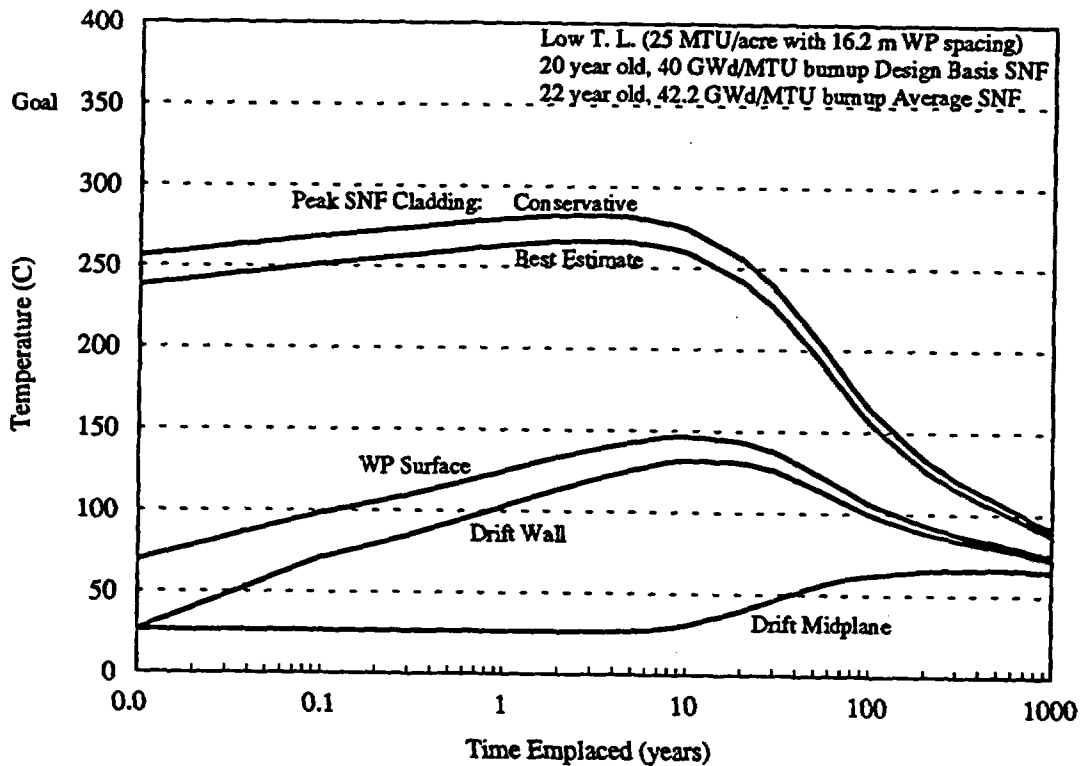


Figure 6.5-16. 21 PWR Multi-Purpose Canister, Low Thermal Load (#3), Multi-Purpose Canister Design Basis Fuel

6.5.1.2 12 PWR Multi-Purpose Canister

A two-dimensional finite-element thermal model of the small 12 PWR flux trap MPC conceptual design was developed from design drawings supplied in the *MPC Conceptual Design Report* (CRWMS M&O 1994k). Model detail included the separate layers of the basket tube design. Intimate contact was assumed between the layers of stainless steel and aluminum, and also between the tube guides and inner shell. The MPC fill gas was assumed to be helium. The multibarrier disposal container for the 12 PWR MPC, described in Appendix B, was also modeled. The analysis is described in detail in a supporting design analysis (CRWMS M&O 1995f).

The finite-element code ANSYS was used to model the two-dimensional cross-section of the MPC/WP. Time and position-dependent temperatures for the WP surface were exported from the emplacement model, described in Section 6.2.1.1.2, and applied as time-varying boundary conditions. The other time-varying conditions used in the model were the design basis SNF decay heat outputs applied as volumetric heat generations to the assembly areas of the model and use smeared material properties. The effective conductivity for the assembly area was developed as described in Section 6.2.1.2 and it represents the resistance due to heat transfer in a 15x15 PWR assembly. The heat loads for the assembly areas were interpolated from the Oak Ridge National Laboratory database of SNF characteristics for each of the assumed design basis SNF types. The heat load will decrease logarithmically with time as the fission products decay. The heat loads were applied volumetrically and were multiplied by an axial heat peaking factor to approximate the axial center of the WP with a two-dimensional model. An SNF assembly is much hotter at the mid-length than at the ends, and it is conservative to assume the two-dimensional WP model represents the hottest cross-section of the MPC/WP.

The boundary conditions and heat loads were applied and solved out to 1,000 years for each of the five thermal loading scenarios described in Section 6.2.1.1.2 and for each of the PWR design basis SNF types described in Table 6.5-1. Table 6.5-3 summarizes the peak temperatures and the time of occurrence for each of the cases analyzed. The thermal loading scenarios indicated in Table 6.5-3 are defined in Table 6.2-2, and the design basis SNF descriptions are provided in Table 6.5-1. Both "conservative" estimates of peak cladding temperatures using the Wooton-Epstein correlation and "best estimate" predictions using the effective conductivity method are presented in the table. Peak cladding temperatures using effective conductivity are calculated directly in the ANSYS program. Wooton-Epstein calculations for each time step in the ANSYS analysis were also performed for comparison.

Table 6.5-3. 12 PWR Multi-Purpose Canister Thermal Analysis Results

| Thermal Load | Design Basis SNF | Peak Cladding | | | | Peak Basket | | MPC shell | | WP Surface | |
|--------------|------------------|-----------------------|-----|---------------|-----|-------------|-----|-----------|-----|------------|-----|
| | | Conservative Estimate | | Best Estimate | | °C | yrs | °C | yrs | °C | yrs |
| | | °C | yrs | °C | yrs | | | | | | |
| High #1 | MGDS | 280 | 5 | 258 | 5 | 243 | 8 | 200 | 40 | 184 | 60 |
| | MPC | 248 | 10 | 232 | 20 | 223 | 30 | 196 | 40 | 184 | 60 |
| High #2 | MGDS | 275 | 2 | 251 | 3 | 233 | 7 | 180 | 30 | 160 | 50 |
| | MPC | 238 | 8 | 221 | 10 | 209 | 10 | 174 | 30 | 160 | 50 |
| | Historic | 256 | 5 | 235 | 5 | 221 | 8 | 177 | 30 | 160 | 50 |
| Low #1 | MGDS | 267 | 0.5 | 242 | 0.6 | 221 | 0.7 | 148 | 3 | 101 | 20 |
| | MPC | 219 | 2 | 199 | 2 | 183 | 3 | 134 | 6 | 101 | 20 |
| Low #2 | MGDS | 272 | 1 | 247 | 1 | 227 | 2 | 160 | 5 | 118 | 10 |
| | MPC | 227 | 3 | 208 | 4 | 194 | 4 | 148 | 8 | 118 | 10 |
| Low #3 | MGDS | 278 | 2 | 254 | 2 | 236 | 2 | 173 | 8 | 137 | 10 |
| | MPC | 237 | 4 | 219 | 5 | 206 | 6 | 163 | 8 | 137 | 10 |

The historic MPC PWR design basis of 10-years-old, 40 GWd/MTU was evaluated so that the current solution results can be compared to previous analyses (CRWMS M&O 1994i). The thermal history for this SNF type at 83 MTU/acre (20.5 kgU/m²) is presented in Figure 6.5-17. Figure 6.5-18 displays the temperature profile across the MPC basket and disposal container for the time of peak internal temperatures (five years). The peak conservative estimate for SNF cladding temperature was 256°C, which is comfortably below the cladding temperature limit of 350°C.

Figures 6.5-19 and 6.5-20 display the thermal history of the 12 PWR MPC with disposal container at 83 MTU/acre (20.5 kgU/m²) for the MGDS design basis SNF and the MPC design basis SNF, respectively. The highest temperatures occur for MGDS design basis SNF owing to its relatively young age of 10 years. The conservative estimate of peak cladding temperature for this case was 275°C, which is less than the thermal design goal of 350°C. Peak temperatures for the MPC design basis SNF were 37°C less than that for the MGDS design basis. Just as for the 21 PWR MPC with disposal container, peak temperatures occur between the time of emplacement and the time of peak drift wall temperatures.

Figure 6.5-21 displays the temperature contours in the 12 PWR MPC with disposal container at the time of peak temperatures, three years. The thermal loading for this case was 83 MTU/acre (20.5 kgU/m²) and the MGDS design basis SNF was assumed. Figures 6.5-22, 6.5-23, and 6.5-24 display the temperature contours for the same case at 10, 50, and 100 years respectively. By 100 years the temperature drop across the WP (from center to edge) has dropped to less than 40°C.

Figures 6.5-25 and 6.5-26 display the thermal history of the 12 PWR MPC with disposal container at 100 MTU/acre (24.7 kgU/m²) for the MGDS and MPC SNF design bases, respectively. While 83 MTU/acre is considered a more likely scenario for a high thermal loading, a higher thermal loading of 100 MTU/acre was also evaluated to bound the WP internal temperatures. The combination of short WP spacing and high thermal loading resulted in the highest conservative estimation of peak cladding temperature (280°C). Just as for the 21 PWR cases, above-boiling, near-field temperatures persisted past 1,000 years.

Figures 6.5-27 and 6.5-28 display the thermal history of the 12 PWR MPC with disposal container at 25 MTU/acre (6.2 kgU/m²) with the long WP spacing (low thermal loading #1) for the MGDS design basis SNF and the MPC design basis SNF, respectively. As in the 21 PWR MPC, peak internal temperatures are similar to those for the high thermal loadings because the peaks occur before any effects of thermal loading have been realized. Figures 6.5-29 and 6.5-30 display the thermal history of the 12 PWR MPC with disposal container for low thermal loading #2 and for the MGDS design basis SNF and the MPC design basis SNF, respectively. Because the WP spacing is similar to that for high thermal loading #2, similar temperatures are predicted for the first few years of emplacement. Figures 6.5-31 and 6.5-32 display the thermal history of the 12 PWR MPC with disposal container for low thermal loading #3 and for the MGDS design basis SNF and the MPC design basis SNF, respectively. The highest internal temperature occurred where the MGDS design basis SNF and the shortest WP spacing (9.2 m) were used. The peak temperatures occur before drift-to-drift effects emerge, such that the WP spacing drives the peak near-field temperatures and high thermal loading #1 and low thermal loading #3 have nearly the same peak cladding temperatures.

The thermal evaluation of the 12 PWR MPC conceptual design with respect to the repository has considered a number of thermal loading scenarios and design basis SNF types. For each repository thermal loading scenario, a three-dimensional repository emplacement and two-dimensional WP evaluation were performed. The results of the thermal evaluations indicate that the 12 PWR MPC with disposal container design satisfies the thermal limitations for disposal in the MGDS.

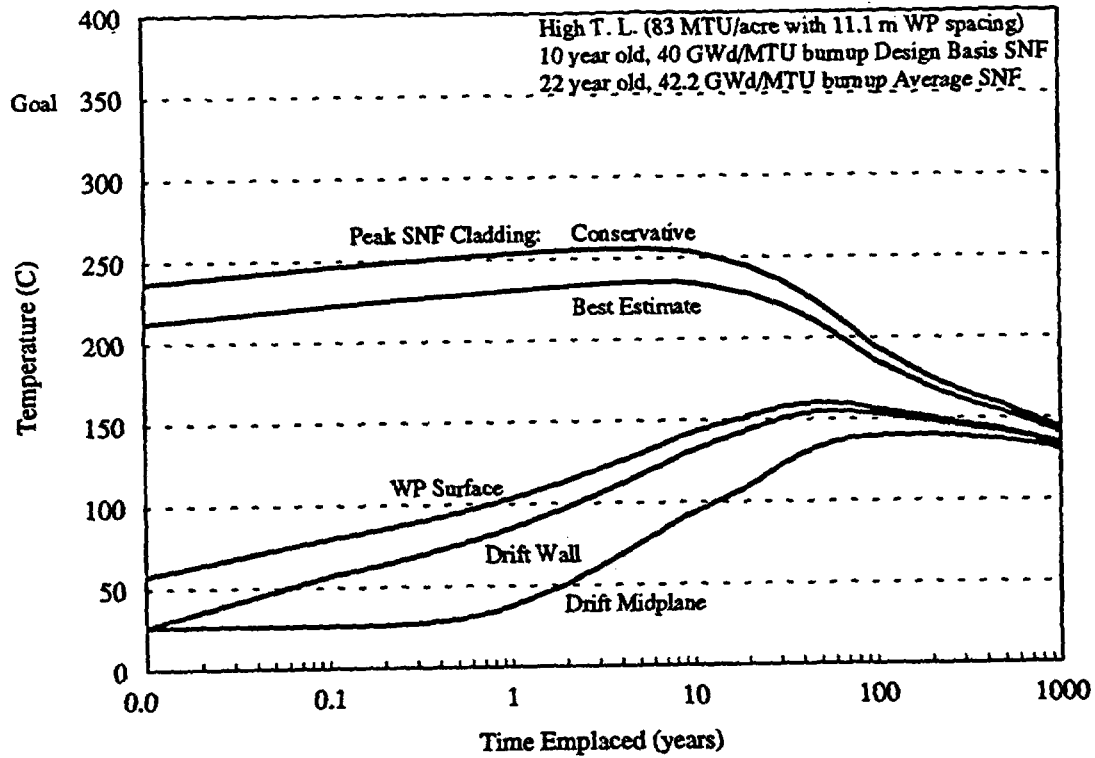


Figure 6.5-17. 12 PWR Multi-Purpose Canister, High Thermal Load (#2), Historic Design Basis Fuel

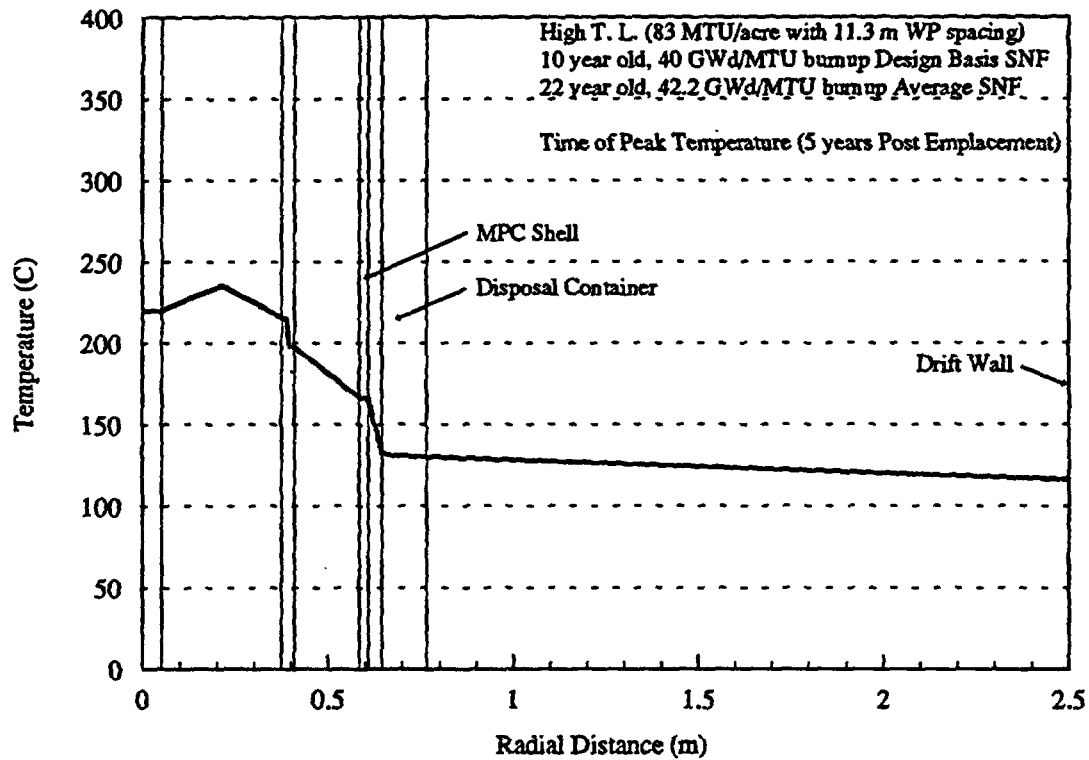


Figure 6.5-18. Temperature Profile in 12 PWR Multi-Purpose Canister

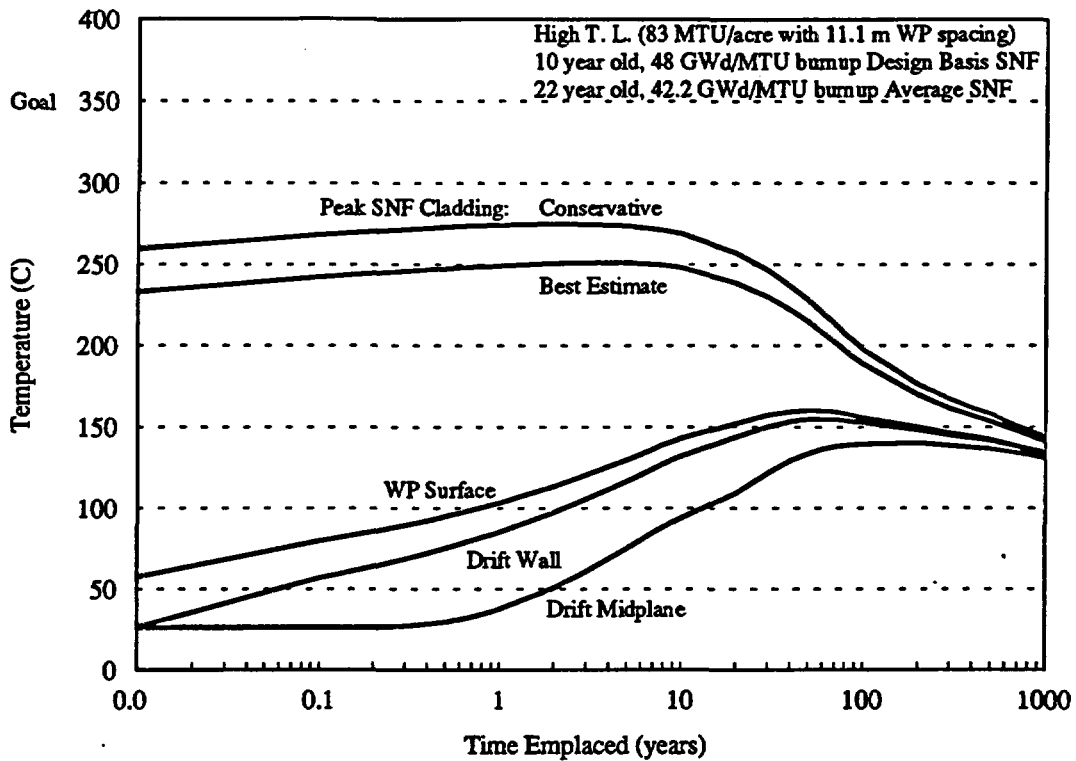


Figure 6.5-19. 12 PWR Multi-Purpose Canister, High Thermal Load (#2), MGDS Design Basis Fuel

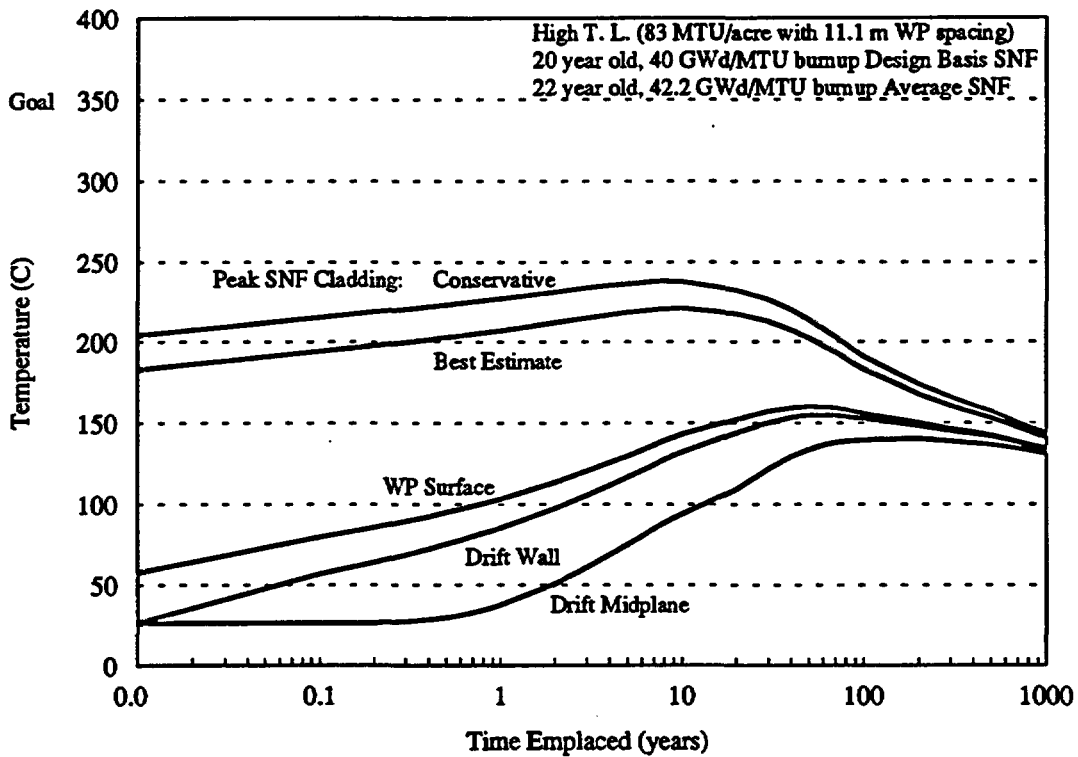


Figure 6.5-20. 12 PWR Multi-Purpose Canister, High Thermal Load (#2), Multi-Purpose Canister Design Basis Fuel

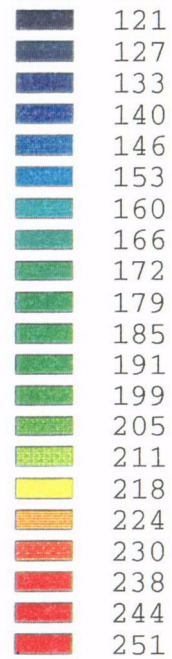
INTENTIONALLY LEFT BLANK

ANSYS 5.0 A
MAR 27 1995

Temperature

Min =120

Max =251



Degrees C

83 MTU/acre

10-year-old SNF
48 GWd/MTU

C05

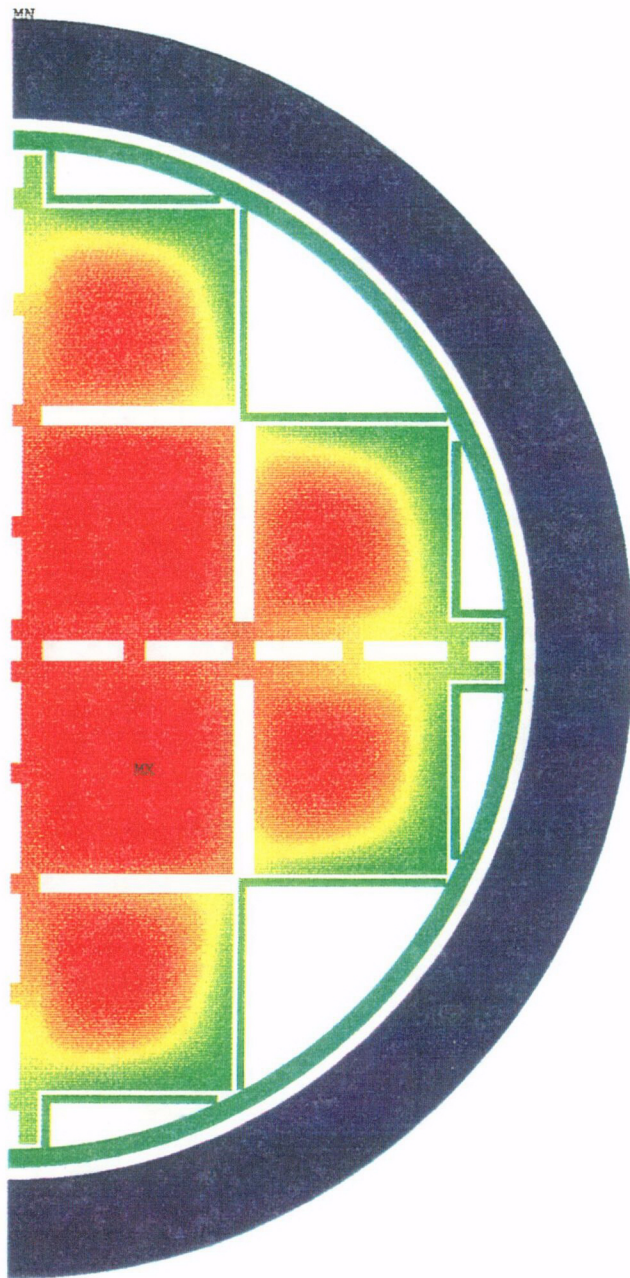
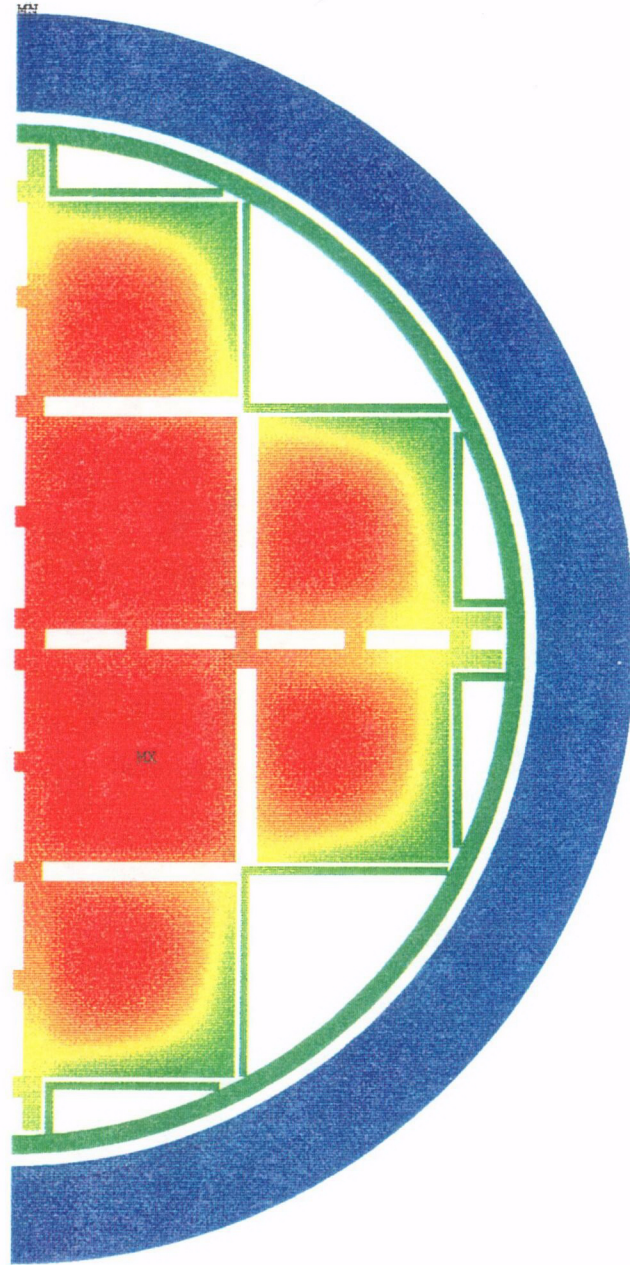
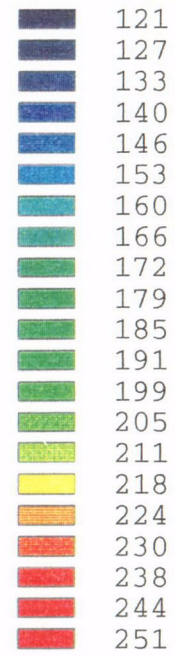


Figure 6.5-21. 12 PWR Multi-Purpose Canister Peak Temperatures at 3 Years

ANSYS 5.0 A
MAR 27 1995



Temperature
Min =142
Max =248



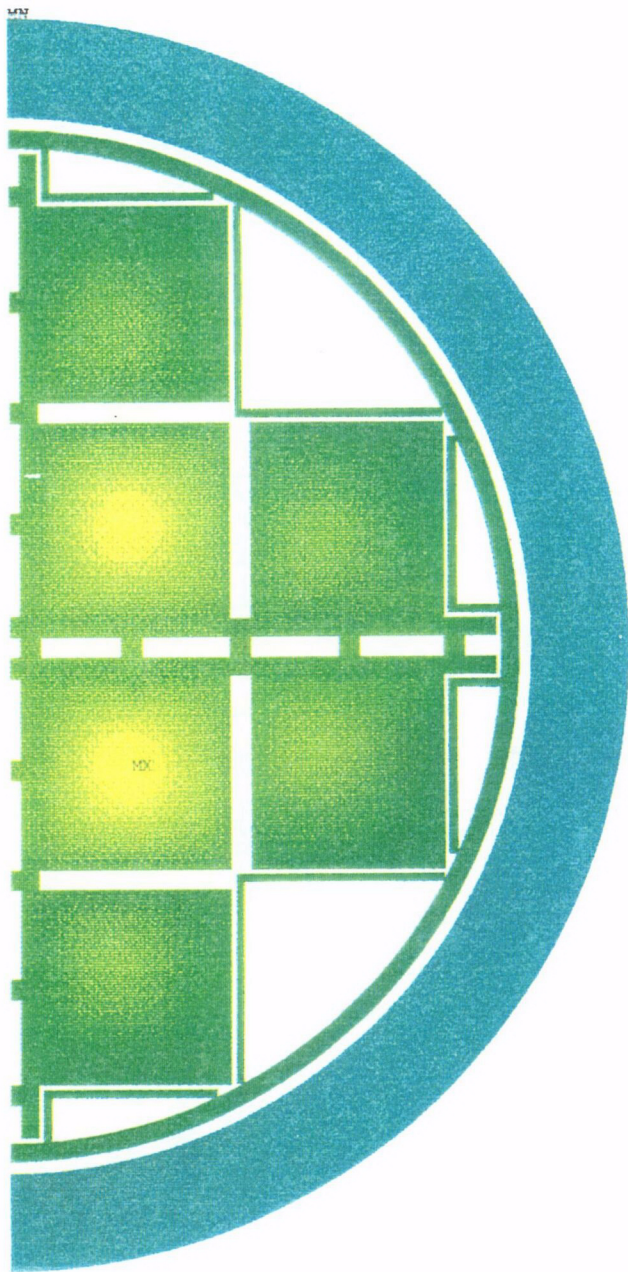
Degrees C

83 MTU/acre

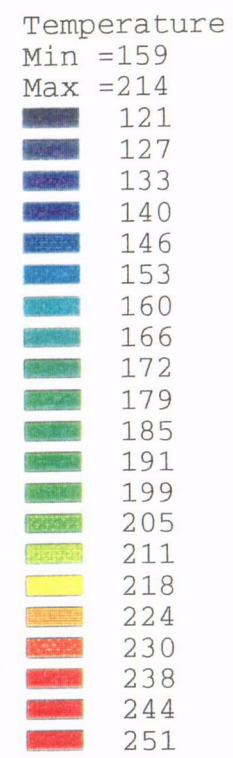
10-year-old SNF
48 GWd/MTU

CO6

Figure 6.5-22. 12 PWR Multi-Purpose Canister Temperatures at 10 Years



ANSYS 5.0 A
MAR 27 1995



Degrees C

83 MTU/acre

10-year-old SNF
48 GWd/MTU

C07

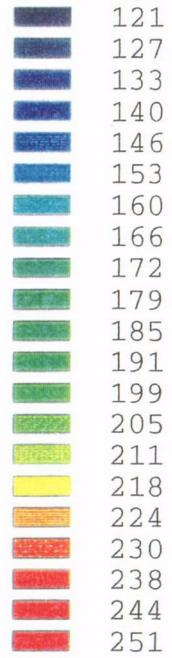
Figure 6.5-23. 12 PWR Multi-Purpose Canister Temperatures at 50 Years

ANSYS 5.0 A
MAR 27 1995

Temperature

Min =156

Max =188



Degrees C

83 MTU/acre

10-year-old SNF

48 GWd/MTU

C08

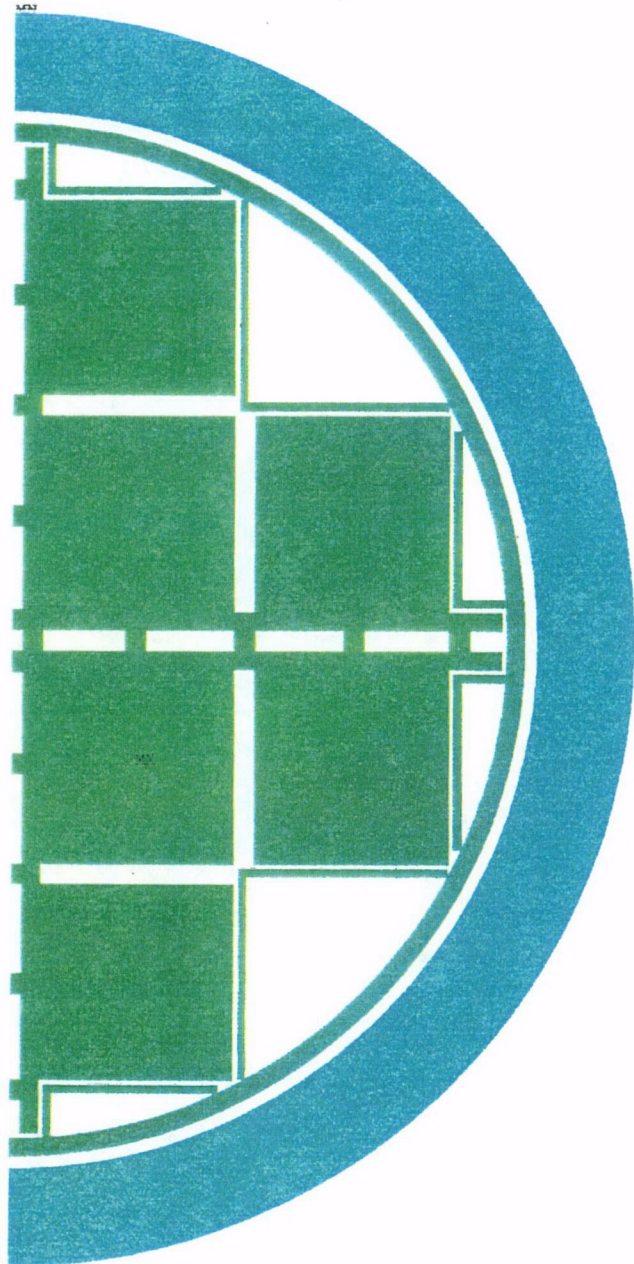


Figure 6.5-24. 12 PWR Multi-Purpose Canister Temperatures at 100 Years

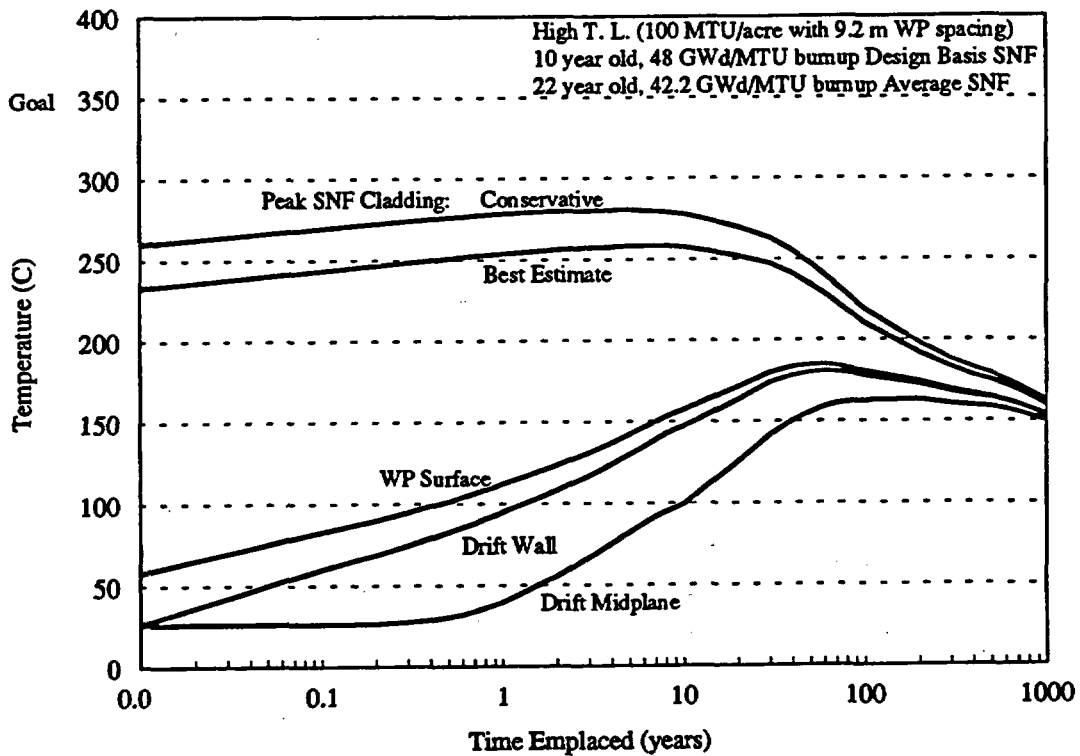


Figure 6.5-25. 12 PWR Multi-Purpose Canister, High Thermal Load (#1), MGDS Design Basis Fuel

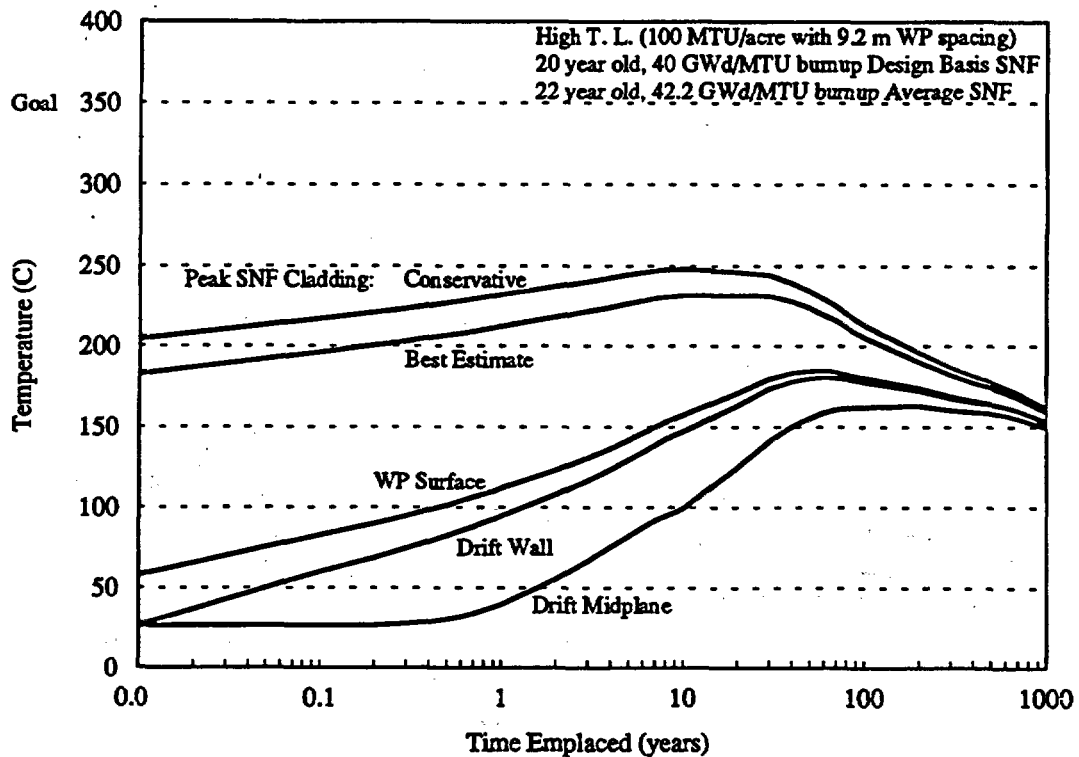


Figure 6.5-26. 12 PWR Multi-Purpose Canister, High Thermal Load (#1), Multi-Purpose Canister Design Basis Fuel

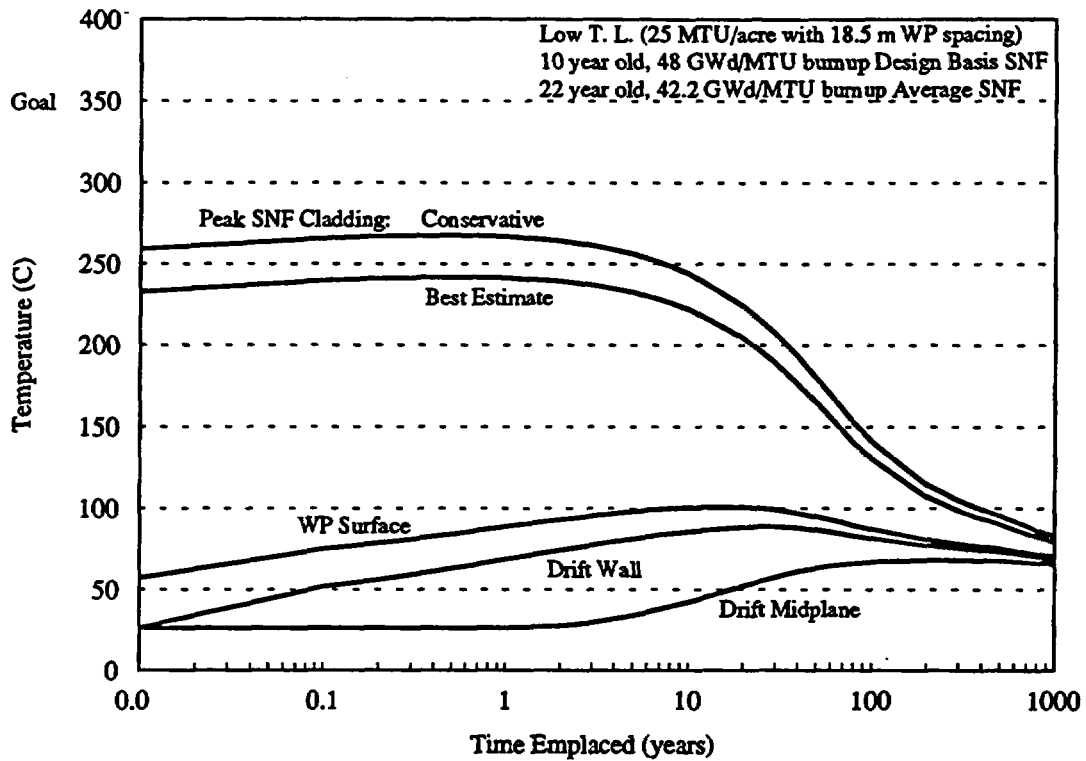


Figure 6.5-27. 12 PWR Multi-Purpose Canister, Low Thermal Load (#1), MGDS Design Basis Fuel

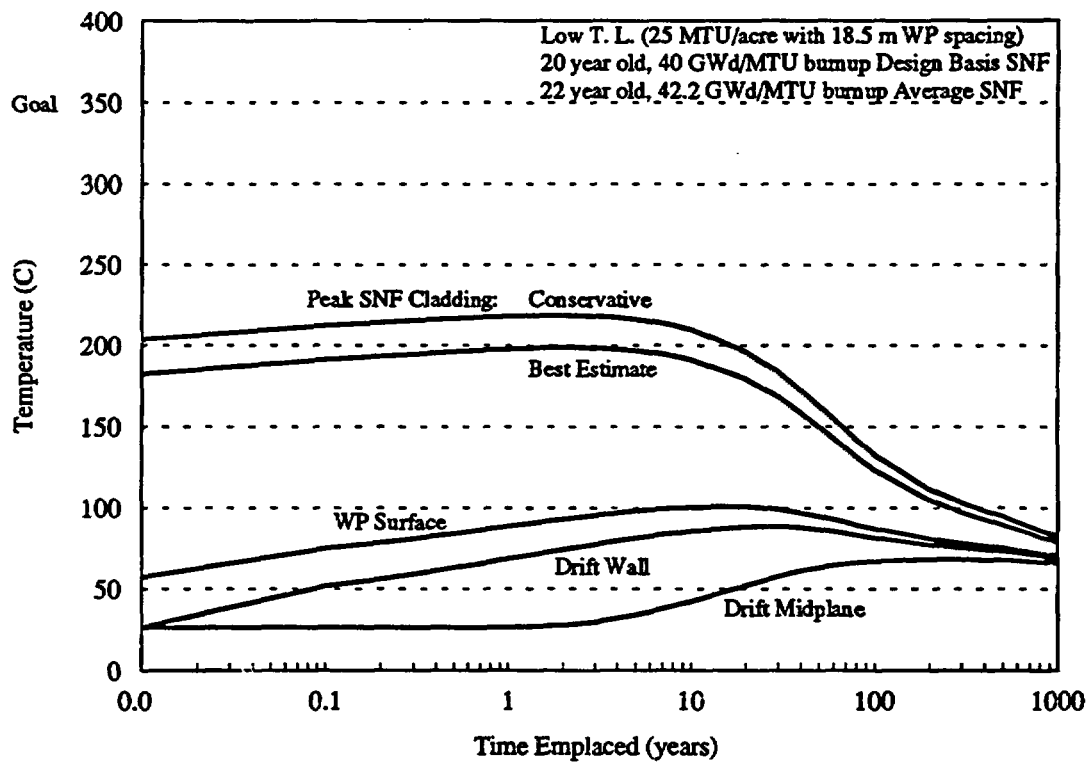


Figure 6.5-28. 12 PWR Multi-Purpose Canister, Low Thermal Load (#1), Multi-Purpose Canister Design Basis Fuel

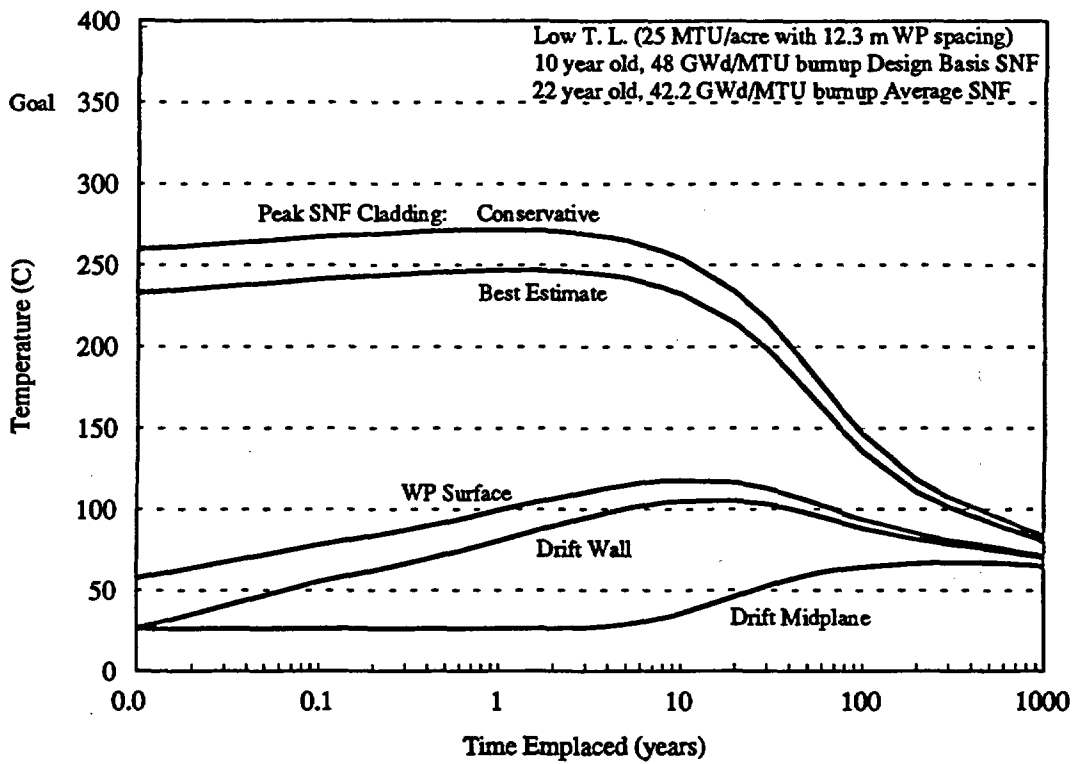


Figure 6.5-29. 12 PWR Multi-Purpose Canister, Low Thermal Load (#2), MGDS Design Basis Fuel

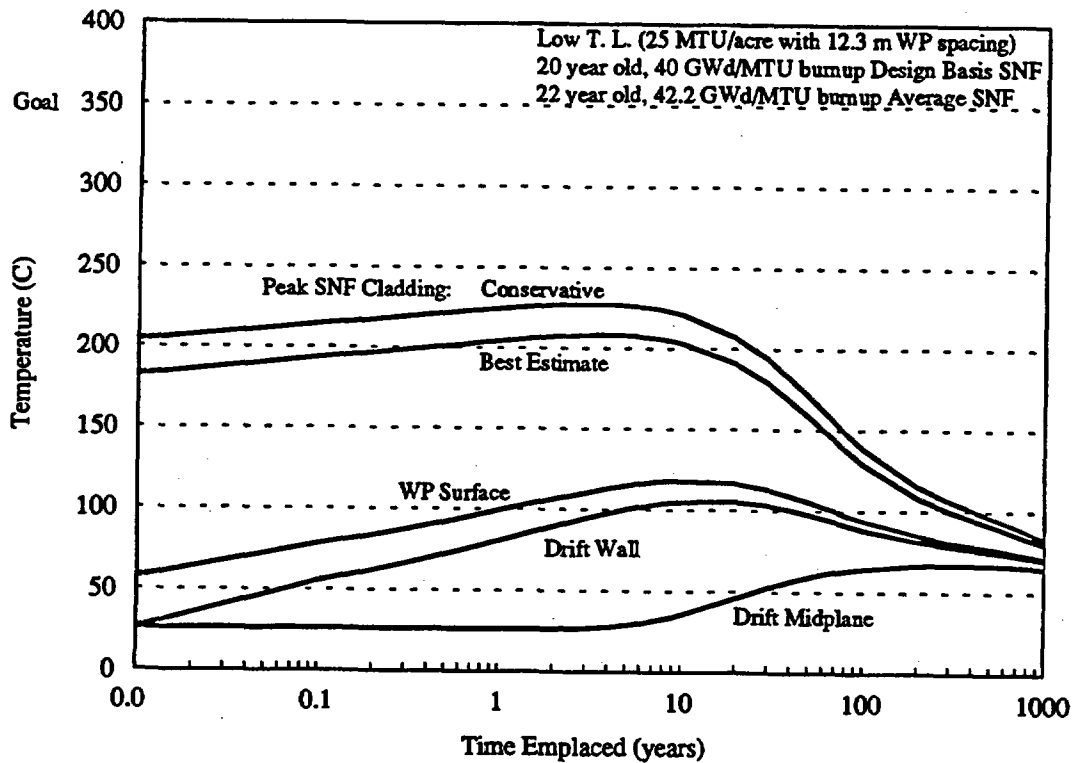


Figure 6.5-30. 12 PWR Multi-Purpose Canister, Low Thermal Load (#2), Multi-Purpose Canister Design Basis Fuel

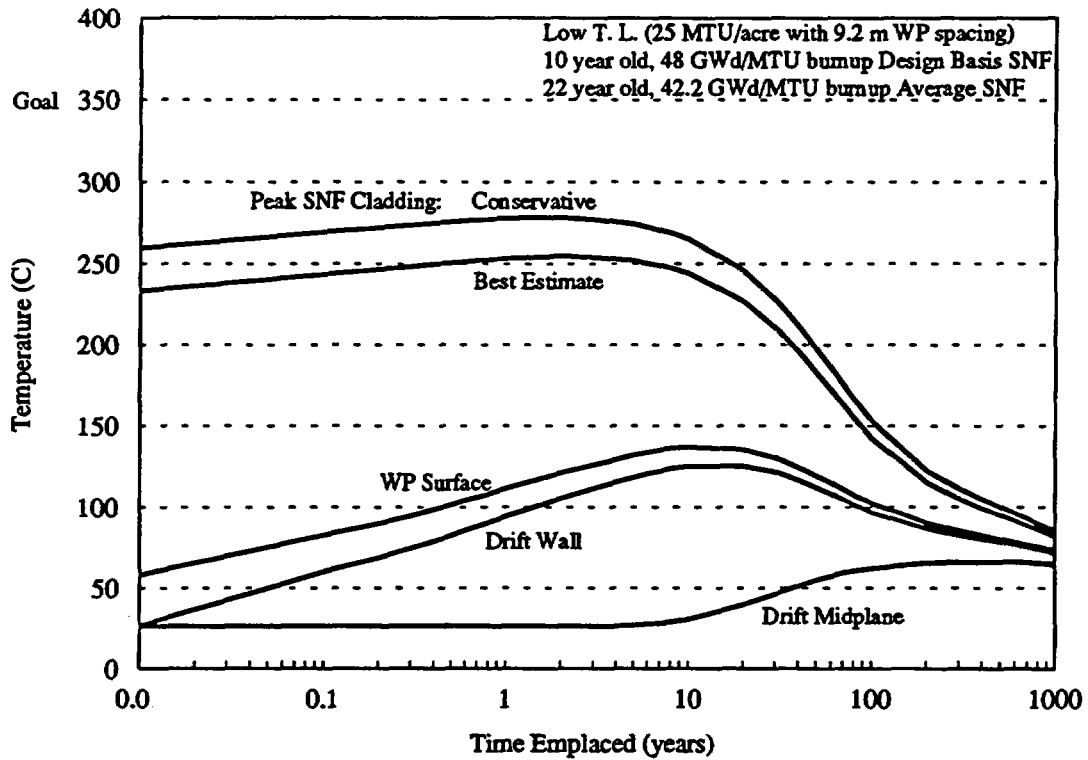


Figure 6.5-31. 12 PWR Multi-Purpose Canister, Low Thermal Load (#3), MGDS Design Basis Fuel

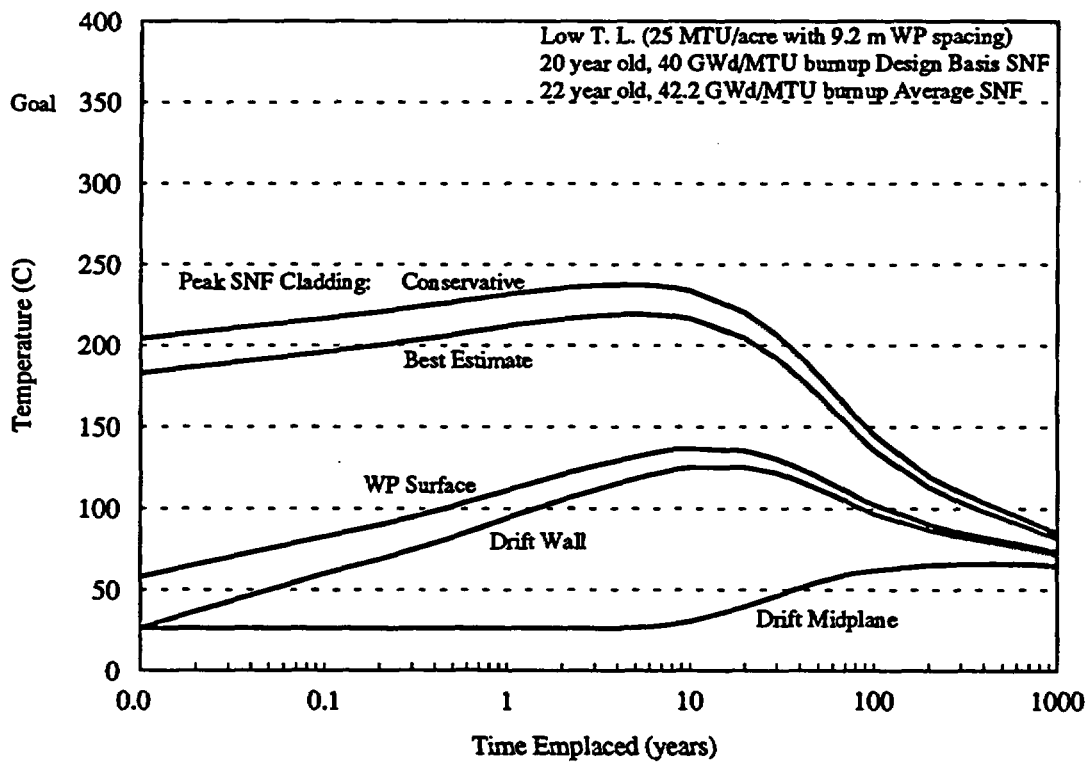


Figure 6.5-32. 12 PWR Multi-Purpose Canister, Low Thermal Load (#3), Multi-Purpose Canister Design Basis Fuel

6.5.1.3 40 BWR Multi-Purpose Canister

A two-dimensional finite-element thermal model of the large 40 BWR burnup credit MPC conceptual design was developed from design drawings supplied in the *MPC Conceptual Design Report* (CRWMS M&O 1994k). Model detail included the separate layers of the basket tube design. Intimate contact was assumed between the layers of stainless steel and aluminum, and also between the tube guides and inner shell. The MPC fill gas was assumed to be helium. The multibarrier disposal container for the MPC, described in Appendix B, was also modeled. The analysis is described in detail in a supporting design analysis (CRWMS M&O 1995g).

The finite-element code ANSYS was used to model the two-dimensional cross-section of the MPC/WP. Time and position-dependent temperatures for the WP surface were exported from the emplacement model, described in Section 6.2.1.1.1, and applied as time-varying boundary conditions. The other time-varying conditions used in the model were the design basis SNF decay heat outputs applied as volumetric heat generations to the assembly areas of the model and use smeared material properties. The effective conductivity for the assembly area for a PWR assembly was developed as described in Section 6.2.1.2. For the purpose of the BWR thermal evaluation, it was assumed that the effective conductivity developed for a PWR assembly can be applied to the peak cladding temperature determination for a BWR assembly. It is expected that the effective conductivity for a BWR will be higher, and therefore slightly conservative temperatures will be predicted using the PWR effective conductivity. The heat loads for the assembly areas were interpolated from the Oak Ridge National Laboratory database of SNF characteristics for the assumed design basis SNF. The heat load will decrease logarithmically with time as the fission products decay. The heat loads were applied volumetrically and were multiplied by an axial heat peaking factor to approximate the axial center of the WP with a two-dimensional model. An SNF assembly is much hotter at the mid-length than at the ends, and it is conservative to assume the two-dimensional WP model represents the hottest cross-section of the MPC/WP.

The boundary conditions and heat loads were applied and solved out to 1,000 years for each of the five thermal loading scenarios described in Section 6.2.1.1.1 with the MGDS BWR design basis SNF type described in Table 6.5-1. Table 6.5-4 summarizes the peak temperatures and the time of occurrence for each of the cases analyzed. The thermal loading scenarios indicated in Table 6.5-4 are defined in Table 6.2-1, and the design basis SNF descriptions are provided in Table 6.5-1. Both "conservative" estimates of peak cladding temperatures using the Wooton-Epstein correlation and "best estimate" predictions using the effective conductivity method are presented in the table. Peak cladding temperatures using effective conductivity are calculated directly in the ANSYS program. Wooton-Epstein calculations for each time step in the ANSYS analysis were also performed for comparison.

Table 6.5-4. 40 BWR Multi-Purpose Canister Thermal Analysis Results

| Thermal Load | Design Basis SNF | Peak Cladding | | | | Peak Basket | | MPC shell | | WP Surface | |
|--------------|------------------|-----------------------|-----|---------------|-----|-------------|-----|-----------|-----|------------|-----|
| | | Conservative Estimate | | Best Estimate | | °C | yrs | °C | yrs | °C | yrs |
| | | °C | yrs | °C | yrs | | | | | | |
| High #1 | MGDS | 301 | 2 | 288 | 2 | 280 | 3 | 213 | 30 | 188 | 50 |
| High #2 | MGDS | 297 | 0.9 | 284 | 0.9 | 275 | 1 | 206 | 8 | 165 | 40 |
| Low #1 | MGDS | 294 | 0.5 | 280 | 0.5 | 271 | 0.5 | 190 | 2 | 117 | 8 |
| Low #2 | MGDS | 296 | 0.8 | 282 | 0.8 | 273 | 0.9 | 195 | 4 | 131 | 8 |
| Low #3 | MGDS | 300 | 1 | 287 | 2 | 278 | 2 | 204 | 5 | 146 | 10 |

Figure 6.5-33 displays the thermal history of the 40 BWR MPC with disposal container at 83 MTU/acre (20.5 kgU/m²) for the MGDS design basis SNF. The conservative estimate of peak cladding temperature for this case was 297°C, which is less than the thermal design goal of 350°C. Just as for the 21 PWR MPC with disposal container, peak temperatures occur between the time of emplacement and the time of peak drift wall temperatures. Figure 6.5-34 displays the thermal history of the 40 BWR MPC with disposal container at 100 MTU/acre (24.7 kgU/m²) for the MGDS design basis SNF. This case, which had a short WP spacing and represents an upper bound of possible thermal loadings, resulted in the highest conservative estimation of peak cladding temperatures (301°C).

Figure 6.5-35 displays the temperature contours in the 40 BWR MPC with disposal container at the time of peak temperatures, 0.9 years. The thermal loading for this case was 83 MTU/acre (20.5 kgU/m²) and the MGDS design basis SNF was assumed. Figures 6.5-36, 6.5-37, and 6.5-38 display the temperature contours for the same case at 10, 50, and 100 years, respectively. By 100 years, the temperature drop across the WP (from center to edge) has dropped to less than 50°C.

Figures 6.5-39 and 6.5-40 display the thermal history of the 40 BWR MPC with disposal container at 25 MTU/acre (6.2 kgU/m²) with the MGDS design basis SNF for low thermal loading #1 and low thermal loading #2, respectively. Peak internal temperatures are similar to those for the high thermal loading because the peaks occur before any effects of thermal loading have been realized. Figure 6.5-41 displays the thermal history of the 40 BWR MPC with disposal container for low thermal loading #3 with the MGDS design basis SNF. The highest internal temperature occurred where the MGDS design basis SNF and the shortest WP spacing (16.2 m) were used. The peak temperatures occur before drift-to-drift effects emerge such that the WP spacing drives the peak near-field temperatures and high thermal loading #1 and low thermal loading #3 have nearly the same peak cladding temperatures.

The thermal evaluation of the 40 BWR MPC conceptual design with respect to the repository has considered a number of thermal loading scenarios. For each repository thermal loading scenario, a three-dimensional repository emplacement and two-dimensional WP evaluation were performed. The results of the thermal evaluations indicate that the 40 BWR MPC with disposal container design satisfies the thermal limitations for disposal in the MGDS.

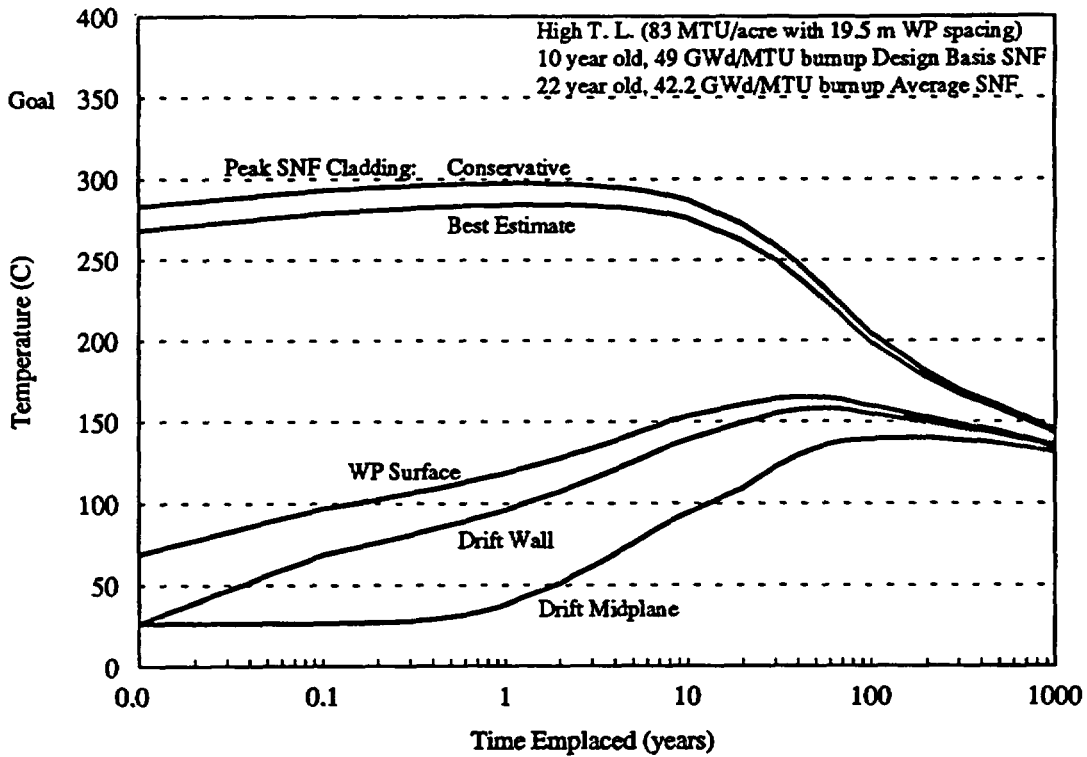


Figure 6.5-33. 40 BWR Multi-Purpose Canister, High Thermal Load (#2), MGDS Design Basis Fuel

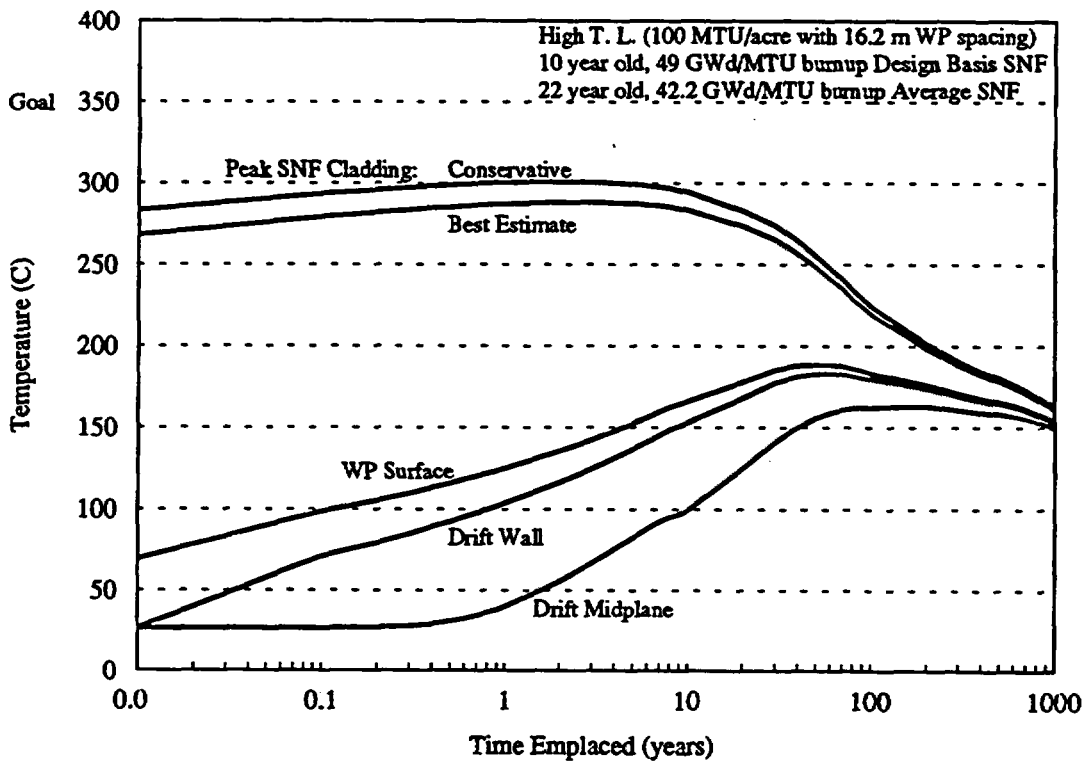


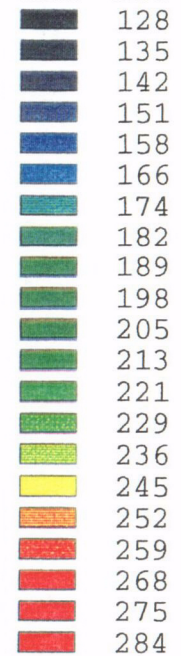
Figure 6.5-34. 40 BWR Multi-Purpose Canister, High Thermal Load (#1), MGDS Design Basis Fuel

ANSYS 5.0 A
MAR 18 1995

Temperature

Min =126

Max =284

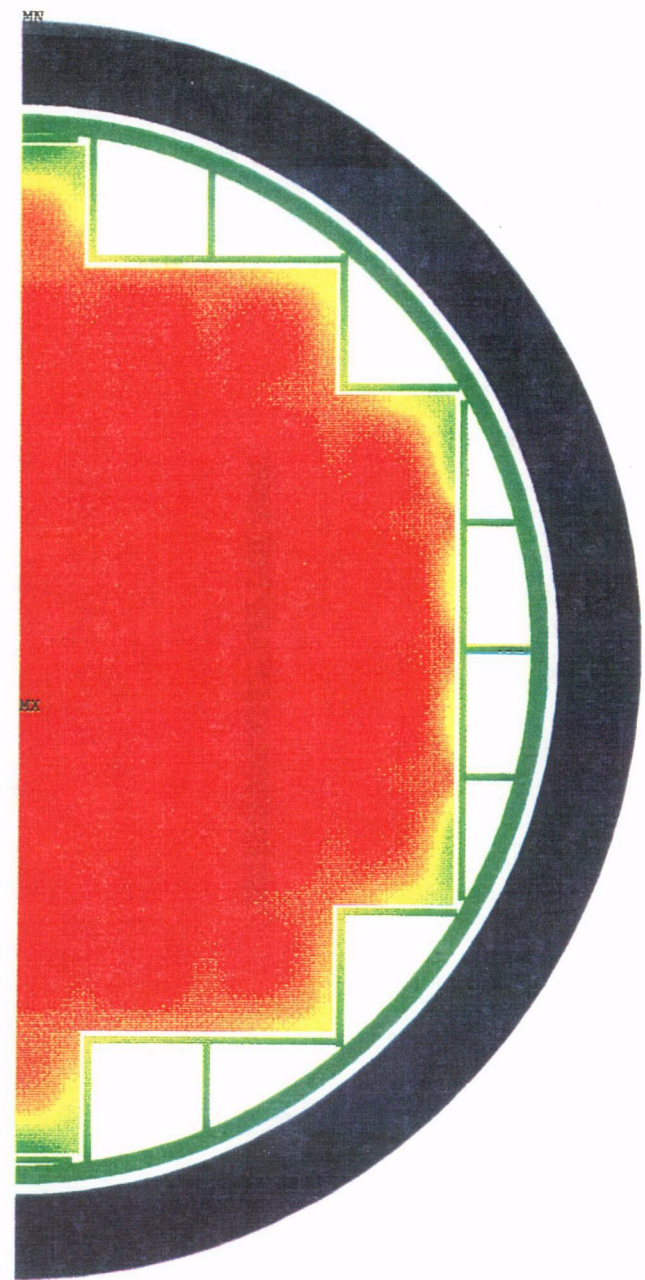


Degrees C

83 MTU/acre

10-year-old SNF
49 GWd/MTU

C09



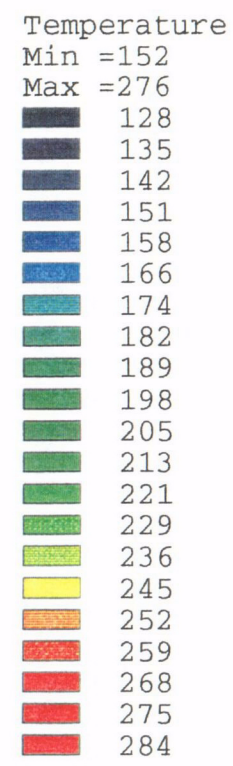
B000000000-01717-5705-00027 REV 00

6.5-43

March 1996

Figure 6.5-35 40 BWR Multi-Purpose Canister Peak Temperatures at 0.9 Years

ANSYS 5.0 A
MAR 18 1995

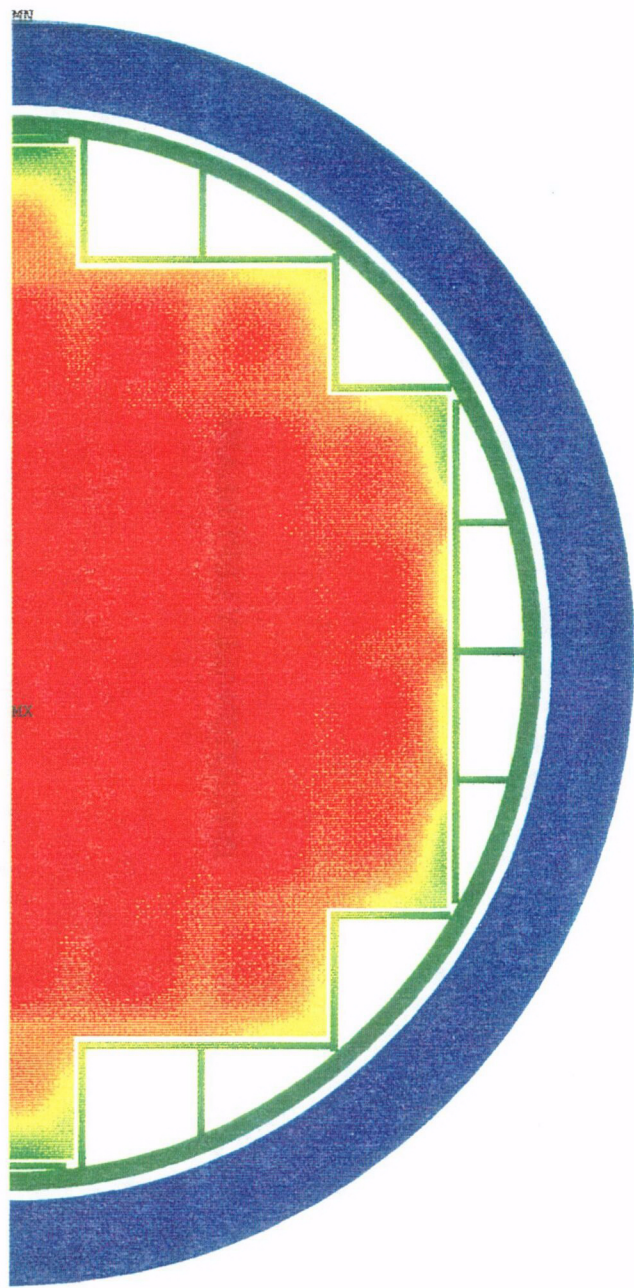


Degrees C

83 MTU/acre

10-year-old SNF
49 GWd/MTU

C10

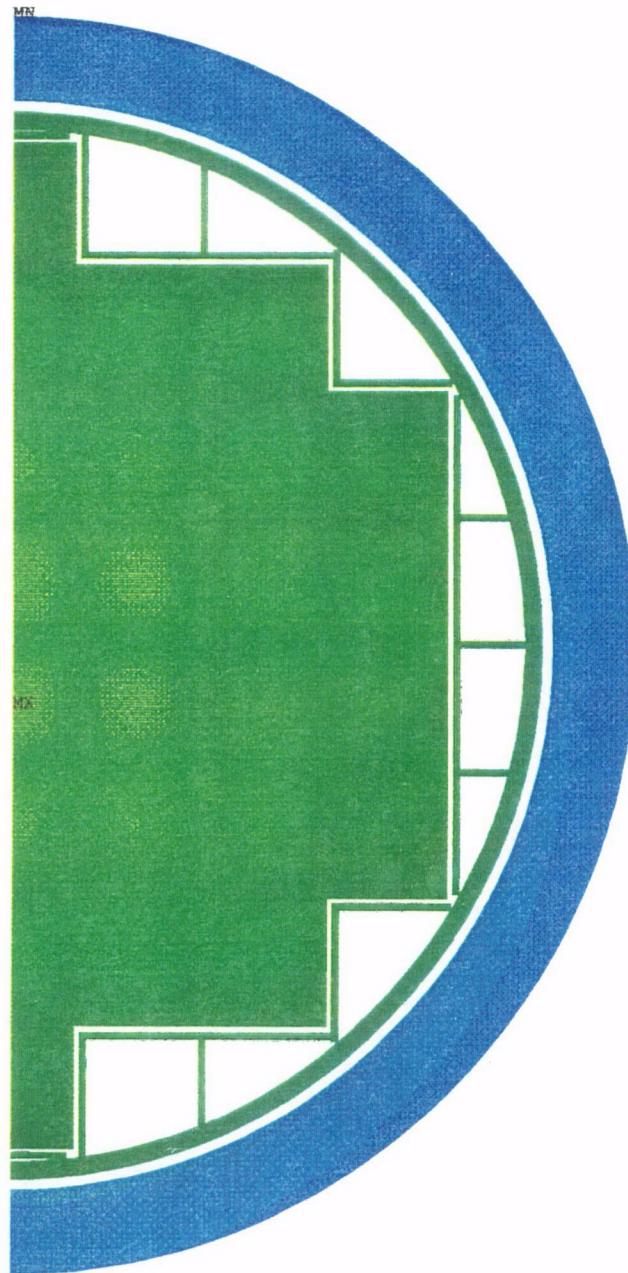


B000000000-01717-5705-00027 REV 00

6.5-45

March 1996

Figure 6.5-36. 40 BWR Multi-Purpose Canister Temperatures at 10 Years



ANSYS 5.0 A
MAR 18 1995

Temperature

Min =164

Max =230

- 128
- 135
- 142
- 151
- 158
- 166
- 174
- 182
- 189
- 198
- 205
- 213
- 221
- 229
- 236
- 245
- 252
- 259
- 268
- 275
- 284

Degrees C

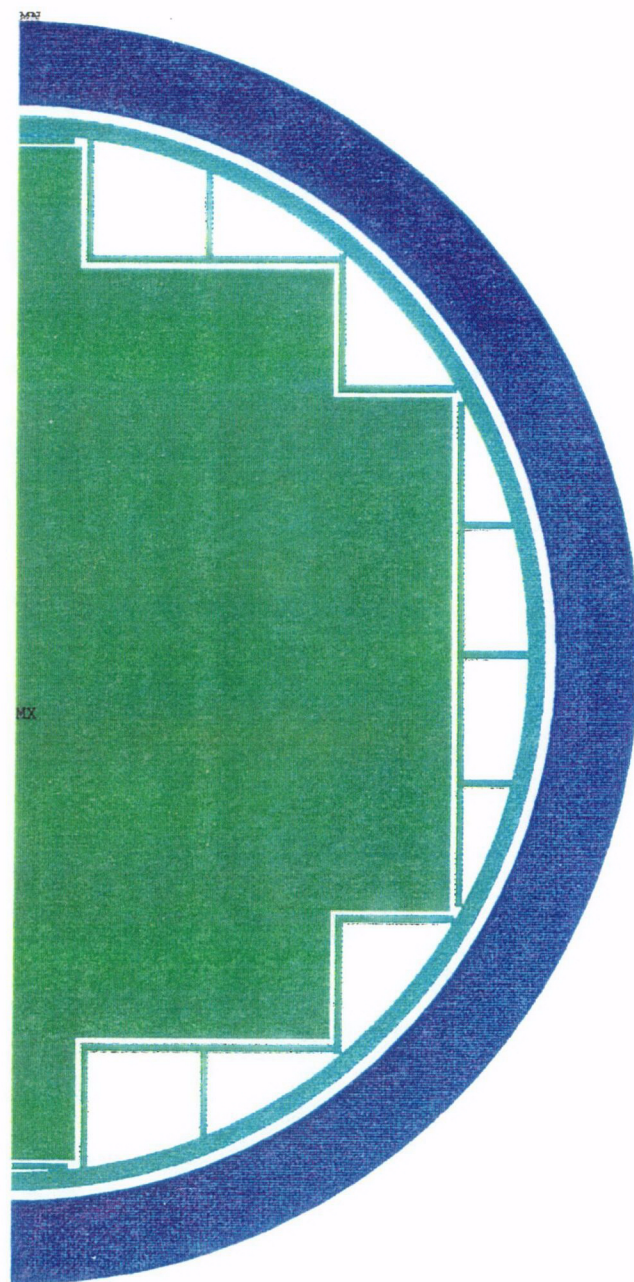
83 MTU/acre

10-year-old SNF

49 GWd/MTU

cll

Figure 6.5-37. 40 BWR Multi-Purpose Canister Temperatures at 50 Years



ANSYS 5.0 A
MAR 18 1995

Temperature

Min =159

Max =199

- 128
- 135
- 142
- 151
- 158
- 166
- 174
- 182
- 189
- 198
- 205
- 213
- 221
- 229
- 236
- 245
- 252
- 259
- 268
- 275
- 284

Degrees C

83 MTU/acre

10-year-old SNF
49 GWd/MTU

C12

Figure 6.5-38. 40 BWR Multi-Purpose Canister Temperatures at 100 Years

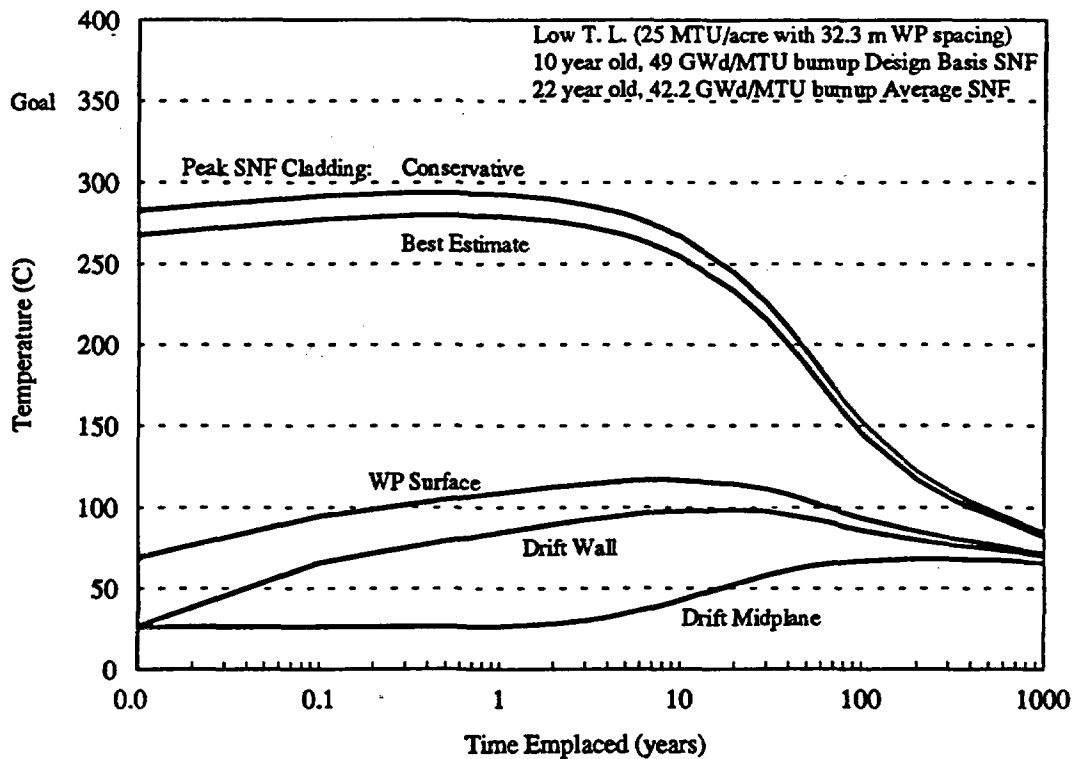


Figure 6.5-39. 40 BWR Multi-Purpose Canister, Low Thermal Load (#1), MGDS Design Basis Fuel

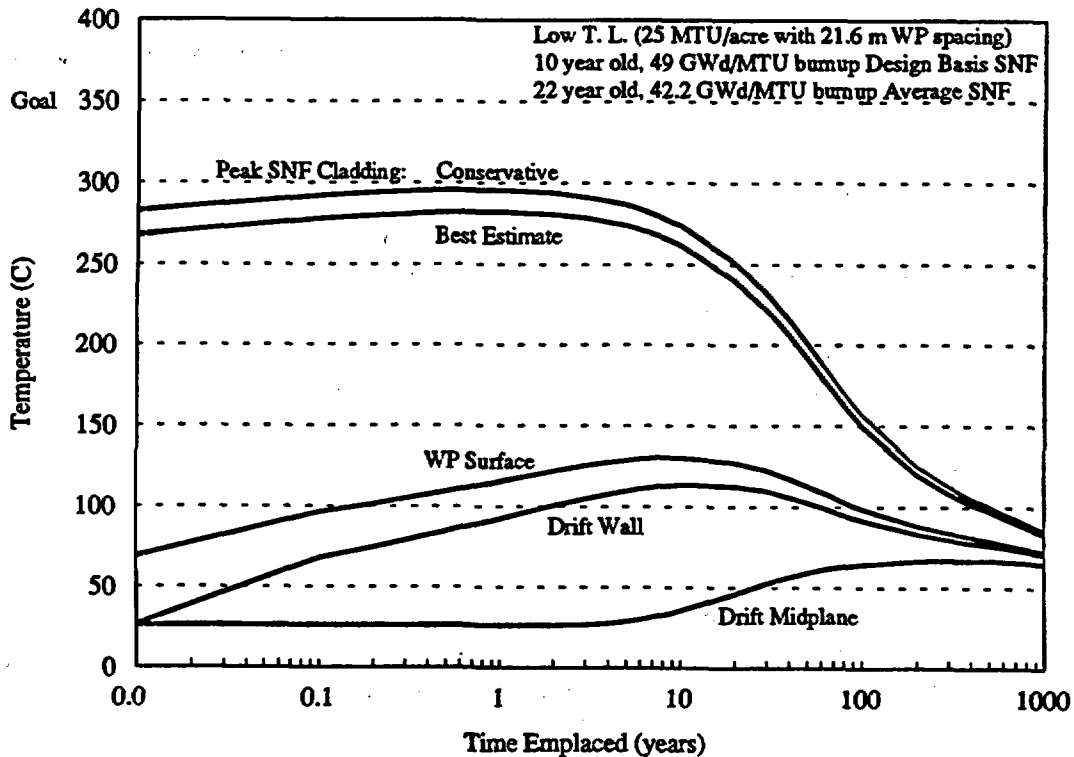


Figure 6.5-40. 40 BWR Multi-Purpose Canister, Low Thermal Load (#2), MGDS Design Basis Fuel

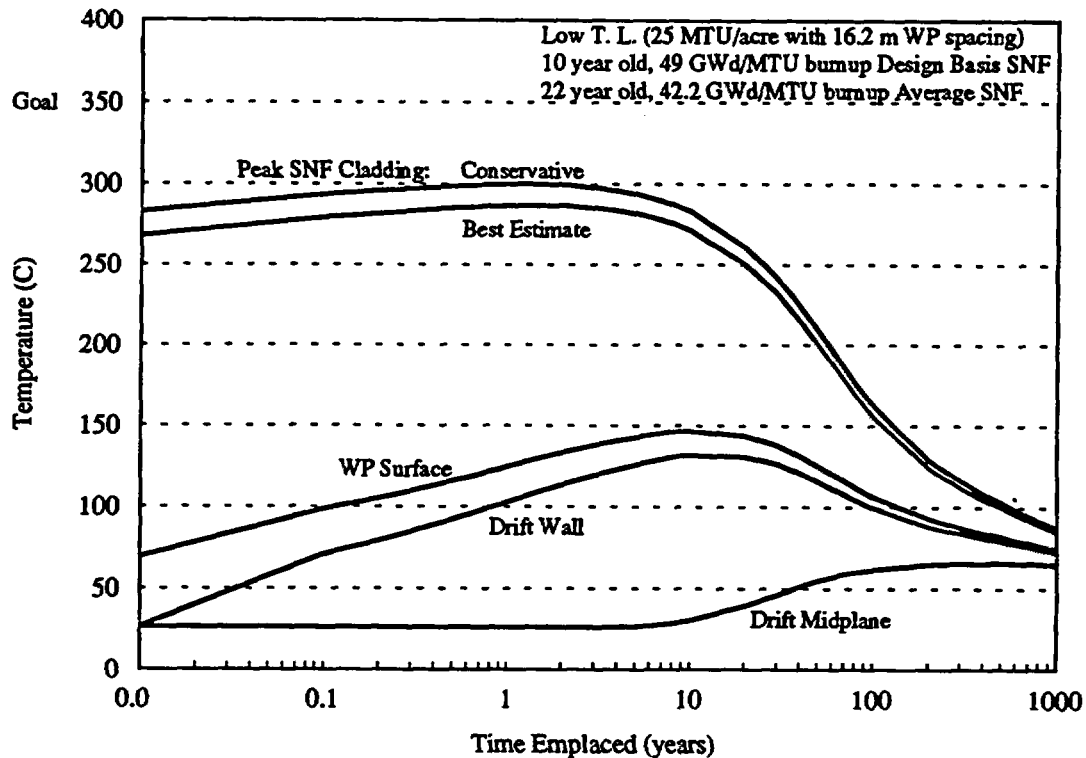


Figure 6.5-41. 40 BWR Multi-Purpose Canister, Low Thermal Load (#3), MGDS Design Basis Fuel

6.5.1.4 Multi-Purpose Canister 24 BWR

A two-dimensional finite-element thermal model of the small 24 BWR burnup credit MPC conceptual design was developed from design drawings supplied in the *MPC Conceptual Design Report* (CRWMS M&O 1994k). Model detail included the separate layers of the basket tube design. Intimate contact was assumed between the layers of stainless steel and aluminum, and also between the tube guides and inner shell. The MPC fill gas was assumed to be helium. The multibarrier disposal container for the 24 BWR MPC, described in Appendix B, was also modeled. The analysis is described in detail in a supporting design analysis (CRWMS M&O 1995h).

The finite-element code ANSYS was used to model the two-dimensional cross-section of the MPC/WP. Time- and position-dependent temperatures for the WP surface were exported from the emplacement model, described in Section 6.2.1.1.2, and applied as time-varying boundary conditions. The other time-varying conditions used in the model were the design basis SNF decay heat outputs applied as volumetric heat generations to the assembly areas of the model and use smeared material properties. Similar to the 40 BWR MPC analysis, the effective conductivity for the assembly area was assumed to be same as described in Section 6.2.1.2 for PWR assemblies. The heat loads for the assembly areas were interpolated from the Oak Ridge National Laboratory database of SNF characteristics for each of the assumed design basis SNF. The heat load will decrease logarithmically with time as the fission products decay. The heat loads were applied

volumetrically and were multiplied by an axial heat peaking factor to approximate the axial center of the WP with a two-dimensional model. An SNF assembly is much hotter at the mid-length than at the ends, and it is conservative to assume the two-dimensional WP model represents the hottest cross-section of the MPC/WP.

The boundary conditions and heat loads were applied and solved out to 1,000 years for each of the five thermal loading scenarios described in Section 6.2.1.1.2 with the MGDS BWR design basis SNF type described in Table 6.5-1. Table 6.5-5 summarizes the peak temperatures and time of occurrence for each of the cases analyzed. The thermal loading scenarios indicated in Table 6.5-5 are defined in Table 6.2-2, and the design basis SNF descriptions are provided in Table 6.5-1. Both "conservative" estimates of peak cladding temperatures using the Wooton-Epstein correlation and "best estimate" predictions using the effective conductivity method are presented in the table. Peak cladding temperatures using effective conductivity are calculated directly in the ANSYS program. Wooton-Epstein calculations for each time step in the ANSYS analysis were also performed for comparison.

Table 6.5-5. 24 BWR Multi-Purpose Canister Thermal Analysis Results

| Thermal Load | Design Basis SNF | Peak Cladding | | | | Peak Basket | | MPC shell | | WP Surface | |
|--------------|------------------|-----------------------|-----|---------------|-----|-------------|-----|-----------|-----|------------|-----|
| | | Conservative Estimate | | Best Estimate | | °C | yrs | °C | yrs | °C | yrs |
| | | °C | yrs | °C | yrs | | | | | | |
| High #1 | MGDS | 265 | 8 | 252 | 8 | 244 | 8 | 201 | 40 | 184 | 60 |
| High #2 | MGDS | 259 | 4 | 244 | 4 | 235 | 5 | 182 | 20 | 160 | 50 |
| Low #1 | MGDS | 251 | 0.6 | 234 | 0.6 | 224 | 0.8 | 152 | 3 | 101 | 20 |
| Low #2 | MGDS | 255 | 1 | 239 | 1 | 229 | 2 | 163 | 5 | 118 | 10 |
| Low #3 | MGDS | 262 | 2 | 247 | 2 | 237 | 2 | 176 | 8 | 137 | 10 |

Figure 6.5-42 displays the thermal history of the 24 BWR MPC with disposal container at 83 MTU/acre (20.5 kgU/m²) for the MGDS design basis SNF. The conservative estimate of peak cladding temperature for this case was 259°C, which is comfortably less than the thermal design goal of 350°C. Just as for the 21 PWR MPC with disposal container, peak temperatures occur between the time of emplacement and the time of peak drift wall temperatures. Figure 6.5-43 displays the thermal history of the 24 BWR MPC with disposal container at 100 MTU/acre (24.7 kgU/m²) for the MGDS design basis SNF. This case, which had a short WP spacing and represents an upper bound of possible thermal loadings, resulted in the highest conservative estimation of peak cladding temperatures (265°C).

Figure 6.5-44 displays the temperature contours in the 24 BWR MPC with disposal container at the time of peak temperatures, four years. The thermal loading for this case was 83 MTU/acre (20.5 kgU/m²) and the MGDS design basis SNF was assumed. Figures 6.5-45, 6.5-46, and 6.5-47 display the temperature contours for the same case at 10, 50, and 100 years, respectively. By 100 years the temperature drop across the WP (from center to edge) has dropped to less than 40°C.

Figures 6.5-48 and 6.5-49 display the thermal history of the 24 BWR MPC with disposal container at 25 MTU/acre (6.2 kgU/m²) with the MGDS design basis SNF for low thermal loading #1 and low thermal loading #2, respectively. Peak internal temperatures are similar to those for the high thermal loading because the peaks occur before any effects of thermal loading have been realized. Figure 6.5-50 displays the thermal history of the 24 BWR MPC with disposal container for low thermal loading #3 with the MGDS design basis SNF. The highest internal temperature occurred where the MGDS design basis SNF and the shortest WP spacing (9.2 m) were used. The peak temperatures occur before drift-to-drift effects emerge such that the WP spacing drives the peak near-field temperatures and high thermal loading #1 and low thermal loading #3 have nearly the same peak cladding temperatures.

The thermal evaluation of the 24 BWR MPC conceptual design with respect to the repository has considered a number of thermal loading scenarios. For each repository thermal loading scenario, a three-dimensional repository emplacement and two-dimensional WP evaluation were performed. The results of the thermal evaluations indicate that the 24 BWR MPC with disposal container design satisfies the thermal limitations for disposal in the MGDS.